Synthesis and Structural Characterization of Bismuth(III)-, Lead(II)- and Scandium(III)-Containing Heteropolytungstates

by

Nickolet Ncube

A thesis submitted in partial fulfilment of the requirements for the degree of:

Doctor of Philosophy
in Chemistry

Approved Dissertation Committee:

Prof. Dr. Ulrich Kortz (supervisor, Jacobs University, Bremen)

Prof. Dr. Detlef Gabel (Jacobs University, Bremen)

Prof. Dr. Emmanuel Cadot (Université de Versailles, France)

Dr. John V. Skilton (Consultancy Service, Bremen)

Date of Defense: 24th August 2020

Department of Life Sciences & Chemistry

STATUTORY DECLARATION

Family Name, Given/First Name	Ncube, Nickolet
Matriculation number	20329539
What kind of thesis are you submitting? Bachelor-, Master- or PhD-Thesis	PhD-Thesis

English: Declaration of Authorship

I hereby declare that the thesis submitted was created and written solely by myself without any external support. Any sources, direct or indirect, are marked as such. I am aware of the fact that the contents of the thesis in digital form may be revised with regard to usage of unauthorized aid as well as whether the whole or parts of it may be identified as plagiarism. I do agree my work to be entered into a database for it to be compared with existing sources, where it will remain in order to enable further comparisons with future theses. This does not grant any rights of reproduction and usage, however.

The Thesis has been written independently and has not been submitted at any other university for the conferral of a PhD degree; neither has the thesis been previously published in full.

German: Erklärung der Autorenschaft (Urheberschaft)

Ich erkläre hiermit, dass die vorliegende Arbeit ohne fremde Hilfe ausschließlich von mir erstellt und geschrieben worden ist. Jedwede verwendeten Quellen, direkter oder indirekter Art, sind als solche kenntlich gemacht worden. Mir ist die Tatsache bewusst, dass der Inhalt der Thesis in digitaler Form geprüft werden kann im Hinblick darauf, ob es sich ganz oder in Teilen um ein Plagiat handelt. Ich bin damit einverstanden, dass meine Arbeit in einer Datenbank eingegeben werden kann, um mit bereits bestehenden Quellen verglichen zu werden und dort auch verbleibt, um mit zukünftigen Arbeiten verglichen werden zu können. Dies berechtigt jedoch nicht zur Verwendung oder Vervielfältigung.

Diese Arbeit wurde in der vorliegenden Form weder einer anderen Prüfungsbehörde vorgelegt noch wurde das Gesamtdokument bisher veröffentlicht.

…………………………………………………………………………………………

Date, Signature

ACKNOWLEDGEMENTS

I dedicate this dissertation to my mother who raised me to love education and believe in myself. I am who I am today because of her love, endless prayers and encouraging words.

First of all, I would like to express my deepest gratitude to my supervisor Prof. Dr. Ulrich Kortz, for accepting me into his research group. Looking back at the last three and a half years I can only say I am blessed to have studied under his supervision. I am grateful for his continuous support and guidance, his motivation and unparalleled knowledge. I am also grateful for his open-door policy and for caring not only about the science but also the human behind the science. I admire his commitment to educating young people and giving equal opportunities to everyone regardless of their race, age, gender, or socioeconomic status. I will always remember him for this! Besides my supervisor, I would also like to thank Prof. Dr. Detlef Gabel, Prof. Dr. Emmanuel Cadot and Dr. John Skilton for accepting to be a part of my thesis and defense committee.

I thank my fellow lab mates for their help. In particular, I am extremely grateful to Dr. Saurav Bhattacharya for solving most of the crystal structures of my compounds and to Dr. Ali Mougharbel for his technical assistance over the course of my studies. I also thank Dr. Joydeb Goura for his helpful advice and the many times he guided me, especially during the paper writing process. I am humbled and grateful to know Dr. Muhammad Qasim, a colleague and very good friend/brother who helped me adapt to the POM lab and assisted me in innumerable ways. I also appreciate undergraduate students such as Diarra Thiam, Lisa Tichagwa, Sihana Ahmedi and Jovana Spalevic for the experimental work they did under my supervision.

In addition, I would like to thank my family and friends. I am indebted to my mother, brother, and sister for their undying emotional and spiritual support in my life in general and specifically throughout my doctoral studies. I cannot begin to express my gratitude to Mark Philip Schaub

whose presence has made my life sweeter. His relentless support and belief in my abilities mean the world to me. Additionally, I wish to thank a number of amazing women I call sisters. They are my cheerleaders and support system, and I am held by their prayers and words of encouragement. Linda Kokwaro, Alisha Johnson, Stephanie Tindjou, Nadine Lehnen, Nelisa Tebeka and Nothizile Ncube, may the good Lord richly bless you all!

Last but not the least

"…Blessing and glory and wisdom, thanksgiving and honour and power and might, be to our God forever and ever. Amen." Revelation 7:12

ABSTRACT

Polyoxometalates (POMs) are discrete, anionic metal-oxides of early d-block metals in high oxidation states that exhibit unmatched structural variety and associated physicochemical properties leading to interest in many diverse areas including catalysis, magnetism, material science and biomedicine. Chapter 1 is an introduction of POMs covering the historical background, structural properties as well as some applications. Chapter 2 presents the state of the art of bismuth(III)-, lead(II)- and scandium(III)-containing POMs. Chapter 3 is about the analytical techniques used as well as synthetic procedures of the used POM precursors. Chapter 4 focuses on the synthesis and structural characterization of bismuth(III)-containing POMs and eight novel compounds are reported. This chapter is divided into two subsections, (i) synthesis of four isostructural Keggin-type ions $[Bi(\alpha\text{-}XW_{11}O_{39})_2]^{n-}$, X = Si (**1**), Ge (**2**), n = 13; X = P (**3**), As (**4**), n = 11) and two Wells-Dawson-type ions $[Bi(\alpha_2\text{-}X_2W_{17}O_{61})_2]^{17-}$ X = P (**5**), As (**6**), n = 17, and (ii) synthesis of the 1:1 complexes $[\{Bi(H_2O)SiW_{11}O_{39}\}_4]^{20-}$ (**7**) and $\{[Bi(H_2O)SiW_{11}O_{39}]^{5-}\}_\infty$ (**8**), the latter being an infinite one-dimensional structure in the solid state. Chapter 5 reports two novel lead(II)-substituted Keggin-type heteropolytungstates, $[Pb(\alpha\text{-}XW_{11}O_{39})]^{6-}$ (X = Si (**9**), Ge (**10**)). This work suggests that Pb^{2+} and Bi^{3+} mimic the structural chemistry of lanthanide ions in POM chemistry. Chapter 6 presents the synthesis and structural characterization of two scandium(III)-containing heteropolytungstates, $[(Na(H_2O))_2Sc_2(P_2W_{15}O_{56})_2]^{16-}$ (**11**) and $[Sc(HPW_7O_{28})_2]^{13-}$ (**12**). Chapter 7 summarizes all the work presented in this dissertation and discusses the future prospects of this work. Chapter 8 shows some incomplete results including the synthesis of $[Sc_4(H_2O)_{10}(B\text{-}\beta\text{-}Te^{IV}W_9O_{33})_2]^{4-}$ (**13**), $[Sc_4(H_2O)_{10}(B\text{-}\beta\text{-}As^{III}W_9O_{33})_2]^{6-}$ (**14**) $\{[(Sc(H_2O)_4)_2(H_2W_{12}O_{42})]^{4-}\}_\infty$ (**15**), $[Bi_2(W_3O_{10})(B\text{-}\alpha\text{-}BiW_9O_{33})_3]^{23-}$ (**16**), $[Bi_2(H_2O)_6W_2O_4(B\text{-}\beta\text{-}BiW_9O_{33})_2]$ (**17**), $[Sc_2Na_2(H_2O)_2(B\text{-}\alpha\text{-}GeW_9O_{34})_2]^{12-}$ (**18**) and $[Sc_2(B\text{-}\beta\text{-}GeW_8O_{31})_2]^{14-}$ (**19**), respectively.

TABLE OF CONTENTS

LIST OF FIGURES

X

LIST OF TABLES

LIST OF COMPOUNDS OBTAINED WITH ABBREVIATIONS

Compound	Abbreviation
$Na_{0.25}K_{12.75}[Bi(\alpha\text{-}SiW_{11}O_{39})_2]\cdot 25H_2O$	**NaK-1**
$Na_{0.5}K_{12.5}[Bi(\alpha\text{-}GeW_{11}O_{39})_2]\cdot 28H_2O$	**NaK-2**
$K_{11}[Bi(\alpha\text{-}PW_{11}O_{39})_2]\cdot 39H_2O$	**K-3**
$K_{17}[Bi(\alpha_2\text{-}P_2W_{17}O_{61})_2]\cdot 38H_2O$	**K-4**
$Cs_{11-x}Na_x[Bi(\alpha\text{-}As^VW_{11}O_{39})_2]\cdot xH_2O$	**CsNa-5**
$K_{17-x}Rb_x[Bi(\alpha_2\text{-}As^V_2W_{17}O_{61})_2]\cdot xH_2O$	**KRb-6**
$K_{20}[(Bi(H_2O)SiW_{11}O_{39})_4]\cdot 40\ H_2O$	**K-7**
$K_5[Bi(H_2O)SiW_{11}O_{39}]\cdot 12H_2O$	**K-8**
$K_6[Pb(\alpha\text{-}SiW_{11}O_{39})]\cdot 12H_2O$	**K-9**
$K_6[Pb(\alpha\text{-}GeW_{11}O_{39})]\cdot 16H_2O$	**K-10**
$Na_{16}[(Na_2(H_2O)_2Sc_2(P_2W_{15}O_{56})_2]\cdot 20H_2O$	**Na-11**
$Na_{13}[Sc(HPW_7O_{28})_2]\cdot 27H_2O$	**Na-12**
Incomplete and inconclusive results	
$Na_4[Sc_4(H_2O)_{10}(B\text{-}\beta\text{-}Te^{IV}W_9O_{33})_2]\cdot xH_2O$	**Na-13**
$Na_6[Sc_4(H_2O)_{10}(B\text{-}\beta\text{-}As^{III}W_9O_{33})_2]\cdot xH_2O$	**Na-14**
$Na_4[(Sc(H_2O)_4)_4(H_2W_{12}O_{42})]\cdot xH_2O$	**Na-15**
$Na_{23}[Bi_2(W_3O_{10})(B\text{-}\alpha\text{-}BiW_9O_{33})_3]\cdot xH_2O$	**Na-16**
$Na_8[Bi_2(H_2O)_6W_2O_4(B\text{-}\beta\text{-}BiW_9O_{33})_2]\cdot xH_2O$	**Na-17**
$Na_{12}[Sc_2Na_2(H_2O)_2(B\text{-}\alpha\text{-}GeW_9O_{34})_2]\cdot xH_2O$	**Na-18**
$Na_{14}[Sc_2(B\text{-}\beta\text{-}GeW_8O_{31})_2]\cdot xH_2O$	**Na-19**

CHAPTER 1. INTRODUCTION OF POLYOXOMETALATES

Polyoxometalates (POMs) are discrete metal-oxo anions of early *d*-block metals in high oxidation states (V^{5+}, Nb^{5+}, Ta^{5+}, Mo^{6+} and W^{6+}).[1-3] These polynuclear, robust compounds have an unmatched structural and compositional variety that offers a unique combination of physical properties, such as thermal and oxidative stability, acidity, redox potentials and high solubility in many aqueous and organic media.[4] A combination of these unique properties results in a wide range of potential applications in various areas such as magnetism, catalysis, biomedicine and materials science.

1.1 Historical Background

The earliest known polyoxometalate was reported by Berzelius in 1826 where he described a yellow precipitate which is now known as ammonium 12-phosphomolybdate, $(NH_4)_3[PMo_{12}O_{40}]_{aq}$. This compound was synthesized by mixing ammonium molybdate with phosphoric acid.[2] C. Marignac (1862) performed the first systematic study of POMs in which the compositions of two isomers of 12-tungstosilicic acid and their salts were determined. From then on, there were tremendous developments in the field of POM chemistry where several hundreds of compounds were synthesized and analysed worldwide, however more work would later be done to understand their structures. In 1908, A. Miolati and R. Pizzighelli developed a structural hypothesis based on Alfred Werner's coordination theory where they proposed the structure of potassium 12-tunsgtosilicate and other related compounds.[5] This work was further developed by A. Rosenheim, an influential scientist in POM chemistry in the first three decades of the twentieth century. This work resulted in the Miolati-Rosenheim theory which suggested that the 12-heteropoly acid with composition $H_7[P(W_2O_7)_6]$ could be formed by the replacement of oxygen atoms by $[W_2O_7]^{2-}$ anions from a hypothetical $H_7[PO_6]$. [6]

In 1929, L. Pauling criticized this theory. He noted that there was no evidence of the existence of $[W_2O_7]^{2-}$ anions due to the fact that the crystal radii of both Mo^{6+} and W^{6+} would favour an octahedral coordination geometry as compared to the tetrahedral geometry of hypothetical $[W_2O_7]^{2-}$. As such he proposed that the structure of 12-tungsto anions was based on an arrangement of twelve MO_6 octahedra surrounding a central XO_4 tetrahedron. Pauling´s proposal was not completely accurate as it only considered the possibility of corner-sharing between the MO_6 octahedra to minimize electrostatic repulsion.[7] Pauling's proposal was partly confirmed by J. F. Keggin in 1933 who provided the first conclusive information on $H_3[PW_{12}O_{40}]\cdot 5H_2O$ using X-ray diffraction. In his work the actual connection of the WO_6 octahedral units could be elucidated. He showed that the polyanion was indeed based on WO_6 octahedra but that these were linked by not only corners but also by edges, as previously proposed by Pauling [8]

More work would later be done by notable names such as J. S Anderson, who suggested the structure of the 6-molybdoperiodate ion $[IMo_6O_{24}]^{5-}$ (no experimental work was involved)[9] and H. T. Evans (1948) for the structure of $[TeMo_6O_{24}]^{6-}$, [10] I. Lindqvist (1950) for the novel heptamolybdate $[Mo_7O_{24}]^{6-}$ [11] and B. Dawson (1953) for a structure closely related to the Keggin anion, $[P_2W_{18}O_{62}]^{6-}$.[12] Therefore, by the end of the first half of the century the Keggin, Anderson-Evans, Lindqvist and Wells-Dawson structures were well known and these were the basis for the discovery of a lot of novel compounds with exciting structures. To date many more novel compounds with varied structures and compositions have been synthesized and can now be characterized by experimental techniques such as X-Ray Diffraction (XRD) Crystallography, multinuclear NMR, Infrared (IR) and Raman spectroscopy.

1.2 General Synthesis of POMs

The process of the formation of POMs is based on the rational/programmed self-assembly of metal oxide building blocks. More specifically, POMs are formed by condensation reactions that take place when an aqueous solution of a metal oxide (and a suitable heteroatom) is acidified (see equations below).[13]

$$7MoO_4^{2-} + 8H^+ \leftrightarrows [Mo_7O_{24}]^{6-} + 4H_2O \text{ (Heptamolybdate ion)}$$

$$12WO_4^{2-} + HPO_4^{2-} + 23H^+ \leftrightarrows [PW_{12}O_{40}]^{3-} + 12H_2O \text{ (Keggin ion)}$$
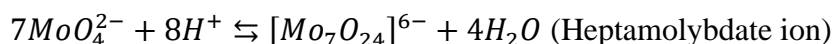
In general, alkaline salts soluble in water such as $Na_2WO_4 \cdot 2H_2O$ and $Na_2MoO_4 \cdot 2H_2O$, are utilized. For heteroatoms, oxoacids such as H_3PO_4 and H_3AsO_4 or alkaline salts such as Na_2SiO_3 are typically used, however oxides such as Sb_2O_3 and Bi_2O_3 can be used if they are dissolved in concentrated hydrochloric acid, or GeO_2 in concentrated hydroxide solution to avoid hydrolysis.[14]

There are several factors that need to be taken into consideration for the successful synthesis of POMs. Some of these factors are:

- the ratio of the addenda and heteroatoms (M/X),

- the temperature at which the reaction takes place,

- the final pH of the reaction solution, which is very important because there is a range of pH where a polyanion can exist and is stable,

- the type of solvent and the nature of the countercations(e.g. the divacant $[\gamma\text{-PW}_{10}O_{36}]^{7-}$ polyanion is isolated only as a caesium salt.[15] It is important to choose appropriate countercations in order to isolate pure compounds in either crystalline form or as precipitates.[16]

In POM chemistry, the most common methods of identification and structural characterization are in the solid state (IR spectroscopy and X-Ray Diffraction Crystallography).

1.3 Composition and Classification of POMs

POMs are classified as either isopolyanions $[M_mO_y]^{p-}$ or heteropolyanions $([X_xM_mO_y]^{q-}$ where with x ≤ m). "X" is the heteroatom and "M" is the addenda atom. Typical heteroatoms are usually p block elements such as Si^{IV}, Ge^{IV}, P^{V}, $As^{III/V}$, $Sb^{III/V}$, Te^{IV}, Bi^{III}.[3] Addenda atoms are Group V and VI transition metals in their d^0 or d^1 electronic configurations.[1-2]
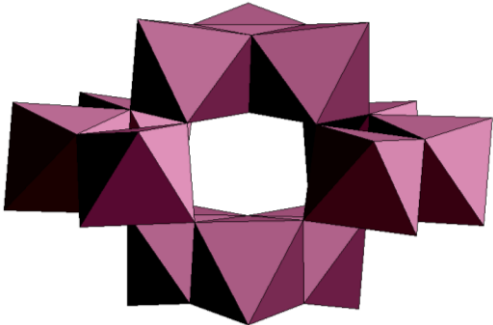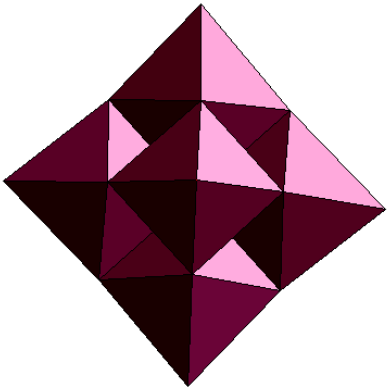
The structures of POMs are mainly composed of MO_6 octahedra which are joined via corner-, edge- or face-shared oxygen bridges to form discrete anionic molecules. In the corner- and edge-sharing models, the addenda atoms (metal ions) do not lie at the centre of its octahedron but are displaced strongly towards the exterior of the POM structure. These models are more favourable than the face-sharing model where the metallic centres are closer to each other thereby causing more repulsion and decreased stability of the polyanion.[17-18]
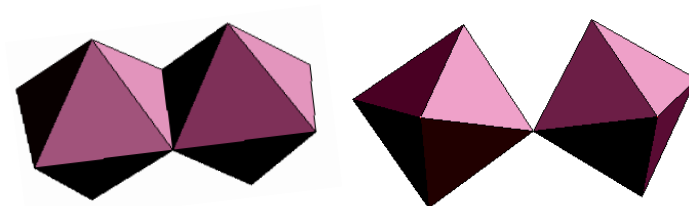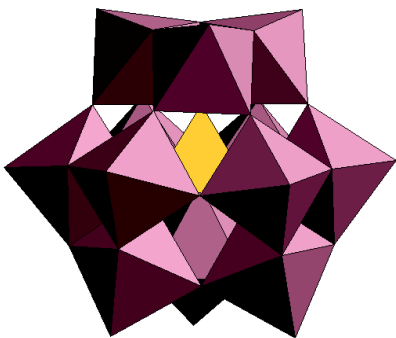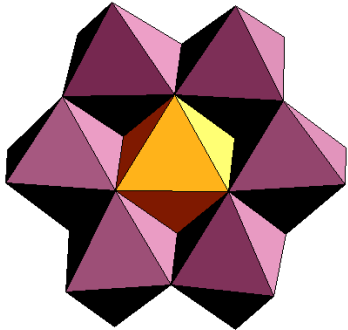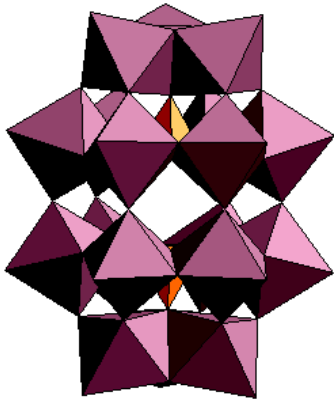
Figure 1.1. Polyhedral representation of the two favourable sharing models between two MO_6 octahedral units, edge-sharing (left) and corner-sharing (right).
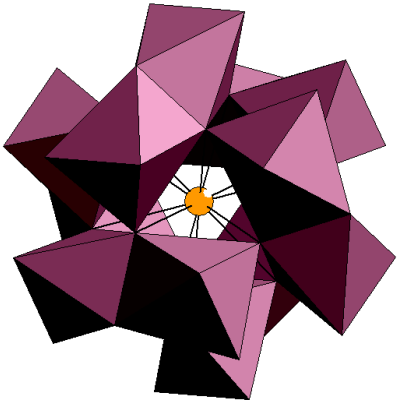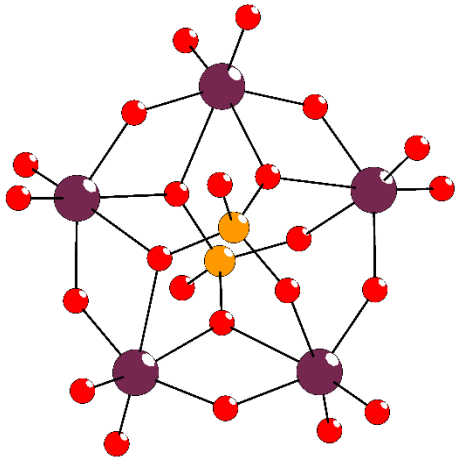
Table 1.1. Polyhedral representations of common isopolyanions.

Isopolyanions
Paratungstate-B $[H_2W_{12}O_{42}]^{10-}$	This centrosymmetric anion consists of four corner-sharing W_3O_{13} groups which are constructed by the assembly of three WO_6 octahedra via edges. The structure contains a central cavity where the two protons are attached to the triply bridging O atoms of W_3O_{13} and these help stabilize this structure by hydrogen-bonding. [19]
Lindqvist $[M_6O_{19}]^{n-}$	The $[M_6O_{19}]^{n-}$ structure (O_h symmetry) is an arrangement of six edge-shared MO_6 octahedra with one O atom common to each of them. [11] This structure is known for M = Mo^{6+}, W^{6+}, V^{5+}, and Ta^{5+}. Some examples are $[Mo_6O_{19}]^{2-}$, $[W_6O_{19}]^{2-}$, $[Ta_6O_{19}]^{8-}$, $[V_6O_{19}]^{8-}$. [20–22]

Table 1.2. Polyhedral/ball-and-stick representations of common heteropolyanions.
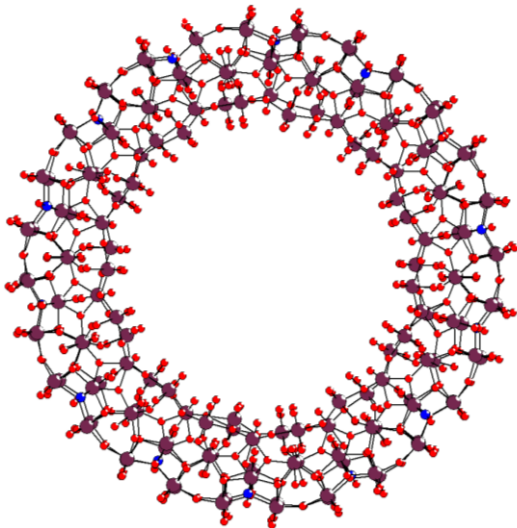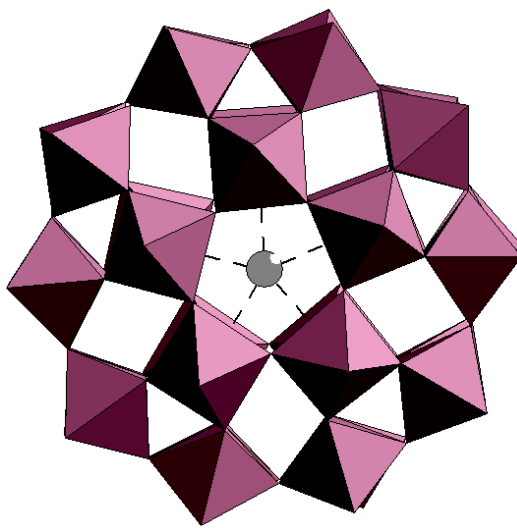
Heteropolyanions	
Keggin $[XM_{12}O_{40}]^{n-}$ 	This polyanion can also be represented as $[(XO_4)M_{12}O_{36}]^{n-}$. It is composed of a central XO_4 tetrahedron surrounded by four M_3O_{13} triads. Each triad is built up by three edge-shared MO_6 octahedra. The triads are connected *via* corners sharing a common oxygen resulting in a T_d point group symmetry. [23]
Anderson-Evans $[XM_6O_{24}]^{n-}$ 	This polyanion is composed of six edge-sharing MO_6 octahedra surrounding a central, edge-sharing heteroatom of octahedral geometry (XO_6) leading to a planar arrangement and D_{3d} point group symmetry. [10]
Wells-Dawson $[X_2M_{18}O_{62}]^{6-}$ 	The anion (D_{3h} point group symmetry) consists of two fused $[A\text{-}\alpha\text{-}XM_9O_{34}]^{n-}$ connected via corners. Each $[A\text{-}\alpha\text{-}XM_9O_{34}]^{n-}$ consists of a central PO_4 tetrahedron surrounded by nine WO_6 octahedra linked together by sharing both corners and edges. [12]

Dexter–Silverton $[XMo_{12}O_{42}]^{n-}$	This anion consists of a CeO_{12} core (icosahedron) which is surrounded by six Mo_2O_9 units. Each Mo_2O_9 unit, which consists of two face-sharing octahedra, is connected to four adjacent units via shared corners. Two corners are on the shared face and the other two are the innermost ones opposite the shared face. Each Mo atom has two cis terminal oxygen atoms, and this structure is only known for molybdates with Ce^{3+}, Ce^{4+}, Th^{4+}, U^{5+} and Np^{5+} heteroatoms.[2, 24]
Strandberg $[P_2Mo_5O_{23}]^{6-}$	The Strandberg anion has five MoO_6 units joined to form a ring. The units are linked to each other by sharing edges except for one where a corner is shared. The structure contains two PO_4 tetrahedra that are attached to the ring, one above and the other below, each having three oxygen atoms in common with the ring. Each MO_6 unit has four shared and two unshared oxygen atoms and each PO_4 tetrahedron has one unshared oxygen. [25]

Allmann-Waugh $[MnMo_9O_{32}]^{6-}$	This anion consists of a central MnO_6 group and on the same level is connected to three MoO_6 units which are joined via three non-adjacent edges of the central MnO_6 octahedron. Above and below this central layer of four octahedra are two triads. In each of these triads the three MoO_6 octahedra have one vertex in common, and each MoO_6 of the triad shares two adjacent edges with the other two octahedra.[26]
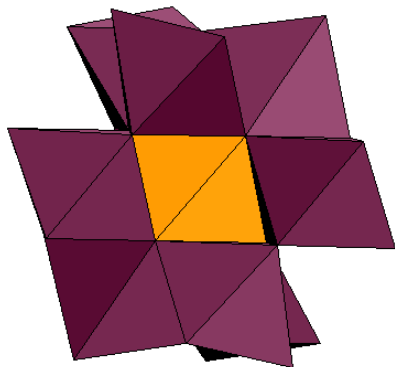
Table 1.3. Polyhedral/ball-and-stick representations of common large polyanions.

Large Polyanions	
"Bielefeld-wheel" ([Mo$_{154}$(NO)$_{14}$O$_{448}$H$_{14}$(H$_2$O)$_{70}$]$^{28-}$	This wheel-shaped anion consists of 140 MoO$_6$ octahedra and 14 {Mo(NO)O$_6$} pentagonal bipyramids. It can be described as a tetradecamer with an approximate D$_{7d}$ symmetry.[27, 28]
Pope-Jeannin-Preyssler [Na(H$_2$O)P$_5$W$_{30}$O$_{110}$]$^{14-}$	The doughnut-shaped anionic cluster consists of five PW$_6$O$_{22}$ subunits which are derived from [PW$_{12}$O$_{40}$]$^{3-}$ (Keggin ion) that has lost two sets of corner-shared triads. These subunits are arranged in a crown such that the resulting point group symmetry is D$_{5h}$. However, the presence of a tightly bound sodium atom in the polyanion structure results in the reduction of the symmetry to C$_{5v}$. The internal sodium cation has been successfully replaced by several cations of similar size such as K$^+$, Ca^{2+}, Y^{3+}, Bi^{3+} and U^{4+}. [29-31]

Contant-Tézé $[H_7P_8W_{48}O_{184}]^{33-}$	This crown-shaped polyanion is formed by the connection of four $\{P_2W_{12}O_{48}\}$ subunits which are derived from the Wells-Dawson structure that has lost six adjacent WO_6 octahedra, one from each cap and four from the belt region of the polyanion. The resulting point symmetry is D_{4h}.[32]
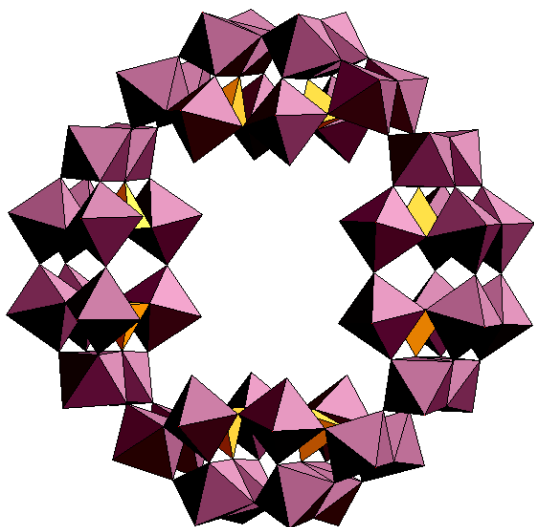
1.4 The Keggin Polyanion, $[XM_{12}O_{40}]^{n-}$

Of all polyoxometalates, those that assume the Keggin structure are the most studied. The condensation of MO_6 octahedra around an XO_4 tetrahedron results in this structural type and the majority of heteropolytungstates adopt either the Keggin structure or structures that are derived from fragments of the Keggin ion. Although there is a high range of possibilities of the central heteroatom (X), P and Si are the most abundant.

The Keggin structure contains 40 oxygen atoms which result in four types of M-O bonds; M-O_t, X-O_a, M-O_a and M-O_b bonds where O_t are terminal/surface oxygens, O_a are the oxygen atoms directly bound to the central heteroatom X, and O_b atoms are bridging oxygen atoms. Transition metals or other elements of the periodic table mostly attach to the most basic oxygen atoms in the Keggin which are the bridging ones. [33,34]]
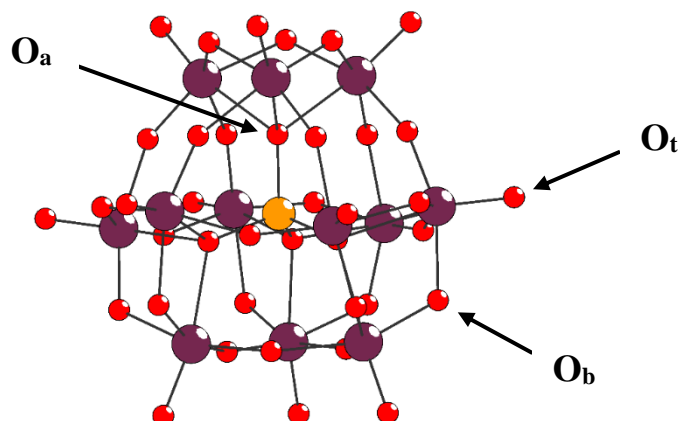
Figure 1.2. Ball-and-stick representation of the Keggin anion. Colour code: W, dark-pink; X (heteroatom), orange; O, red.

1.5 Rotational Isomers of the Keggin Polyanion: Baker-Figgis Isomers

In 1970 L. C. W. Baker and J. S. Figgis ascertained that five isomers of the Keggin ion exist. The α-Keggin is the parent or plenary ion where none of the triads are rotated. A 60° rotation of one of the M_3O_{13} triads of the α anion about the three-fold rotation axis leads to the β structure. The rotation of the remaining triads result in three additional isomers, γ, δ and ε where two, three and all triads are rotated by 60°, respectively.[35] In the α- and β- isomers, the M_3O_{13} triads are connected via vertices (corners) only, while in the γ-, δ- and ε- structures they are connected by edges. The rotation of one triad leads to the reduction of symmetry of the anion from T_d to C_{3v} . The addenda atoms (M = W or Mo) in heteropolyanions are known to be displaced towards the unshared vertices of their respective octahedra thereby minimizing electrostatic repulsion between the metal atoms. The replacement of the corner-shared links in the α- and β- isomers with one to six edge-shared links in the γ, δ and ε structures results in addenda atoms being closer together in the γ-, δ- and ε- isomers.[36] In the β- isomer, the newly formed corner-shared W-O-W bonds between the rotated triad and the rest of the polyanion have shorter W-W distances (3.65 vs 3.72 Å) and more acute W-O-W angles (~145°-155 °) as compared to the α-Keggin isomer. This results in the β- isomer being less stable due to the increase in coulombic repulsion and less favourable pπ-dπ interactions. Moving to γ-, δ- and ε-

isomers, the isomers are even less stable than the α- and β- isomers.[2]
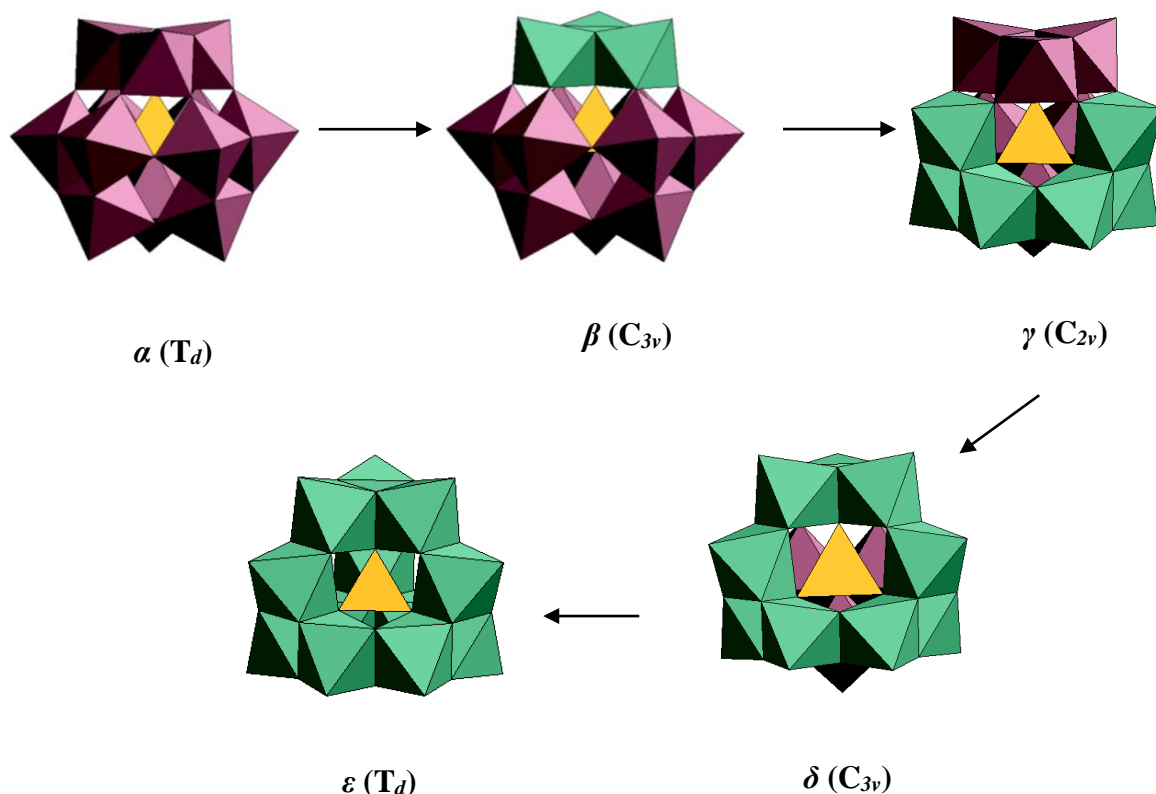
Figure 1.3. Polyhedral representation of the five rotational isomers of the Keggin anion. Colour code: WO_6, dark-pink and green octahedra (octahedra involved in isomerism); XO_4, orange tetrahedra.

1.6 Lacunary Derivatives of the Keggin Polyanion

Besides the Baker-Figgis isomers, other structural derivatives of the Keggin ion exist. When octahedra are eliminated through controlled base hydrolysis of the plenary ion, the result is the formation of lacunary POMs. For example, $[SiW_{12}O_{40}]^{4-}$ is a stable polyanion in acidic media but upon increasing the pH of the solution, one or several W-O bonds can be broken leading to monolacunary $[SiW_{11}O_{39}]^{8-}$, dilacunary $[\gamma\text{-}SiW_{10}O_{36}]^{8-}$ and trilacunary $[SiW_9O_{34}]^{10-}$ species. Where three octahedra are lost, the resulting structure can be further categorized based on whether the three octahedra eliminated are from a corner-shared triad or an edge-shared triad. The letter **A** is placed before the α- if the eliminated triad is corner-shared; $[A\text{-}\alpha\text{-}SiW_9O_{34}]^{10-}$, and **B** if the eliminated triad is edge-shared; $[B\text{-}\alpha\text{-}SiW_9O_{34}]^{10-}$.[37]
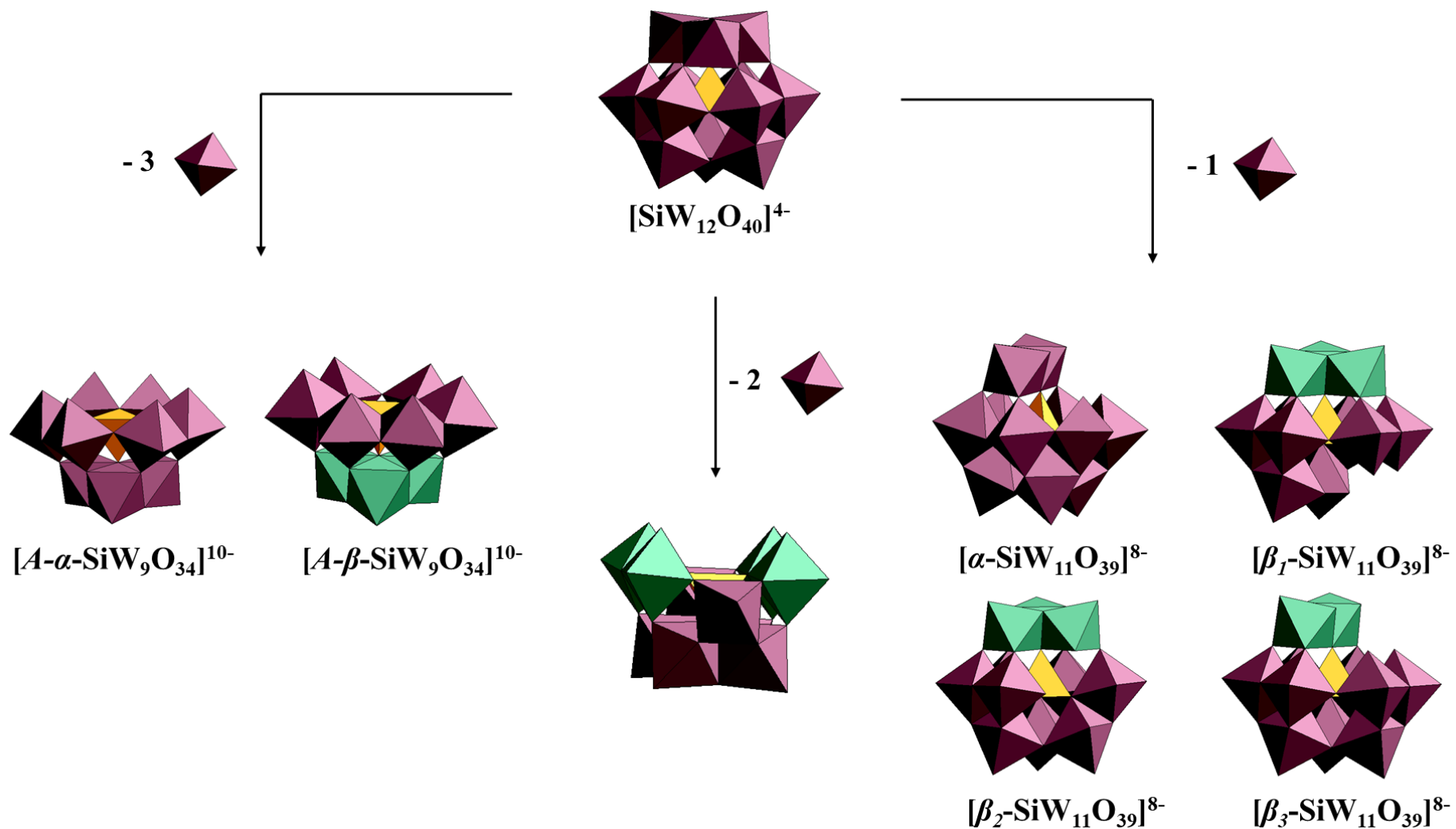
Figure 1.4. Polyhedral representation of the lacunary derivatives of $[SiW_{12}O_{40}]^{4-}$. Colour code: WO_6, dark-pink and green octahedra(rotated triad); SiO_4, orange tetrahedra.

1.7 Lacunary Derivatives of the Wells-Dawson Polyanion

Lacunary derivatives of the Wells-Dawson ion; $[P_2W_{18}O_{62}]^{6-}$ have been reported. To date, α-,

β- and γ- isomers are known but only the α- and β- isomers are the most stable.[2, 12, 38-41]The

Wells-Dawson ion behaves similarly to the Keggin ion in that upon base hydrolysis of both,

lacunary/vacant species are formed. Four lacunary species of $[P_2W_{18}O_{62}]^{6-}$ are known, namely,

the two monolacunary ions; $[\alpha_1\text{-} P_2W_{17}O_{61}]^{10-}$ and $[\alpha_2\text{-} P_2W_{17}O_{61}]^{10-}$ where W-O is lost from

the belt position of the plenary structure and from the cap respectively; the trilacunary $[B\text{-}\alpha\text{-}$

$P_2W_{15}O_{56}]^{12-}$ which lacks an entire edge-shared triad and the hexalacunary $[P_2W_{12}O_{48}]^{14-}$ where

an addenda atom from the bottom and top caps, as well as four from the belt area of the plenary

ion are lost [42-44] Just like the Keggin lacunary species, the vacant/lacunary sites of the Wells-

Dawson species can be filled by a wide variety of elements, such transition and post-transition

metals and, lanthanides.
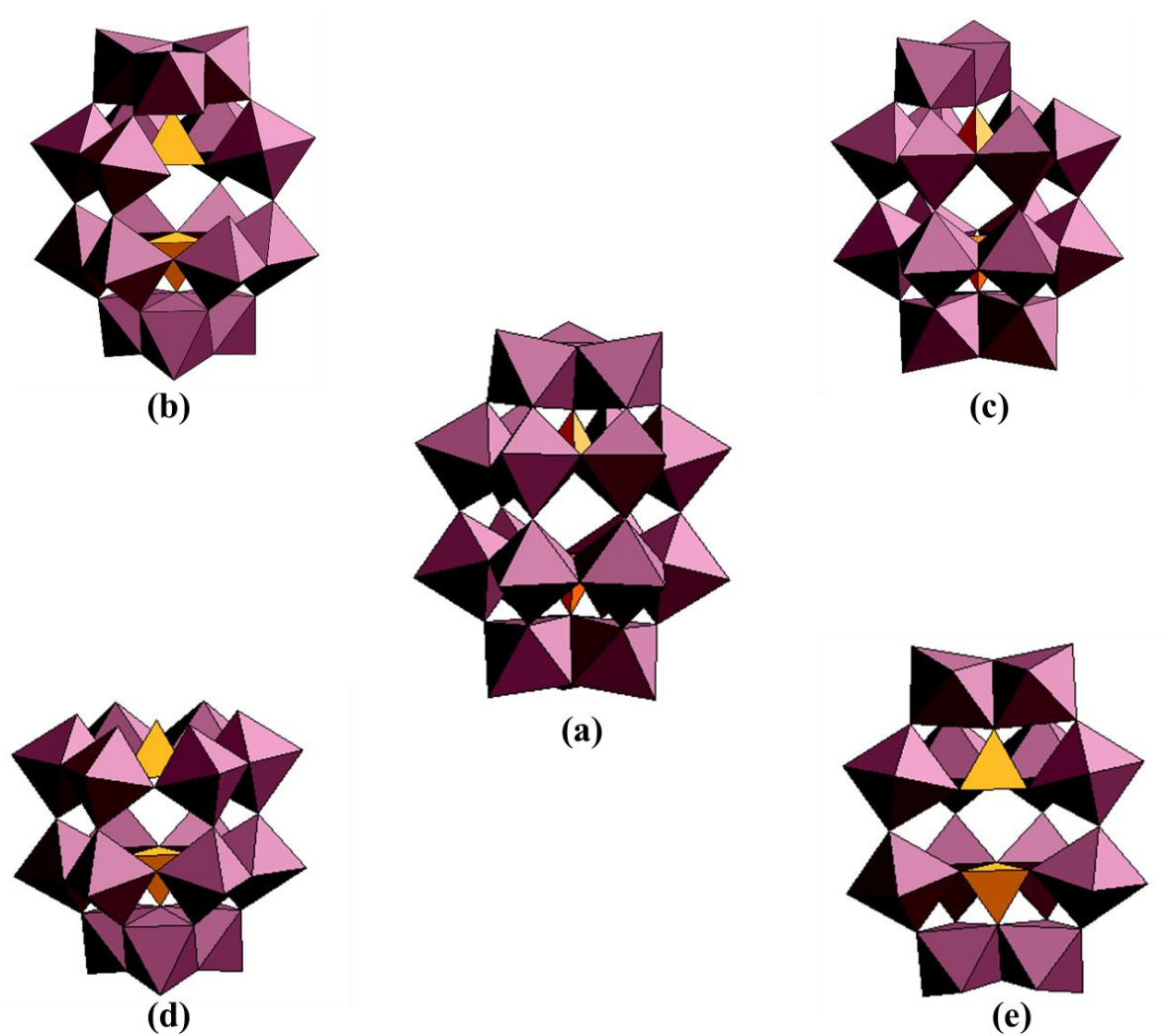
Figure 1.5. Polyhedral representations of $[\alpha\text{-}P_2W_{18}O_{62}]^{6-}$ (a) and its lacunary derivatives; monolacunary $[\alpha_1\text{-}P_2W_{17}O_{61}]^{10-}$ (b) and $[\alpha_2\text{-}P_2W_{17}O_{61}]^{10-}$ (c), trilacunary $[P_2W_{15}O_{56}]^{12-}$ (d) and hexalacunary $[P_2W_{12}O_{48}]^{14-}$(e). Colour code: WO_6, dark-pink octahedra; PO_4, orange tetrahedra.

1.8 Physicochemical Properties and Applications of POMs

Polyoxometalates (POMs) have unique physicochemical properties that stem from a wide range of sizes (~6-25 Å), structure and elemental composition, solubility, charge density and redox potentials.[45] POMs are usually isolated as hydrated salts. Keggin-type heteropoly acids (HPA) and their salts have gained an increasing interest in the field of catalysis.[46] Besides having a strong Bronsted acidity, they are efficient oxidants due to their ability to undergo fast reversible multi-electron redox transformations under very mild conditions.[47] POMs are great electron reservoirs since they can gain or lose electrons without any major structural changes. This in turn has led to POMs being great acid as well as redox catalysts which are capable of catalysing various chemical processes such as the rapid oxidation of H_2O to O_2 at ambient temperature, with low over-potential and high turnover frequency as well as catalysis of the reduction of CO_2 to CO in the presence of H_2 under light.[48]

The solubility of POMs greatly depends on the counter cations that are employed to co-crystallize with the polyanion. Li, Na and K salts of POMs are water soluble whereas salts of organic cations (e.g., tetrabutylammonium (TBA)) are soluble only in non-aqueous media.[49] The ability to adjust the solubility as well as their size, charge, surface area and polarity has led to POMs being known for their antiviral, enzyme inhibition, anticancer and antibacterial properties. POMs have gained a lot of attention in biomedicine for the treatment of various diseases, including HIV/AIDS, cancer, diabetes, Alzheimer's and infectious diseases.[50–53]

POMs have also been found to be promising co-crystallization agents in the investigation and resolution of crystal structures of various biomolecules. This is because they are capable of binding to positively charged regions of biomolecules by electrostatic interactions, thus rigidifying flexible loops or other regions thereby promoting crystallization.[54-56]

1.9 References

[1]   F. Secheresse, *Polyoxometalate Chemistry : Some Recent Trends*, World Scientific,
       2013.

[2]   M. T. Pope, *Heteropoly and Isopoly Oxometalates*, Springer-Verlag, 1983.

[3]   J. J. Borrás-Almenar, E. Coronado, A. Müller, M. Pope, Eds. , in *Polyoxometalate
       Molecular Science.*, Springer Netherlands, Dordrecht, 2003.

[4]   C. L. Hill, *Chem. Rev.* **1998**, *98*, 1–2.

[5]   A. Miolati, R. Pizzighelli, *J. Prakt. Chem.* **1908**, *77*, 417–456.

[6]   A. Rosenheim, J. Jaenicke, *Z. Anorg. Allg. Chem.* **1917**, *100*, 304–354.

[7]   L. Pauling, *J. Am. Chem. Soc.* **1929**, *51*, 2868–2880.

[8]   J. F. Keggin, *Nature.* **1933**, *132*, 351–351.

[9]   J. S. Anderson, *Nature.* **1937**, *140*, 850–850.

[10]   H. T. Evans, *J. Am. Chem. Soc.* **1948**, *70*, 1291–1292.

[11]   I. Lindqvist, *Acta Cryst.* **1950**, *3*, 159–160.

[12]   B. Dawson, *Acta Cryst.* **1953**, *6*, 113–126.

[13]   A. Proust, R. Thouvenot, P. Gouzerh, *Chem. Commun.* **2008**, 1837.

[14]   G. Hervé, A. Tézé, R. Contant, in *Polyoxometalate Molecular. Science.*, Springer
       Netherlands, Dordrecht, 2003, 33–54.

[15]   W. H. Knoth, R. L. Harlow, *J. Am. Chem. Soc.* **1981**, *103*, 1865–1867.

[16]   M. T. Pope, A. Müller, *Introduction to Polyoxometalate Chemistry : From Topology via
       Self-Assembly to Applications*, Kluwer Academic Publishers, 2006.

[17]   A. Tézé, G. Hervé, *J. Inorg. Nucl. Chem.* **1977**, *39*, 2151–2154.

[18]   D. L. Keppert, **1972**, 499.

[19]   I. Lindqvist, *Acta Cryst.* **1952**, *5*, 667–670.

[20]   H. K. Chae, W. G. Klemperer, V. W. Day, *Inorg. Chem.* **1989**, *28*, 1423–1424.

[21]   J. Fuchs, W. Freiwald, H. Hartl, *Acta Cryst. B.* **1978**, *34*, 1764–1770.

[22]   O. Nagano, Y. Sasaki, *Acta Cryst. B.* **1979**, *35*, 2387–2389.

[23]   J. F. Keggin, *Nature.* **1933**, *132*, 351.

[24]   D. D. Dexter, J. V. Silverton, *J. Am. Chem. Soc.* **1968**, *90*, 3589–3590.

[25]   R. Strandberg, L. Niinistö, J. Møller, G. Schroll, K. Leander, C.-G. Swahn, *Acta Chem. Scand.* **1973**, *27*, 1004–1018.

[26]   J. L. T. Waugh, D. P. Shoemaker, L. Pauling, IUCr, *Acta Cryst.* **1954**, *7*, 438–441.

[27]   A. Müller, A, E. Krickemeyer, J. Meyer, H. Bögge, F. Peters, W. Plass, E. Diemann, S. Dillinger, F. Nonnenbruch, M. Randerath, C. Menke. *Angew. Chem., Int. Ed.* **1995**, *34*, 2122.

[28]   A. Müller, S. K. Das, V. P. Fedin, E. Krickemeyer, C. Beugholt, H. Bögge, M. Schmidtmann, B. Hauptfleisch. *Z. Anorg. Chem.* **1999**, *625*, 1187.

[29]   C. Preyssler, *Bull. Soc. Chim. Fr.* **1970**, *1*, 30.

[30]   M. H. Alizadeh, S. P. Harmalker, Y. Jeannin, J. Martin-Frere, M. T. Pope, *J. Am. Chem. Soc.* **1985**, *107*, 2662.

[31]   K. C. Kim, M. T. Pope, G. J. Gama, M. H. Dickman, *J. Am. Chem. Soc.* **1999**, *121*, 11164.

[32]   Contant, R.; Tézé, A. *Inorg.Chem.* **1985**, *24*, 4610– 4614.

[33]   J. F. Keggin, *Proc. R. Soc. A Math. Phys. Eng. Sci.* **1934**, *144*, 75–100.

[34]   L. C. W. Baker, L. Lebioda, J. Grochowski, H. G. Mukherjee, *J. Am. Chem. Soc.* **1980**, *102*, 3274–3276.

[35]   L. C. W. Baker, J. S. Figgis, *J. Am. Chem. Soc.* **1970**, *92*, 3794–3797.

[36]   M. T. Pope, *Inorg. Chem.* **1976**, *15*, 2008–2010.

[37]   A.P. Ginsberg, Ed., *Inorganic Syntheses*, John Wiley & Sons, Inc., Hoboken, NJ, USA, 1990, *27*, 85–96.

[38]   W. Hsein, *J. Biol. Chem.* **1920**, *1*, 189.

[39]   R. Acerete, C. F. Hammer, L. C. W. Baker, *Inorg. Chem.* **1984**, *23*, 1478–1482.

[40]   K. Y. Matsumoto, Y. Sasaki, *J. Chem. Soc. Chem. Commun.* **1975**, 691–692.

[41]   R. Contant, R. Thouvenot, *Inorg. Chim. Acta* **1993**, *212*, 41–50.

[42]   L. E. Briand, G. T. Baronetti, H. J. Thomas, *Appl. Catal. A Gen.* **2003**, *256*, 37–50.

[43]   R. Massart, R. Contant, J. M. Fruchart, J. P. Ciabrini, M. Fournier, *Inorg. Chem.* **1977**, *16*, 2916–2921.

[44]   A.P. Ginsberg, Ed., *Inorganic Syntheses*, John Wiley & Sons, Inc., Hoboken, NJ, USA, 1990, *27*, 104-111.

[45]   M. T. Pope, *Inorg. Chem.* **1972**, *11*, 1973–1974.

[46]   D. E. Katsoulis, *Chem. Rev.* **1998**, *98*, 359–388.

[47]   M. Ammam, *J. Mater. Chem. A* **2013**, *1*, 6291.

[48]   I. V. Kozhevnikov, *Chem. Rev.* **1998**, *98*, 171–198.

[49]   T. Minato, K. Suzuki, K. Kamata, N. Mizuno, *Chem. Eur. J.* **2014**, *20*, 5946–5952.

[50]   J. Iqbal, M. Barsukova-Stuckart, M. Ibrahim, S. U. Ali, A. A. Khan, U. Kortz, *Med. Chem. Res.* **2013**, *22*, 1224–1228.

[51]   S. G. Sarafianos, U. Kortz, M. T. Pope, M. J. Modak, *Biochem. J.* **1996**, *319 (2)*, 619.

[52]   R. Raza, A. Matin, S. Sarwar, M. Barsukova-Stuckart, M. Ibrahim, U. Kortz, J. Iqbal, *Dalton. Trans.* **2012**, *41*, 14329.

[53]   S.-Y. Lee, F. Amelie, W. Li, H. Theodor, K. Brylev, V. E. Fedorov, L. Joanna, A. Haider, H.-J. Pietzsch, H. Zimmermann, et al., *Biochem. Pharmacol.* **2015**, *93*, 171–181.

[54]   T. A. Steitz, *Angew. Chemie. Int. Ed.* **2010**, *49*, 4381–4398.

[55]   A. Bijelic, A. Rompel, *Acc. Chem. Res.* **2017**, *50*, 1441–1448.

[56]   A. Blazevic, A. Rompel, *Coord. Chem. Rev.* **2016**, *307*, 42–64.

CHAPTER 2. STATE OF THE ART

2.1 Bismuth-Containing POMs

POMs are formed when heteroatoms and addenda atoms condense to form derivatives of the same POM structure or completely new structural types due to the different modes of coordination of these atoms. Additionally, endless polyoxometalate variations have been reported where an electrophilic group such as a transition element is inserted into the otherwise very nucleophilic vacant sites of lacunary POMs. One of the research objectives of this dissertation was to explore the reaction of bismuth, a pentavalent post-transition metal with lacunary heteropolyanion precursors. The field of bismuth(III)-containing POMs remains largely unexplored because of the difficulty in the design and synthesis of bismuth(III)-containing POMs due to the steric effects of the lone pair and the large ionic radius (≥ 1 Å) of Bi^{3+}.[1] As a result not so many POMs incorporating Bi^{3+} have been reported. C. Xiaobing and coworkers classified Bi-containing POMs into four different categories based on the position of Bi^{3+} in the polyanion:[2]

1. <u>Bismuth in the primary heteroatom site.</u>

This class represents polyanions in which Bi^{3+} is a central (primary) heteroatom with a trigonal-bipyramidal coordination geometry such as $[B\text{-}\alpha\text{-}BiW_9O_{33}]^{9-}$ [3], $[H_3BiW_{18}O_{60}]^{6-}$ [4] and $[Bi_2W_{22}O_{74}(OH)_2]^{12-}$ [5]. The coordination geometry of Bi^{3+} in this case is three and the Bi-O bond lengths are in the range of 2.05(8) - 2.16(6) Å. Because of the presence of a lone pair of electrons in Bi^{3+}, the formation of a complete spherical structure is prevented.
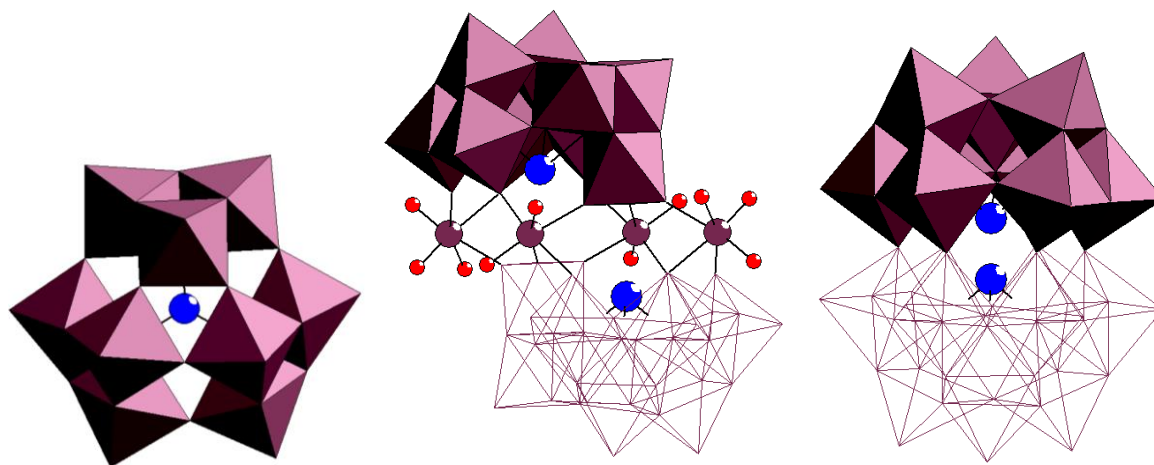
Figure 2.1. Combined polyhedral/ball-and-stick representation of $[B\text{-}\alpha\text{-}BiW_9O_{33}]^{9-}$ (left), $[Bi_2W_{22}O_{74}(OH)_2]^{12-}$ (middle) and $[H_3BiW_{18}O_{60}]^{6-}$ (right).[3-5] Colour code: WO6, dark-pink octahedra; W, dark-pink; Bi, blue; O, red.

2.   Bismuth as a Secondary Heteroatom

In this category, Bi^{3+} is a substituting atom that fills the vacant site that is left upon removal of some addenda atoms. The first example of heteropolyanions with Bi^{3+} as a secondary heteroatom was reported by J. Wang *et.al*. The two polyanions; $M_2Bi_2([B\text{-}\beta\text{-}MW_9O_{34})_2]^{14-}$ (M $= Co^{2+}, Zn^{2+}$) consist of two $[B\text{-}\beta\text{-}MW_9O_{34}]^{12-}$ subunits that are connected to each other by two M^{2+} and two Bi^{3+} ions in a coplanar fashion.[6] The Neumann group reported a nearly isostructural heteropolyanion; $[Bi_2Zn_2(\alpha\text{-}ZnW_9O_{34})_2]^{14-}$ where the trivacant fragments in the former example are based on $[\beta\text{-}MW_{12}O_{40}]^{6-}$ from which a non-rotated edge-shared triad is removed as compared to the latter where the edge shared triad is removed from $[\alpha\text{-}MW_{12}O_{40}]^{6-}$.[7] In both examples, the coordination number of Bi^{3+} is five and the Bi-O bond lengths are in the range of 2.061(2)- 2.289(2) Å for the three shorter bonds and 2.378(2) and 2.544(5) Å for the two longer Bi–O bonds.
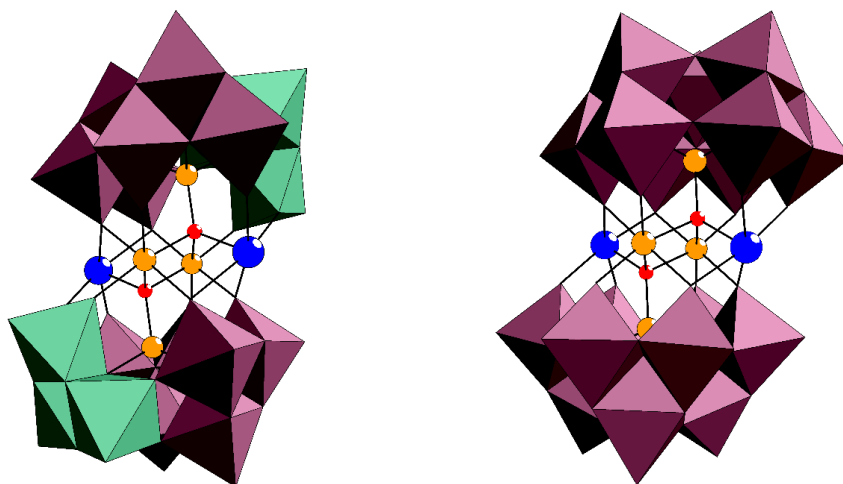
Figure 2.2. Combined polyhedral/ball-and-stick representation of $M_2Bi_2([B\text{-}\beta\text{-}MW_9O_{34})_2]^{14\text{-}}$ (M = Co^{2+}, Zn^{2+}) (left) and $[Bi_2Zn_2(\alpha\text{-}ZnW_9O_{34})_2]^{14\text{-}}$(right). [6-7] Colour code: WO_6 octahedra, green (rotated triads) and dark-pink; Bi, blue; M, orange; O, red.

Mizuno and co-workers reported three polyanions; consisting of two Bi^{3+} ions sandwiched by two $[A\text{-}\alpha\text{-}SiW_9O_{34}]^{10-}$ and $[\gamma\text{-}SiW_{10}O_{36}]^{8-}$ units; $([Bi_2(A\text{-}\alpha\text{-}SiW_9O_{32})_2(OAc)(H_2O)_2]^{7\text{-}}$ and $[Bi_2(\gamma\text{-}SiW_{10}O_{36})_2]^{10\text{-}}$ respectively) and a polyanion containing four Bi^{3+} ions that sandwich two $[\gamma\text{-}SiW_{10}O_{36}]^{8-}$ units; $[Bi_4O(\gamma\text{-}SiW_{10}O_{36})_2(OAc)]^{7\text{-}}$. In all three cases, the coordination number of Bi^{3+} is four and the Bi-O bond distances are in the range of 2.088(8) - 2.385(11) Å.[8]
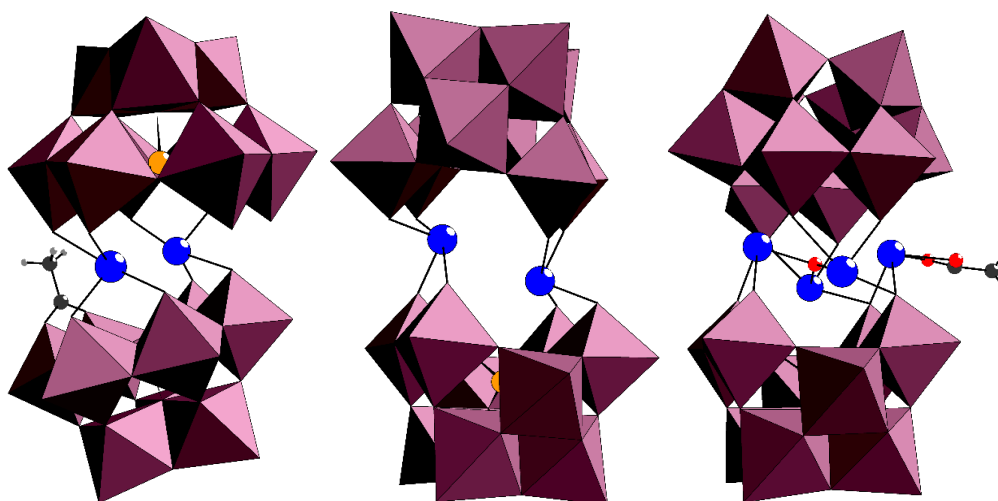
Figure 2.3. Combined polyhedral/ball-and-stick representation of $[Bi_2(A\text{-}\alpha\text{-}SiW_9O_{32})_2(OAc)(H_2O)_2]^{7\text{-}}$ (left), $[Bi_2(\gamma\text{-}SiW_{10}O_{36})_2]^{10\text{-}}$ (middle) and $[Bi_4O(\gamma\text{-}SiW_{10}O_{36})_2(OAc)]^{7\text{-}}$ (right). [8] Colour code: WO_6 octahedra, dark-pink; Bi, blue; Si, orange; C, black; O, red.

3.   Linking/ Bridging site

Bi^{3+} has also been reported to act as a linking (bridging) atom. In 1998 Villanneau *et al*. reported the first isopolyanion in which Bi^{3+} connects two monolacunary Lindqvist-type fragments which act as tetradentate ligands; $[Bi\{M_5O_{13}(OMe)_4(NO)\}_2]^{3-}$ (M = Mo, W). This resulted in an 8-coordinated Bi^{3+} ion with Bi-O bond distances of 2.42(1)-2.46(9) Å.[9] In 2010, aryldiazenido derivatives; $[Bi\{Mo_5O_{13}(OMe)_4(NNAr)\}_2]^{3-}$ (Ar = C_6F_5 and O_2N-*p*-C_6H_4) were reported where Bi-O distances range from 2.321(7) to 2.642(7) Å.[10]
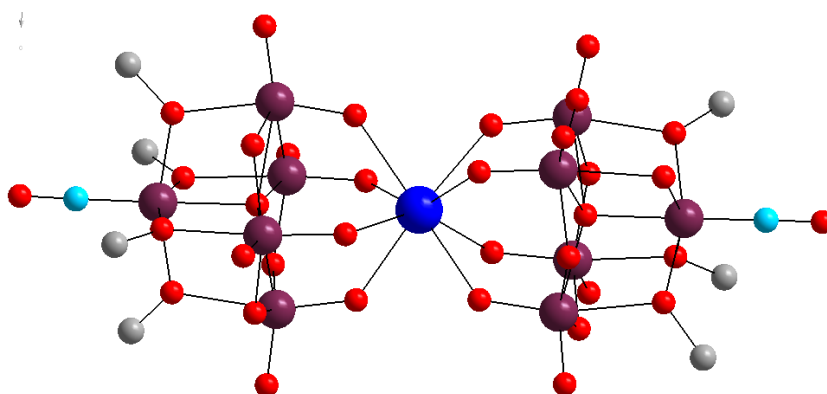
Figure 2.4. Ball-and-stick representation of $[Bi\{M_5O_{13}(OMe)_4(NO)\}_2]^{3-}$ (M = Mo, W).[9] Colour code: M, dark pink; Bi, blue; N, turquoise; C, grey; O, red.

In 2007, Xu and co-workers reported a novel 1D structure where Bi^{3+} connects paratungstate-B ions leading to a polymeric chain; $[Bi(H_2W_{12}O_{42})]^{7-}$. The coordination number of Bi^{3+} is four and Bi-O bond distances are in the range of 2.346(12)–2.518(15) A. [11]
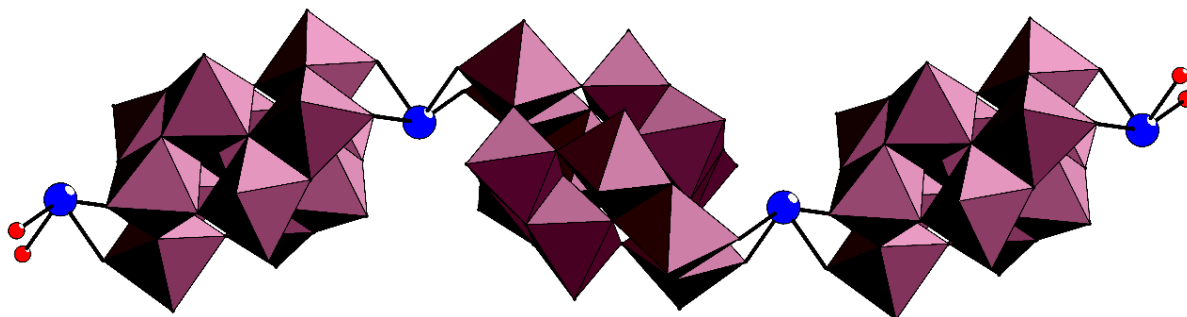
Figure 2.5. Combined polyhedral/ball-and-stick representation of $[Bi(H_2W_{12}O_{42})]^{7-}$.[11] Colour code: WO_6, dark-pink octahedra; Bi, blue; O, red.

4.   Grafted on addenda/ Capping

Bi^{3+} can be terminally grafted onto an addenda atom. Sokolov *et.al* reported a compound where Bi^{3+} is directly connected (grafted on) to $[HSiW_{12}O_{40}]^{3-}$, via one terminal oxo group of the POM unit. In the resulting neutral complex $[Bi(DMF)_7(HSiW_{12}O_{40})]$, Bi^{3+} is coordinated to seven molecules of DMF with an average Bi-O bond distance of 2.409(17) Å, and has a weak interaction with the terminal oxygen ligand of $[HSiW_{12}O_{40}]^{3-}$ (Bi-O distance of 2.851(3) Å), leading to a coordination number of 8. [12] Adonin *et.al* reported the decanuclear $[Mo_8O_{26}(BiX_3)_2]^{4-}$ (X = Cl, Br, I) anions where two {BiX_3}fragments coordinate β-$[Mo_8O_{26}]^{4-}$ anions, *via* two terminal oxygen atoms each resulting in a distorted square pyramidal coordination geometry of Bi^{3+} (coordination number of five, Bi-O distances of 2.58 - 2.65 Å) formed by two halides and by two oxygen atoms in the equatorial plane.[13]
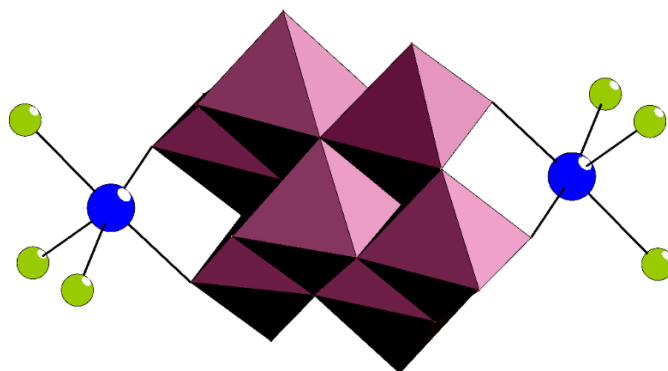
Figure 2.6. Combined polyhedral/ball-and-stick representation of $[Mo_8O_{26}(BiX_3)_2]^{4-}$ (X = Cl, Br, I).[13] Colour code: MoO_6, dark-pink octahedra; Bi, blue; X, lime.

Additional examples of Bi^{3+} acting as a capping atom are $[PMo_{12}O_{40}Bi_2(H_2O)_2]$ (Bi-O distances of 2.211(8)-2.730(8)Å)[2] and $[(Bi-(dmso)_3)_4V_{13}O_{40}]$ in which the Bi^{3+} centres adopt a tetrahedral geometry.[14]

5.   Bismuth encapsulated in a polyoxometalate host.

Bi^{3+} has been reported to replace Na^+ in the Pope-Jeannin-Preyssler ion; $[Na(H_2O)P_5W_{30}O_{110}]^{14-}$. In the resulting $[BiP_5W_{30}O_{110}]^{12-}$, the Bi^{3+} guest is located in the inner

(central) cavity, on the fivefold axis, but is shifted from the equatorial position towards the opening of the polyanion. The average Bi-O bond distance are 3.05 Å.[15]
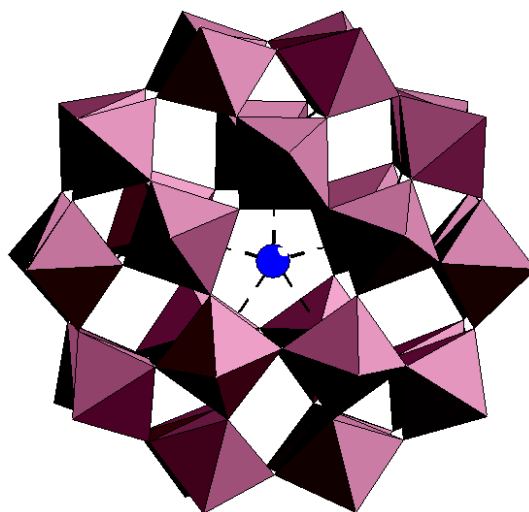
Figure 2.7. Combined polyhedral/ball-and-stick representation of $[BiP_5W_{30}O_{110}]^{12-}$.[15] Colour code: WO_6, dark-pink octahedra; Bi, blue.

In all the examples presented above, the trivalent Bi^{3+} ion assumes varied coordination geometries such as three, four, five and eight. However, an 8-coordinated Bi^{3+} ion in heteropolytungstate chemistry had never been reported until Mizuno et.al and our research group published several POMs with an 8-coordinated Bi^{3+} ion. [16-17]

2.2 Scandium-Containing POMs

For many decades, *d*-block metals have been incorporated into POMs generating a huge class of compounds with unique physicochemical properties. A commonly used approach in the synthesis of novel POMs has been to react *d*-block metals electrophiles with lacunary POM precursors which are excellent multidentate, inorganic, nucleophilic O-donor ligands. As a result, a large pool of transition-metal substituted POMs with diverse structures from monomeric to multimeric have been synthesized and characterized. Our research group has successfully incorporated many *3d*-transition metals such as Ti^{4+}, Cr^{3+}, $Mn^{2+/3+/4+}$, Fe^{3+}, Co^{2+}, Ni^{2+}, Cu^{2+} and Zn^{2+} into various lacunary POMs.[18-39] Interestingly Sc^{3+}-containing POMs have

rarely been incorporated into lacunary POMs due to the difficulty in crystallizing these compounds and the obvious high cost of scandium salts.[40] In 2010, two organo-soluble scandium containing POMs, isolated as white powders; $TBA_{5.5}K_{0.5}Na_{0.5}H_{0.5}[\alpha_1\text{-}Sc(H_2O)_4P_2W_{17}O_{61}]$ and $TBA_4[\alpha\text{-}Sc(H_2O)PW_{11}O_{39}]$ [41] were reported but the first crystal structure of a scandium-containing heteropolytungstate was first reported by J. Niu and co-workers in 2012. They presented a two-dimensional organic-inorganic hybrid structure; $\{[Cu(en)_2(H_2O)]_2[Cu(en)_2]_2[(\alpha\text{-}SiW_{11}O_{39})Sc(H_2O)]_2(C_2O_4)\}\cdot 8H_2O$ made by the hydrothermal reaction of monolacunary $[\alpha\text{-}SiW_{11}O_{39}]^{8-}$ with Sc^{3+} in the presence of mixed ligands of oxalate and ethylene diamine (en = ethylene diamine). The structure consists of an oxalate bridging two $\{Sc(H_2O)(\alpha\text{-}SiW_{11}O_{39})\}$ sub-units.[42]
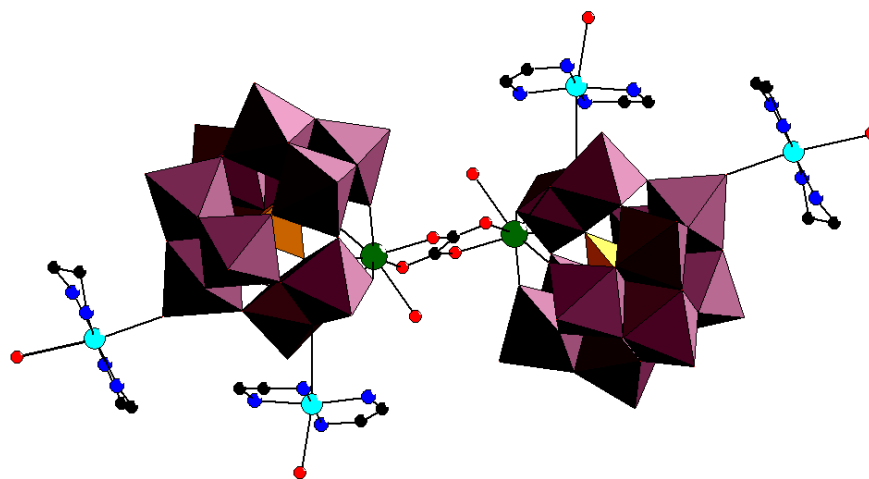
Figure 2.8. Combined polyhedral/ball-and-stick representation of $\{[Cu(en)_2(H_2O)]_2[Cu(en)_2]_2[(\alpha\text{-}SiW_{11}O_{39})Sc(H_2O)]_2(C_2O_4)\}$.[42] Colour code: WO_6, dark-pink octahedra; SiO_4, orange tetrahedra; Cu, turquoise; Sc, green; C, black; N, blue, O, red.

Since 2012, five Sc-containing POMs have been reported with varying nuclearity ranging from 4 to 11. In 2017, Zheng *et.al* reported $[Sc_4(H_2O)_{10}(B\text{-}\beta\text{-}SbW_9O_{33})_2]^{6-}$ and $[Sc_4(C_2O_4)_4(B\text{-}\beta\text{-}SbW_9O_{33})_2][Sc_4(H_2O)_2(C_2O_4)_4(B\text{-}\beta\text{-}SbW_9O_{33})_2]^{28-}$ synthesized by the reactions of $[B\text{-}\alpha\text{-}SbW_9O_{33}]^{9-}$ with Sc^{3+} under different reaction conditions. The resulting polyanions consist of two trivacant $[B\text{-}\beta\text{-}SbW_9O_{33}]^{9-}$ units which are connected by four Sc^{3+} ions forming a Krebs-

type polyoxoanion and an extended inorganic-organic hybrid based on two different types of tetra-scandium(III)-substituted POMs as building units, respectively. [43]
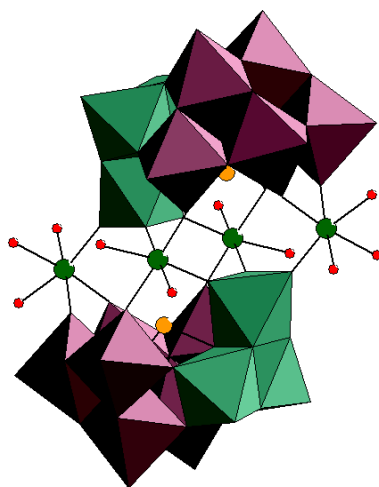
Figure 2.9. Combined polyhedral/ball-and-stick representation of $[Sc_4(H_2O)_{10}(B\text{-}\beta\text{-}SbW_9O_{33})_2]^{6-}$.[43] Colour code:$WO_6$, dark-pink and green (rotated triad) octahedra; Sc, green; Sb, orange; O, red.
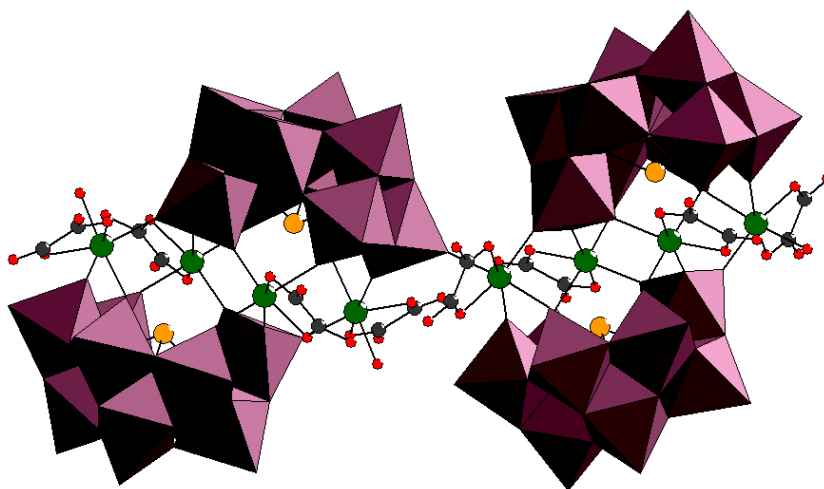
Figure 2.10. Combined polyhedral/ball-and-stick representation of $[Sc_4(C_2O_4)_4(B\text{-}\beta\text{-}SbW_9O_{33})_2][Sc_4(H_2O)_2(C_2O_4)_4(B\text{-}\beta\text{-}SbW_9O_{33})_2]^{28-}$.[43] Colour code: WO_6, dark-pink octahedra; Sc, green; Sb, orange; O, red; C, black.

Later in 2017, Zheng *et.al* reported the first series of hexameric scandium-containing POMs namely, undeca-Sc^{3+}-containing $[Sc_{11}W_6O_{20}(OH)_2(H_2O)_{16}(SbW_9O_{33})_6]^{27-}$, hepta-$Sc^{3+}$-containing $[Sc_7Sb_2W_6O_{20}(H_2O)_8(SbW_9O_{33})_6]^{31-}$ and hexa-Sc^{3+}-containing $[Sc_6Sb_2W_6O_{19}(H_2O)_6(SbW_9O_{33})_6]^{32-}$. $[Sc_{11}W_6O_{20}(OH)_2(H_2O)_{16}(SbW_9O_{33})_6]^{27-}$ is the largest

scandium containing polyoxometalate to date [40]
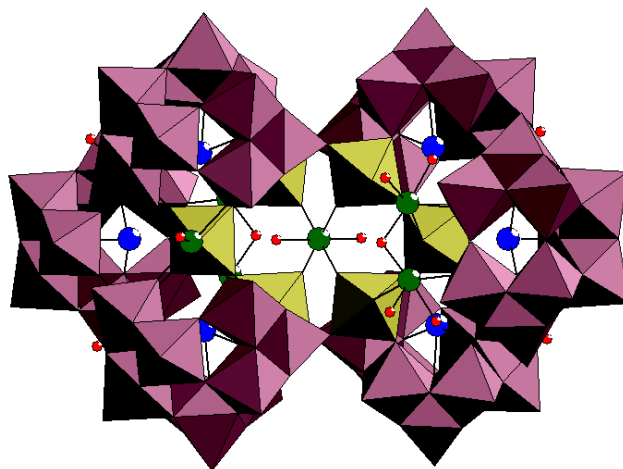
Figure 2.11. Combined polyhedral/ball-and-stick representation of $[Sc_{11}W_6O_{20}(OH)_2(H_2O)_{16}(SbW_9O_{33})_6]^{27-}$.[40] Colour code: WO_6, dark-pink and lime green octahedra; Bi, blue; Sb, orange; Sc, green; O, red.

In 2020, Zhengguo. and co-workers reported three novel scandium-containing heteropolytungstates $[Sc_3(H_2O)_3NO_3(PW_9O_{34})_2]^{10-}$, $[Sc_8(H_2O)_2(GeW_9O_{34})_2(GeW_6O_{26})_2]^{12-}$ and $[Sc_{11}(W_6O_{10})_2(OH)_2(H_2O)_{16}(BiW_9O_{33})_6]^{27-}$ which were synthesized by reactions of Sc^{3+} ions with trilacunary Keggin precursors, $[A\text{-}\alpha\text{-}XW_9O_{34}]^{n-}$ (X = P, Ge, n = 9, 10 respectively) and $[B\text{-}\alpha\text{-}BiW_9O_{33}]^{9-}$, in a NaOAc/HOAc buffer solution.[44]
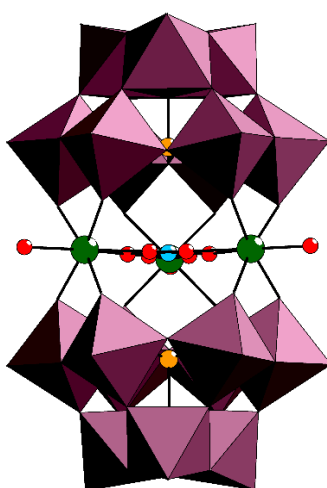
Figure 2.12. Combined polyhedral/ball-and-stick representation of $[Sc_3(H_2O)_3NO_3(PW_9O_{34})_2]^{10-}$.[44] Colour code: WO_6, dark-pink octahedra; P, orange; Sc, green; O, red; N, light blue.

In polyoxopalladate chemistry, Sc^{3+} has been incorporated in the centre of the nanocube to form;

$[Sc^{III}O_8Pd^{II}_{12}(PhAs^VO_3)_8]^{5-}$.[45]
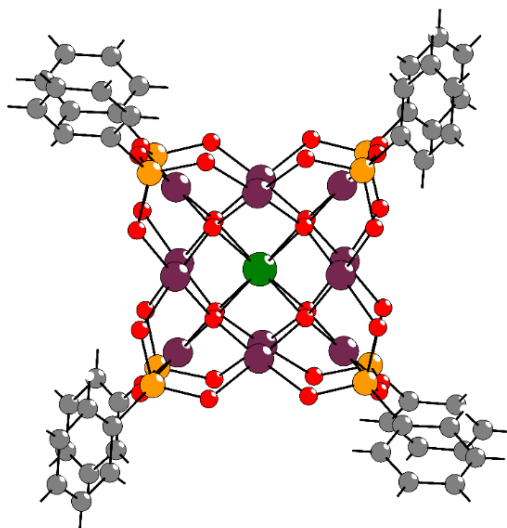
Figure 2.13. Ball-and-stick representation of $[ScO_8Pd^{II}_{12}(PhAs^VO_3)_8]^{5-}$.[45] Colour code: Pd, dark-pink; As, orange; Sc, green; O, red; C, grey.

The existing scandium(III)-containing heteropolytungstates are derived from a few lacunary POM ($[Li(\alpha_1\text{-}P_2W_{17}O_{61})]^{9-}$, $[\alpha\text{-}PW_{11}O_{39}]^{7-}$, $[A\text{-}\alpha\text{-}PW_9O_{34}]^{9-}$, $[\alpha\text{-}SiW_{11}O_{39}]^{8-}$, $[B\text{-}\alpha\text{-}BiW_9O_{33}]^{9-}$ and $[B\text{-}\alpha\text{-}SbW_9O_{33}]^{9-}$). Because of the limited library of scandium(III)-containing metal oxo clusters, we were inspired to investigate the reactions of Sc^{3+} with other POM precursors one of which was the trilacunary $[\alpha\text{-}P_2W_{15}O_{56}]^{12-}$ whose reactions with various transition metal ions such as Cu^{2+}, Co^{2+}, Zn^{2+}, Ni^{2+}, Tl^{3+}, Mn^{2+}, Cd^{2+}, Fe^{2+}, Fe^{3+} and Ti^{4+} have been extensively explored. [46-57]

2.3 Lead-Containing POMs

Even though POM chemistry has advanced greatly since the 19th century, there remains some areas that are still poorly explored. After publishing four bismuth-containing heteropolytungstates, we were inspired to explore the reactivity of Pb^{2+} with heteropolytungstates since this ion is isostructural to Bi^{3+} and lead(II)-containing POMs are extremely rare, especially ones derived from lacunary POM precursors.

The first structural characterization of a Pb(II)- containing POM, K$_7$[PbGaW$_{11}$O$_{39}$]·16H$_2$O, was described by Tourné *et al.* in 1982. The structure is a monolacunary tungstogallate based on the Keggin structure. The Pb^{2+} ion occupies the vacant site that would otherwise be occupied by a W-O unit in a plenary Keggin structure. The resulting coordination number of Pb^{2+} is four with Pb-O distances of 2.37 - 3.11 Å. [58] A year later, Tourné and co-workers reported [PbPW$_{11}$O$_{39}$]$^{5-}$ which was only characterized by two-dimensional ^{183}W NMR (COSY and 2D INADEQUATE). The crystal structure of this polyanion is still unknown but is assumed to be the same as [PbGaW$_{11}$O$_{39}$]$^{7-}$.[59]
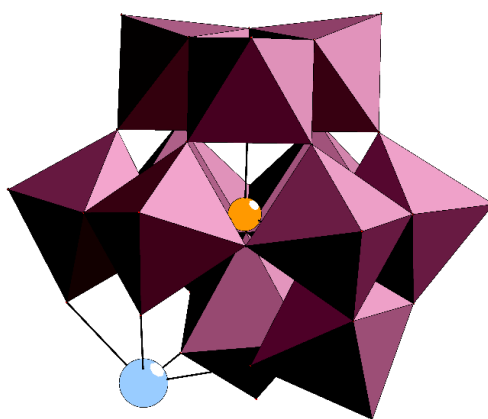
Figure 2.14. Combined polyhedral/ball-and-stick representation of [PbGaW$_{11}$O$_{39}$]$^{7-}$.[58] Colour code: WO$_6$ octahedra, dark-pink; Pb, light blue; Ga, orange; O, red.

In 2009 the second lead(II)-containing POM structure was reported by Mizuno and co-workers. [Pb(γ-SiW$_{10}$O$_{32}$)$_2$(μ-O)$_4$]$^{6-}$ is a derivative of the "inorganic cryptand" [(γ-SiW$_{10}$O$_{32}$)$_2$(μ-O)$_4$]$^{8-}$.

The dimeric γ-Keggin structure consists of one Pb^{2+} ion encapsulated by two $[(\gamma\text{-}SiW_{10}O_{32})_2(\mu\text{-}O)_4]^{8-}$ where Pb^{2+} has a coordination number of 10 and the Pb-O distances range from 2.67-2.90 Å. The position of Pb^{2+} deviates from the centre and the Pb^{2+} ion is positioned at one of two disordered sites.[60]
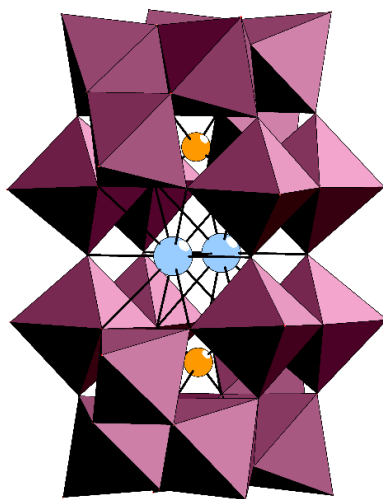
Figure 2.15. Polyhedral/Ball-and-stick representation of $[Pb(\gamma\text{-}SiW_{10}O_{32})_2(\mu\text{-}O)_4]^{6-}$ showing the two disordered positions of Pb^{2+}.[59] Colour code: WO_6, dark-pink octahedra; Pb, light blue; Si, orange; O, red.

Since then, there have not been any POMs reported that are based on lacunary POM species. However, in 2016 Sokolov and co-workers presented two novel complexes based on Pb^{2+} and the non-lacunary Keggin-type $[SiW_{12}O_{40}]^{4-}$ anion; $\{Pb_2(\mu_2\text{-}DMF)_2(DMF)_8(SiW_{12}O_{40})\}$ and $\{Pb_2(\mu_2\text{-}DMF)_2(DMF)_8(SiW_{12}O_{40})\}\cdot DMF$ as well as the Wells–Dawson anion $[P_2W_{18}O_{62}]^{6-}$; $\{(Pb(\mu_2\text{-}DMF)_3(DMF)_6)(Pb(DMF)_6)(P_2W_{18}O_{62})\}$. $\{Pb_2(\mu_2\text{-}DMF)_2(DMF)_8(SiW_{12}O_{40})\}$ can be described as an infinite chain of $[SiW_{12}O_{40}]^{4-}$ anions and Pb^{2+} cations where the Pb atoms form dimers *via* two bridging DMF molecules and two oxygen ligands of the terminal of Keggin anions which are also bridged between two lead atoms.

The coordination spheres of each Pb atom are completed by four DMF molecules resulting in a coordination number of 8. In $\{Pb_2(\mu_2\text{-}DMF)_2(DMF)_8(SiW_{12}O_{40})\}\cdot DMF$, Pb^{2+} and Keggin

anions form a chain structure in which the Pb^{2+} ions are connected to the dimers through two DMF molecules and its coordination sphere is completed by four terminal DMF molecules and a terminal oxo ligand of the Keggin anion resulting in a coordination number of 7. In $\{(Pb(\mu_2\text{-}DMF)_3(DMF)_6)(Pb(DMF)_6)(P_2W_{18}O_{62})\}$, the Dawson anion is connected to 6 Pb atoms of two different types. Two Pb^{2+} ions form a dimeric unit $[(DMF)_3Pb(\mu\text{-}DMF)_3Pb(DMF)_3]^{4+}$ which coordinates to the belt part of the polyanion resulting in a coordination number of 8. One Pb^{2+} ion is connected with the polyanion *via* one of the terminal O atoms of the capping face (W_3O_{13}), and 5 DMF molecules resulting in a coordination number of 6. The Pb-O distances range from 2.810 Å- 2.889 Å [61]

In 2018 Haitao Yu et.al reported four hybrids; $[M(P_4Mo^V_6O_{31})_2]^{n-}$; $[PbMn(H_2O)_2]_2H_2\{Mn[Mo_6O_{12}(OH)_3(HPO_4)_3(PO_4)]_2\}_2{}^{10-}$ Each $\{M(P_4Mo_6)_2\}$ cluster is covalently bound to four $[PbM(H_2O)_2]^{4+}$ fragments by sharing the oxygen atoms. In turn, each $[PbM(H_2O)_2]^{4+}$ fragment bridges four $\{M(P_4Mo_6)_2\}$ clusters. Pb-O bond lengths range from 2.361(4) Å - 2.855(3) Å and the resulting coordination number of Pb^{2+} is 6.[62]

In 2019, Yuguang, Lu et.al reported $[Pb(DMF)_7]_2[SiW_{12}O_{40}]$ and $[Pb(DMF)_4(H_2O)_2][Pb_2(\mu_2\text{-}DMF)_2(DMF)_8][PW_{12}O_{40}]_2$ where the former is composed of Pb-DMF complex and Keggin-type $[SiW_{12}O_{40}]^{4-}$polyoxoanion, in which the Pb^{2+}coordinates to the polyoxoanion by different Pb-O bonds, while the latter is composed of $[Pb(DMF)_4(H_2O)_2]^{2+}$, dimeric $[Pb_2(\mu_2\text{-}DMF)_2(DMF)_8]^{4+}$ cations, and two kinds of Keggin-type $[PW_{12}O_{40}]^{2-}$ polyoxoanions resulting in a coordination number of 8 in both compounds.[63]

Since 2009, no lead(II)-containing-POM based on lacunary Keggin and Wells-Dawson heteropolytungstates have been reported, however the handful of compounds known show that Pb^{2+} can have diverse coordination numbers ranging from 4 to 10.

2.4 References

[1]   T. Hanaya, K. Suzuki, R. Sato, K. Yamaguchi, N. Mizuno, *Dalton. Trans.* **2017**, *46*, 7384–7387.

[2]   J. Song, J. Wang, Z. Ruisha, C. Xiaobing, *Chem. Res. Chin. Univ* **2017**, *33*, 333–338.

[3]   B. Botar, T. Yamase, E. Ishikawa, *Inorg. Chem. Commun.* **2000**, *3*, 579–584.

[4]   Y. Ozawa, Y. Sasaki, *Chem. Lett.* **1987**, *16*, 923–926.

[5]   I. Loose, E. Droste, M. Bösing, H. Pohlmann, M. H. Dickman, C. Rosu, M. T. Pope, B. Krebs, *Inorg. Chem.* **1999**, *38*, 2688–2694.

[6]   Y. Liu, B. Liu, G. Xue, H. Hu, F. Fu, J. Wang, *Dalton. Trans.* **2007**, *0*, 3634.

[7]   S. R. Amanchi, A. M. Khenkin, Y. Diskin-Posner, R. Neumann, *ACS Catal.* **2015**, *5*, 3336–3341.

[8]   T. Hanaya, K. Suzuki, R. Sato, K. Yamaguchi, N. Mizuno, *Dalton. Trans.* **2017**, *46*, 7384–7387.

[9]   R. Villanneau, A. Proust, F. Robert, P. Gouzerh, *J. Chem. Soc. Dalton. Trans.* **1999**, 421–426.

[10]   C. Bustos, D. M. L. Carey, K. Boubekeur, R. Thouvenot, A. Proust, P. Gouzerh, *Inorg. Chim. Acta* **2010**, *363*, 4262–4268.

[11]   Z. H. Xu, X. L. Wang, Y. G. Li, E. B. Wang, C. Qin, Y. L. Si, *Inorg. Chem. Commun.* **2007**, *10*, 276–278.

[12]   A. A. Mukhacheva, S. A. Adonin, P. A. Abramov, M. N. Sokolov, *Polyhedron.* **2018**, *141*, 393–397.

[13]   S. A. Adonin, E. V. Peresypkina, M. N. Sokolov, I. V. Korolkov, V. P. Fedin, *Inorg. Chem.* **2014**, *53*, 6886–6892.

[14]   J. Tucher, L. C. Nye, I. Ivanovic-Burmazovic, A. Notarnicola, C. Streb, *Chem. Eur. J.* **2012**, *18*, 10949–10953.

[15]   A. Hayashi, T. Haioka, K. Takahashi, B. S. Bassil, U. Kortz, T. Sano, M. Sadakane, *Z. Anorg. Allg. Chem.* **2015**, *641*, 2670−2676.

[16]   M. N. K. Wihadi, A. Hayashi, K. Ichihashi, H. Ota, S. Nishihara, K. Inoue, N. Tsunoji, T. Sano, M. Sadakane, *Eur. J. Inorg. Chem.* **2019**, 357–362.

[17]   N. Ncube, S. Bhattacharya, D. Thiam, J. Goura, A. S. Mougharbel, U. Kortz, *Eur. J. Inorg. Chem.* **2019**, 363–366.

[18]   K. Y. Wang, B. S. Bassil, X. Xing, B. Keita, J. K. Bindra, K. Diefenbach, N. S. Dalal, U. Kortz, *Eur. J. Inorg. Chem.* **2016**, 5519–5529.

[19]   K. Y. Wang, Z. Lin, B. S. Bassil, X. Xing, A. Haider, B. Keita, G. Zhang, C. Silvestru, U. Kortz, *Inorg. Chem.* **2015**, *54*, 10530–10532.

[20]   F. Hussain, B. S. Bassil, U. Kortz, O. A. Kholdeeva, M. N. Timofeeva, P. De Oliveira, B. Keita, L. Nadjo, *Chem. Eur. J.* **2007**, *13*, 4733–4742.

[21]   K.-Y. Wang, B. S. Bassil, Z.-G. Lin, A. Haider, J. Cao, H. Stephan, K. Viehweger, U. Kortz, *Dalton. Trans.* **2014**, *43*, 16143–16146.

[22]   G. Al-Kadamany, B. S. Bassil, F. Raad, U. Kortz, *J. Clust. Sci.* **2014**, *25*, 867–878.

[23]   G. A. Al-Kadamany, F. Hussain, S. S. Mal, M. H. Dickman, N. Leclerc-Laronze, J. Marrot, E. Cadot, U. Kortz, *Inorg. Chem.* **2008**, *47*, 8574–8576.

[24]   W. Liu, R. Al-Oweini, K. Meadows, B. S. Bassil, Z. Lin, J. H. Christian, N. S. Dalal, A. M. Bossoh, I. M. Mbomekallé, P. De Oliveira, J. Iqbal, U.Kortz, *Inorg. Chem.* **2016**, *55*, 10936–10946.

[25]   W. Liu, J. H. Christian, R. Al-Oweini, B. S. Bassil, J. Van Tol, M. Atanasov, F. Neese, N. S. Dalal, U. Kortz, *Inorg. Chem.* **2014**, *53*, 9274–9283.

[26]   W. Liu, Z. Lin, B. S. Bassil, R. Al-Oweini, U. Kortz, *Chim. Int. J. Chem.* **2015**, *69*, 537–540.

[27]   B. S. Bassil, M. H. Dickman, M. Reicke, U. Kortz, B. Keita, L. Nadjo, *J. Chem. Soc.*

Dalton. Trans. **2006**, 4253–4259.

[28]   R. Al-Oweini, B. S. Bassil, T. Palden, B. Keita, Y. Lan, A. K. Powell, U. Kortz, *Polyhedron.* **2013**, *52*, 461–466.

[29]   R. Al-Oweini, B. S. Bassil, M. Itani, D. B. Emiroğlu, U. Kortz, *Acta Cryst. Sect. C Struct. Chem.* **2018**, *74*, 1390–1394.

[30]   A. Haider, M. Ibrahim, B. S. Bassil, A. M. Carey, A. N. Viet, X. Xing, W. W. Ayass, J. F. Miñambres, R. Liu, G. Zhang, B Keita, W. Li, G. E. Kostakis, A. K. Powell, U. Kortz, *Inorg. Chem.* **2016**, *55*, 2755–2764.

[31]   R. Al-Oweini, B. S. Bassil, J. Friedl, V. Kottisch, M. Ibrahim, M. Asano, B. Keita, G. Novitchi, Y. Lan, A. Powell, U.Stimming, U. Kortz, *Inorg. Chem.* **2014**, *53*, 5663–5673.

[32]   B. S. Bassil, M. Ibrahim, R. Al-Oweini, M. Asano, Z. Wang, J. Van Tol, N. S. Dalal, K. Y. Choi, R. Ngo Biboum, B. Keita, U. Kortz, *Angew. Chem. Int. Ed.* **2011**, *50*, 5961–5964.

[33]   N. H. Nsouli, A. H. Ismail, I. S. Helgadottir, M. H. Diekman, J. M. Clemente-Juan, U. Kortz, *Inorg. Chem.* **2009**, *48*, 5884–5890.

[34]   U. Kortz, S. Nellutla, A. C. Stowe, N. S. Dalal, U. Rauwald, W. Danquah, D. Ravot, *Inorg. Chem.* **2004**, *43*, 2308–2317.

[35]   U. Kortz, S. Isber, M. H. Dickman, D. Ravot, *Inorg. Chem.* **2000**, *39*, 2915–2922.

[36]   U. Kortz, M. G. Savelieff, B. S. Bassil, M. H. Dickman, *Angew. Chem. Int. Ed.* **2001**, *40*, 3384–3386.

[37]   U. Kortz, S. Matta, *Inorg. Chem.* **2001**, *40*, 815–817.

[38]   I. V. Kalinina, N. V. Izarova, U. Kortz, *Inorg. Chem.* **2012**, *51*, 7442–7444.

[39]   A. H. Ismail, B. S. Bassil, G. H. Yassin, B. Keita, U. Kortz, *Chem. Eur. J.* **2012**, *18*, 6163–6166.

[40]   Z.-W. Cai, T. Yang, Y.-J. Qi, X.-X. Li, S.-T. Zheng, *Dalton. Trans.* **2017**, *46*, 6848–

6852.

[41]　N. Dupré, P. Rémy, K. Micoine, C. Boglio, S. Thorimbert, E. Lacôte, B. Hasenknopf, M. Malacria, *Chem. Eur. J.* **2010**, *16*, 7256–7264.

[42]　D. Zhang, S. Zhang, P. Ma, J. Wang, J. Niu, *Inorg. Chem. Commun.* **2012**, *20*, 191–195.

[43]　Z. W. Cai, B. X. Liu, T. Yang, X. X. Li, S. T. Zheng, *Inorg. Chem. Commun.* **2017**, *80*, 1–5.

[44]　W. Zhang, Z. Lin, Y. Chi, J. Hong, L. Yan, C. Hu, *Chem. Res. Chinese Univ.* **2020**, 1–7.

[45]　M. Barsukova-Stuckart, N. V. Izarova, R. A. Barrett, Z. Wang, J. Van Tol, H. W. Kroto, N. S. Dalal, P. Jiménez-Lozano, J. J. Carbó, J. M. Poblet, M. S. von Gernler, T. Drewello, P. de Oliviera, B. Keita, U. Kortz, *Inorg. Chem.* **2012**, *51*, 13214–13228.

[46]　R. G. Finke, M. W. Droege, P. J. Domaille, *Inorg. Chem.* **1987**, *26*, 3886–3896.

[47]　T. J. R. Weakley, R. G. Finke, *Inorg. Chem.* **1990**, *29*, 1235–1241.

[48]　U. Kortz, S. S. Hamzeh, N. A. Nasser, *Chem. Eur. J.* **2003**, *9*, 2945–2952.

[49]　B. Keita, I. M. Mbomekalle, L. Nadjo, T. M. Anderson, C. L. Hill, *Inorg. Chem.* **2004**, *43*, 3257–3263.

[50]　D. Schaming, J. Canny, K. Boubekeur, R. Thouvenot, L. Ruhlmann, *Eur. J. Inorg. Chem.* **2009**, 5004–5009.

[51]　W. W. Ayass, T. Fodor, E. Farkas, Z. Lin, H. M. Qasim, S. Bhattacharya, A. S. Mougharbel, K. Abdallah, M. S. Ullrich, S. Zaib, J. Iqbal, S. Haragi, G. Szalontai, I. Banyai, L. Zekany, I. Toth, U. Kortz, *Inorg. Chem.* **2018**, *57*, 7168–7179.

[52]　C. J. Gómez-García, J. J. Borrás-Almenar, E. Coronado, L. Ouahab, *Inorg. Chem.* **1994**, *33*, 4016–4022.

[53]　J. F. Kirby, L. C. W. Baker, *J. Am. Chem. Soc.* **1995**, *117*, 10010–10016.

[54]　X. Zhang, Q. Chen, D. C. Duncan, C. F. Campana, C. L. Hill, *Inorg. Chem.* **1997**, *36*,

4208–4215.

[55]   X. Zhang, T. M. Anderson, Q. Chen, C. L. Hill, *Inorg. Chem.* **2001**, *40*, 418–419.

[56]   T. M. Anderson, K. I. Hardcastle, N. Okun, C. L. Hill, *Inorg. Chem.* **2001**, *40*, 6418–
        6425.

[57]   L. Ruhlmann, J. Canny, R. Contant, R. Thouvenot, *Inorg. Chem.* **2002**, *41*, 3811–3819.

[58]   G. F. Tourné, C. M. Tourné, A. Schouten, *Acta Cryst. Sect. B Struct. Cryst. Chem.* **1982**,
        38, 1414–1418.

[59]   C. Brevard, R. Schimpf, G. Tourné, C. M. Tourné, *J. Am. Chem. Soc*. **1983**, *105*, 7059-
        7063.

[60]   A. Yoshida, Y. Nakagawa, K. Uehara, S. Hikichi, N. Mizuno, *Angew. Chem.* **2009**, *121*,
        7189–7192.

[61]   L. I. Udalova, S. A. Adonin, P. A. Abramov, I. V. Korolkov, A. S. Yunoshev, P. E.
        Plyusnin, M. N. Sokolov, *New. J. Chem.* **2016**, *40*, 9981–9985.

[62]   Z. Han, X. Xin, R. Zheng, H. Yu, *Dalton. Trans.* **2018**, *47*, 3356–3365.

[63]   T. Pang, Z. Zhou, D. Li, H. Liu, Z. Zhang, L. Qi, C. Y. Song, G. G. Gao, Y. Lv, *Cryst.
        Res. Technol.* **2019**, *54*, 1900153.

CHAPTER 3. EXPERIMENTAL SECTION

3.1 Instrumentation

All reagents were purchased from commercial sources and used without further purification. Several Sc^{3+} salts with different waters of crystallization and from different commercial sources (and an unknown Chinese source) were used over the course of three years. (see pictures below).

The synthesized compounds were characterized by FT-IR spectroscopy, single crystal X-ray diffraction (XRD), thermogravimetric analysis (TGA), multinuclear NMR spectroscopy and elemental analysis.

3.1.1   Single-Crystal X-Ray Diffraction (XRD)

Single Crystal XRD is one of the most important method for the full determination of structures in POM chemistry. Crystal data of all polyanions were collected on a Bruker Kappa X8 APEX CCD single-crystal diffractometer equipped with a sealed Mo tube and a graphite monochromater ($\lambda_\alpha = 0.71073$ Å). The crystals were mounted in Hampton cryoloops using light oil for data collection at 173 or 100 K or on a glass fibre using glue for data collection at room temperature. The *SHELX* software package (Bruker) was used to solve and refine the structures.[1] An empirical absorption correction was applied using the *SADABS* program (G. M. Sheldrick, *SADABS, Program for empirical X-ray absorption correction*, Bruker-Nonius,

1990). The structures were solved by direct methods and refined by the full-matrix least-squares

method $(\sum w(F_o^2 - F_c^2)^2)$ with anisotropic thermal parameters for all atoms included in the

model. The H atoms of the crystal waters were not allocated.

3.1.2   Fourier Transform Infrared (FT-IR) Spectroscopy

FT-Infrared is a useful technique for compounds in the solid state. Besides the identification of

a fingerprint or characteristic region of a compound, IR allows for the identification of typical

metal-oxygen vibrational absorption bands for POMs. IR spectra of compounds reported were

recorded on KBr disk using a Nicolet-Avatar 370 spectrometer between 400 and 4000 cm^{-1}.

3.1.3   Thermogravimetric and Elemental Analyses

Thermogravimetry provides information regarding thermal stability of compounds and in POM

chemistry it allows for the determination of crystal water molecules as well as some loosely

bound and covalently bound molecules. Measurements were carried out on a TA Instruments

SDT Q600 thermobalance under nitrogen flow. The temperature was ramped from 20 to 600

°C at a rate of 20 °C min^{-1}.

Elemental analysis was used to determine the elemental composition of compounds and is a

useful technique for proving the bulk purity of POMs. The analyses were performed at CNRS,

Service Central d'Analyze, Solaize, France; and at Analytische Laboratorien Prof. Dr. H.

Malissa und G. Reuter GmbH, 51789 Lindlar Germany.

3.1.4   Nuclear Magnetic Resonance (NMR) Spectroscopy

NMR is the most powerful spectroscopic method for the determination of POM structures in

solution. We are also able to ascertain their solution stability by measuring the NMR spectra

over a long period. The NMR spectra of several obtained compounds were recorded in different

solvents on a 400 MHz JEOL ECX instrument at room temperature using 5 mm tubes for ^{31}P

and 10 mm tubes for ^{183}W. The respective resonance frequencies were 162.14 MHz (^{31}P) and

16.69 MHz (^{183}W). The chemical shifts are reported with respect to the references 85% H_3PO_4

(^{31}P) and 1M Na_2WO_4 (^{183}W).

3.1.5   Bond Valence Sum (BVS) Calculations

To determine the oxidation states of the ions, bond valence sum (BVS) calculations were

performed using $\log \frac{(r_0 - r)}{0.37}$ where r_0 is a tabulated parameter expressing the (ideal) bond length

when the element has a valence of 1and r is the actual bond length.[2]

3.2 Synthesis of POM Precursors

3.2.1   Na$_9$ [B-α-AsW$_9$O$_{33}$]·27H$_2$O

As_2O_3 (11 g, 0.056 mol) was added to a hot solution of $Na_2WO_4 \cdot 2H_2O$ (330 g, 1.0 mol) in 350

ml water. 83 ml 11M HCl was added to the reaction mixture over a period of 2 minutes and the

resulting solution heated at 95°C for 10 min and then transferred to a beaker. The product

crystallized overnight and was collected and air dried.[3]

3.2.2   Na$_9$[A-α-AsW$_9$O$_{34}$]·18H$_2$O

To a solution of $Na_2WO_4 \cdot 2H_2O$ (45 g, 136 mmol) in H_2O (40 ml), $Na_2HAsO_4 \cdot 7H_2O$ (4.7 g, 15

mmol) and 8.7 mL of pure acetic acid were successively added. The solid which precipitated

gradually was filtered, washed with ethanol and air-dried with aspiration.[4]

3.2.3   K$_{10}$[α_2-As$_2$W$_{17}$O$_{61}$]·21H$_2$O

To a solution of $K_6[As_2W_{18}O_{62}] \cdot 14H_2O$ (11.85 g, 0.8 mmol) in H_2O (36 ml) was added $KHCO_3$

(36 ml, 36 mmol). The resulting solution was stirred for 40 minutes after which the formed

precipitate was filtered and redissolved in 50 ml of hot water (~ 80°C). A white precipitate

appeared upon cooling to room temperature which was filtered and air-dried.[5]

3.2.4   Na$_9$[B-α-BiW$_9$O$_{33}$]·16H$_2$O

A solution of $Bi(NO_3)_3 \cdot 5H_2O$ (6.5 g, 13.4 mmol) dissolved in 10 ml HCl (6M) was added in

small portions to a hot solution (80ºC) of $Na_2WO_4 \cdot 2H_2O$ (40 g, 121 mmol) in 80 ml H_2O. The

mixture was heated at 80ºC for 1 h and then filtered off. Colourless crystals were obtained upon cooling at room temperature. [6]

3.2.5 $K_8Na_2[A\text{-}\alpha\text{-}GeW_9O_{34}]\cdot25H_2O$

$K_6Na_2[GeW_{11}O_{39}]\cdot13H_2O$ [7] (43.5g, 13.5 mmol) was dissolved in 400 ml H_2O. Then to this solution was added solid anhydrous K_2CO_3 (22.5g, 162.8 mmol) in small portions. After stirring for about 30 min. (pH~ 9.5), a white precipitate appeared slowly. After an additional 20 min. of stirring, the white solid product was collected on a sintered glass frit, washed with 20 ml of saturated KCl solution and air-dried.[8]

3.2.6 $K_6Na_2[\alpha\text{-}GeW_{11}O_{39}]\cdot13H_2O$

GeO_2 (2.092 g, 0.02 mol) was dissolved in a 1M NaOH solution (40ml). An aqueous solution containing $Na_2WO_4\cdot2H_2O$ (72.6 g, 0.22 mol) in 120 mL of water was added to the first solution. The resulting mixture was stirred and heated. Then 80ml of 4M HCl was added dropwise to the hot solution with vigorous stirring. The solution was boiled for about 1 hour and cooled to room temperature. A white precipitate appeared upon adding of 30 g of solid KCl. The precipitate was filtered and redissolved in hot water and then the solution was kept at room temperature for crystallization. [7]

3.2.7 $K_8[\beta_2\text{-}GeW_{11}O_{39}]\cdot14H_2O$

GeO_2 (5.4 g, 0.052 mol) was dissolved in 100 ml of water (solution A). Then, $Na_2WO_4\cdot2H_2O$ (182 g, 0.552mol) was dissolved in 300 ml of water in a separate beaker (solution B). To this solution, 165 mL of 4 M HCl was added with vigorous stirring in small portions over 15 min. Then, solution A was poured into the tungstate solution (solution B), and the pH adjusted to between 5.2 and 5.8 by addition of 4 M HCl solution (40 ml). This pH was maintained for 100 min by the addition of HCl solution. Then, 90 g of solid KCl was added with gentle stirring. After 15min, the precipitate was collected by filtration on a sintered glass filter. [9]

3.2.8   Na$_9$[A-α-PW$_9$O$_{34}$]·13H$_2$O

A mixture of Na$_2$WO$_4$·2H$_2$O (120g, 0.36 mol) and 150g of water was stirred in a 300 mL beaker with a magnetic stirring bar until the solid was completely dissolved. Phosphoric acid (85%) was added dropwise with stirring (4.0 mL, 0.06 mol). After addition of the acid was complete, the measured pH was 8.9 to 9.0. Glacial acetic acid (22.5 mL, 0.40 mol) was added dropwise with vigorous stirring. Large quantities of white precipitate formed during the addition. The final pH of the solution was 7.50. The solution was stirred for 1 h, and the precipitate collected and dried by suction filtration on a medium frit.[10]

3.2.9   K$_7$[α-PW$_{11}$O$_{39}$]·14H$_2$O

To a solution of Na$_2$WO$_4$·2H$_2$O (181.5 g, 0.55 mol) in 300 mL H$_2$O was slowly added 50 mL of 1M H$_3$PO$_4$ and 88 ml glacial acetic acid. This solution was refluxed for 1 hour and then cooled to room temperature. Addition of solid KCl (60 g, 0.81 mol) led to a white precipitate which was collected after 10 minutes and air dried. [11]

3.2.10 Na$_{12}$[α-P$_2$W$_{15}$O$_{56}$]·24H$_2$O

In a 600 ml beaker, K$_6$[α-P$_2$W$_{18}$O$_{62}$]·14H$_2$O (38.5g, 8 mmol) was dissolved in 125 ml of water and then NaClO$_4$·H$_2$O (35g, 0.25mol) added. After vigorous stirring for 20 min, the mixture was cooled in an ice bath. Potassium perchlorate was removed by filtering after almost 3h. A l00 ml solution of Na$_2$CO$_3$ (10.6g, 0.1 mol) in water was added to the filtrate. The fine white precipitate that appeared almost instantaneously was decanted and then filtered on a medium porosity sintered glass frit and dried under suction for 3 hours. The precipitate was washed for 2 minutes using a solution of 4g of NaCl in 25 ml of water, dried under suction for 3 hours, washed for 3 minutes with 25 ml of ethanol, air dried under suction for 3 more hours, then washed again with ethanol and dried under suction, and finally air dried for 3 days. [12]

3.2.11 $K_{10}[\alpha_2\text{-}P_2W_{17}O_{61}]\cdot 20H_2O$

In a I-L beaker a sample of $K_6[\alpha\text{-}P_2W_{18}O_{62}]\cdot xH_2O$ (80g, 0.012 mol) was dissolved in 200 ml of water, and a solution of $KHCO_3$ (20g, 0.2 mol) in 200ml of water was added while stirring. After 1 h, the resultant white precipitate was filtered and dried under suction. The white solid was redissolved in 500ml of hot water (95°C) and snow-like crystals appeared on cooling to room temperature and were filtered after 3 h, dried under suction for a few hours and air-dried for 2 to 3 days. [12]

3.2.12 $Na_{10}[\alpha\text{-}SiW_9O_{34}]\cdot 18H_2O$

$Na_2WO_4\cdot 2H_2O$ (182 g, 0.55 mol) and Na_2SiO_3 (11 g, 0.09 mol) were dissolved in 200 ml of water. Hydrochloric acid (6 M, 130 ml) was added with stirring. The solution was then boiled for 1 h and concentrated to 300 ml. Eventually, the silica residue was filtered off. A solution of anhydrous Na_2CO_3 (50 g, 0.47 mol) in 50 ml of water was added. Then, the lukewarm solution was gently stirred, and the sodium salt precipitated out and was collected and air dried. [13]

3.2.13 $K_8[\alpha\text{-}SiW_{11}O_{39}]\cdot 13H_2O$

Na_2SiO_3 (11 g, 50 mmol) was dissolved with magnetic stirring at room temperature in 100mL of distilled water (the solution was filtered because it was not completely clear) (Solution A). In a I-L beaker, containing a magnetic stirring bar, $Na_2WO_4\cdot 2H_2O$ (182 g, 0.55 mol) was dissolved in 300 ml of boiling distilled water (Solution B). To the boiling Solution B, a solution of 4M HCI (165 ml) was added dropwise for 30 min, with vigorous stirring to dissolve the local precipitate of tungstic acid. Solution A was then added and, quickly, 50ml of 4 M HCI was also added. The pH was between 5 and 6.The solution was kept boiling for 1 h. After cooling to room temperature, the solution was filtered. KCl (150 g, 2.01 mol) was added to the solution, and vigorously stirred. The white solid product was collected on a sintered glass funnel, washed with two 50 ml portions of 1M KCI solution, then washed with 50 ml of cold water, and finally

dried in air. [14]

3.2.14 K$_8$[β_2-SiW$_{11}$O$_{39}$]·14H$_2$O

Na$_2$SiO$_3$ (11 g, 50 mmol) was dissolved in 100 ml of water (Solution A). In a separate 1-L beaker containing a magnetic stirring bar, Na$_2$WO$_4$·2H$_2$O (182 g, 0.55 mol) was dissolved in 300 ml of water. To this solution, 165 mL of 4M HCl was added in 1 ml portions over 10 min, with vigorous stirring (the local formation of hydrated tungstic acid that formed slowly disappeared). Then, Solution A was poured into the tungstate solution, and the pH adjusted to between 5 and 6 by the addition of 4M HCl (40 ml). This pH was maintained by addition of small amounts of 4M HCl for 100 min. Solid potassium chloride (90 g, 1.21 mol) was then added to the solution with gentle stirring. After 15 min, the formed precipitate was collected by filtering through a sintered glass filter. Purification was achieved by dissolving the product in 850 ml of water. The insoluble material was removed by filtration, and the salt precipitated again by addition of solid KCl (80 g, 1.07 mol).The precipitate was filtered, washed with 2M KCl solution (2 portions of 50 mL), and air dried. [15]

3.2.15 Na$_8$[B-α-TeW$_9$O$_{33}$]·19.5H$_2$O

The compound was prepared using the same method as for Na$_9$[SbW$_9$O$_{33}$]·19.5H$_2$O, by replacing Sb$_2$O$_3$ with TeO$_2$ as follows: Na$_2$WO$_4$·2H$_2$O (40 g, 121 mmol) was dissolved in boiling H$_2$O (80 ml). TeO$_2$ (2.14 g, 13.44 mmol) was dissolved in concentrated HCl (10 ml) and the resulting solution added dropwise to the tungsten containing solution. The mixture was refluxed for 1 h then allowed to cool to room temperature. Slow evaporation in air over several days yielded colourless crystals of the target compound which were washed with ice-cold H$_2$O (5 ml) and dried in air. [16]

3.3 References

[1]   G. M. Sheldrick, *Acta Crystallogr. Sect. A Found. Crystallogr.* **2007**, *64*, 112–122.

[2]   I. D. Brown, D. Altermatt, *Acta Crystallogr., Sect. B: Struct. Sci.* **1985**, *41*, 244.

[3]   K. C. Kim, A. Gaunt, M. T. Pope, *J. Clust. Sci.* **2002**, *13*, 423–436.

[4]   R. Contant, R. Thouvenot, Y. Dromzée, A. Proust, P. Gouzerh, *J. Clust. Sci.* **2006**, *17*, 317–331.

[5]   R. Contant, R. Thouvenot, *Can. J. Chem.* **1991**, *69*, 1498–1506.

[6]   B. Botar, T. Yamase, E. Ishikawa, *Inorg. Chem. Commun.* **2000**, *3*, 579–584.

[7]   N. Haraguchi, Y. Okaue, T. Isobe, Y. Matsuda, *Inorg. Chem.* **1994**, *33*, 1015–1020.

[8]   L. H. Bi, U. Kortz, S. Nellutla, A. C. Stowe, J. Van Tol, N. S. Dalal, B. Keita, L. Nadjo, *Inorg. Chem.* **2005**, *44*, 896–903.

[9]   A. Tézé, G. Hervé, *J. Inorg. Nucl. Chem.* **1977**, *39*, 999–1002.

[10]   A.P. Ginsberg, Ed. , *Inorganic Syntheses*, John Wiley & Sons, Inc., Hoboken, NJ, USA, 1990, *27*, 214–217.

[11]   R. Contant, *Can. J. Chem.* **1987**, *65*, 568–573.

[12]   A.P. Ginsberg, Ed. , *Inorganic Syntheses*, John Wiley & Sons, Inc., Hoboken, NJ, USA, 1990, *27*, 107.

[13]   G. Herve, A. Teze, *Inorg. Chem.* **1977**, *16*, 2115–2117.

[14]   A.P. Ginsberg, Ed. , *Inorganic Syntheses*, John Wiley & Sons, Inc., Hoboken, NJ, USA, 1990, *27*, 89-90.

[15]   A. P. Ginsberg, Ed. , *Inorganic Syntheses*, John Wiley & Sons, Inc., Hoboken, NJ, USA, 1990, *27*, 91-92.

[16]   A. J. Gaunt, I. May, R. Copping, A. I. Bhatt, D. Collison, O. Danny Fox, K. Travis Holman, M. T. Pope, *Dalton. Trans.* **2003**, 3009

CHAPTER 4. BISMUTH-CONTAINING POLYOXOMETALATES

4.1 Synthesis and Characterization of Bismuth(III)-Containing Heteropolytungstates, $[Bi(\alpha\text{-}XW_{11}O_{39})_2]^{n\text{-}}$ (X = Si, Ge, n = 13; P, As, n = 11) and $[Bi(\alpha_2\text{-}X_2W_{17}O_{61})_2]^{17\text{-}}$ (X=P, As)

This section is based on the publication; "N. Ncube, S. Bhattacharya, D. Thiam, J. Goura, A. S. Mougharbel, U. Kortz, *Eur. J. Inorg. Chem.* **2019**, 363–366. Bismuth(III)-Containing Heteropolytungstates $[Bi(XW_{11}O_{39})_2]^{n-}$ (X = Si, Ge, *n* = 13; X = P, *n* = 11) and $[Bi(P_2W_{17}O_{61})_2]^{17\text{-}}$, with permission/licensing from John Wiley and Sons, © 2019 Wiley-VCH Verlag GmbH & Co. KGaA, Weinheim. See: https://doi.org/10.1002/ejic.201801391

Herein the syntheses and structural characterization of six bismuth(III)-containing sandwich-type heteropolytungstates with Bi^{3+} in 8-coordination will be discussed. The four isostructural Keggin-type ions $[Bi(\alpha\text{-}XW_{11}O_{39})_2]^{n-}$, X = Si (**1**), Ge (**2**), n = 13; X = P (**3**), As (**5**), n = 11) and the two Wells-Dawson-type ion $[Bi(\alpha_2\text{-}X_2W_{17}O_{61})_2]^{17\text{-}}$, X = P (**4**), As (**6**), n = 17 were prepared *via* simple one-pot synthetic procedures in aqueous medium and structurally characterized in the solid state and in solution by standard analytical techniques. The novel polyanions comprise a Bi^{3+} ion linking two monolacunary $\{XW_{11}\}$ or $\{X_2W_{17}\}$ units in a sandwich-type fashion. The Bi^{3+} ion is coordinated by four oxygens of each monolacunary POM unit, resulting in 8-coordination with square-antiprismatic geometry. Such a coordination mode is rare for Bi^{3+}.
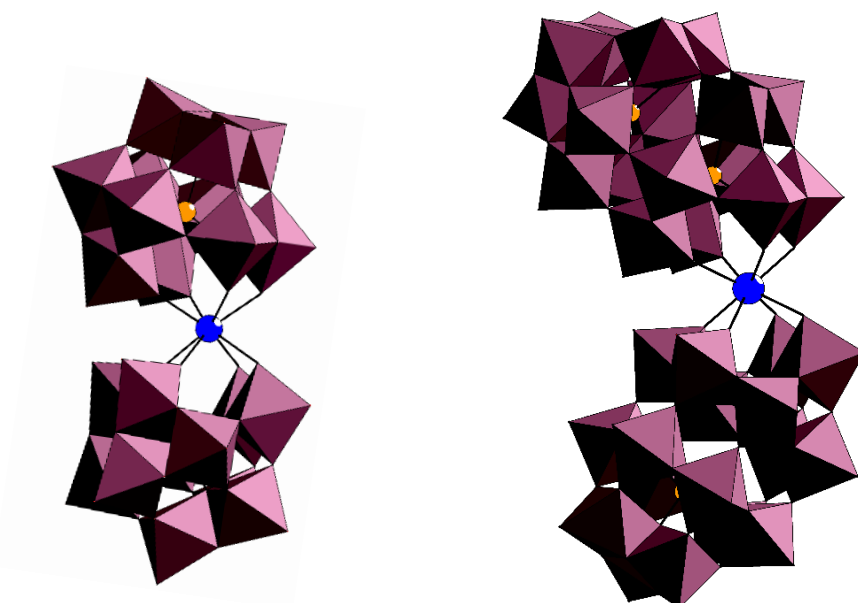
Figure 4.1. Combined polyhedral/ball-and-stick representations of $[Bi(\alpha\text{-}XW_{11}O_{39})_2]^{n-}$ (left) and $[\alpha_2\text{-}Bi(P_2W_{17}O_{61})_2]^{17-}$ (right). Colour code: WO_6, dark-pink octahedra; Bi, blue; heteroatoms (X = Si, Ge, P), orange.

4.1.1 Synthesis

$Na_{0.25}K_{12.75}[Bi(\alpha\text{-}SiW_{11}O_{39})_2]\cdot25H_2O$ (NaK-1)

A solution of the POM precursor $Na_{10}[A\text{-}a\text{-}SiW_9O_{34}]\cdot18H_2O$ (0.260 g, 0.094 mmol) was prepared by dissolving it in 10 ml 1 M KCl solution (pH 10.8). To this solution solid $Bi(NO_3)_3\cdot5H_2O$ (0.06 g, 0.124 mmol) was added under vigorous stirring. The resulting turbid solution was heated at 50 °C for 1 h and filtered while hot. The pH of the solution was 2.1 and 4 drops of 1M KCl solution were added. The solution was left for evaporation open to the air and after one month, small, colorless, cube-shaped crystals of **NaK-1** were obtained. Yield: 60.5 mg, 23% (based on W). The 25 waters of crystallization were determined by TGA (**Figure 4.5**). Elemental analysis % calculated: Na 0.09, K 7.63, Bi 3.21, W 61.8, Si 0.86; found: Na 0.15, K 8.10, Bi 3.03, W 60.5, Si 0.98.

$Na_{0.5}K_{12.5}[Bi(\alpha\text{-}GeW_{11}O_{39})_2]\cdot28H_2O$ (NaK-2)

A solution of the POM precursor $Na_2K_8[\alpha\text{-}GeW_9O_{34}]\cdot25H_2O$ (0.260 g, 0.094 mmol) was prepared by dissolving it in 10 ml 1 M KCl solution (pH, 7.8). Solid $Bi(NO_3)_3\cdot5H_2O$ (0.06 g,

0.124 mmol) was added under vigorous stirring. The resulting turbid solution was heated at 50 °C for 1 h and filtered after cooling. The pH of the solution was 3.5 and 6 drops of a 1M KCl solution were added. The solution was left for evaporation open to the air and filtered daily to remove the white precipitate. After about a month, small, colorless, cube-shaped crystals of **NaK-2** were obtained. Yield: 43.5 mg, 11.3% (based on W). The 28 waters of crystallization were determined by TGA (**Figure 4.6**). Elemental analysis % calculated: Na 0.17, K 7.33, Bi 3.14, W 60.8, Ge 2.18; found: Na 0.19, K 7.58, Bi 3.15, W 61.2, Ge 2.15.

$K_{11}[Bi(\alpha\text{-}PW_{11}O_{39})_2]\cdot 39H_2O$ (K-3)

A solution of the POM precursor $K_7[\alpha\text{-}PW_{11}O_{39}]\cdot 14H_2O$ (0.301 g, 0.094 mmol) was prepared by dissolving the precursor in 10 ml 1 M KCl solution (pH, 5.0). Solid $Bi(NO_3)_3\cdot 5H_2O$ (0.06 g, 0.124 mmol) was then added under vigorous stirring. The resulting turbid solution was heated at 50 °C for 60 minutes and filtered while hot. The pH of the solution was 2.2 and 4 drops of a 1M KCl solution were added. The solution was left for evaporation open to the air and after about one month, colorless, needle-shaped crystals of **K-3** were obtained. Yield: 71 mg, 22.5% (based on W). The 39 waters of crystallization were determined by TGA (**Figure 4.7**). Elemental analysis % calculated: K 6.42, Bi 3.12, W 60.4, P 0.93; found: K 6.60, Bi 3.19, W 60.3, P 0.96.

$K_{17}[Bi(\alpha_2\text{-}P_2W_{17}O_{61})_2]\cdot 38H_2O$ (K-4)

A solution of the POM precursor $K_{10}[\alpha_2\text{-}P_2W_{17}O_{61}]\cdot 20H_2O$ (0.064 g, 0.013 mmol) was prepared by dissolving it in 10 ml 1 M KCl solution (pH, 5.34). To this solution was added solid $Bi(NO_3)_3\cdot 5H_2O$ (0.0104 g, 0.021 mmol) under vigorous stirring. The resulting turbid solution was heated at 50 °C for 60 minutes and filtered after cooling. The pH of the solution was 2.6. Very tiny fluffy rod/needle-shaped crystals of **K-4** formed after 12 hours. Yield: 24 mg, 37.5% (based on W). The 38 waters of crystallization were determined by TGA (**Figure 4.8**). Elemental analysis % calculated: K 6.72, Bi 2.11, W 63.2, P 1.25; found: K 6.68, Bi 2.32,

W 61.9, P 1.24.

$Cs_{11-x}Na_x[Bi(\alpha-As^VW_{11}O_{39})_2]\cdot xH_2O$ (CsNa-5)

A solution of 13 ml the POM precursor $Na_9[A-\alpha-AsW_9O_{34}]\cdot 18H_2O$ (0.14g, 0.050 mmol) in double deionized water was prepared, to which was added dropwise a solution of $Bi(Cl_3)_3\cdot 6H_2O$ (0.032 g, 0.100 mmol) under vigorous stirring. The resulting turbid solution was stirred at room temperature for 90 minutes and filtered. The pH of the resulting solution was 1.8 and it was layered with 6 drops of 0.5M CsCl solution. The solution was left for evaporation open to the air and after about one month, small, colourless, cube-shaped crystals of **(CsNa-5)** were obtained.

$K_{16}Rb[Bi(\alpha_2-As_2W_{17}O_{61})_2]\cdot 39H_2O$ (KRb-6)

A solution of the POM precursor $K_{10}[\alpha_2-As_2W_{17}O_{61}]\cdot 20H_2O$ (0.063 g, 0.0126 mmol) was prepared by dissolving it in 10 ml 1M KCl solution (pH 5.52). Solid bismuth nitrate $Bi(NO_3)_3\cdot 5H_2O$ (0.0104 g, 0.021 mmol) was added slowly under vigorous stirring. The resulting turbid solution was heated at 50 °C for 60 minutes and filtered after cooling. The pH of the solution was 2.79. A few drops of 0.5M RbCl were added and very tiny fluffy rod/ needle shaped crystals of **(KRb-6)** formed immediately and after 12 hours, they could be collected. Yield: 15 mg, 23% (based on W).

4.1.2 Single-Crystal X-Ray Diffraction

Table 4.1. Crystal data and structure refinement for **NaK-1**, **NaK-2**, **K-3**, **K-4**, **CsNa-5** and **KRb-6**.

Compound	**NaK-1**	**NaK-2**	**K-3**	**K-4**	**NaCs-5**	**KRb-6**
Formula Weight (g/mol)	13024.22	6651.34	6696.04	9884.61	7405.21	20146.32
Crystal System	*Triclinic*	*Triclinic*	*Monoclinic*	*Triclinic*	*Triclinic*	*Triclinic*
Space Group	*P*-1	*P*-1	*P*2$_1$/*c*	*P*-1	*P*-1	*P*-1
a (Å)	13.5985(12)	13.6214(10)	18.741(3)	14.5263(11)	13.1346(6)	12.6692(7)
b (Å)	19.5529(17)	19.6371(14)	37.583(5)	22.4722(16)	17.7600(8)	14.5924(9)
c (Å)	20.4324(18)	20.4578(14)	14.090(2)	24.6515(19)	22.4414(10)	43.297(3)
α (°)	110.208(4)	110.366(3)	90	95.810(3)	93.657(2)	90.348(3)
β (°)	105.235(4)	105.400(3)	92.701(9)	102.910(3)	104.051(2)	91.725(3)
γ (°)	98.438(4)	98.493(3)	90	99.110(3)	105.074(2)	100.515(2)
Volume (Å^3)	4746.9(7)	4768.2(6)	9913(2)	7666.4(10)	4858.3(4)	7865.9(8)
Z	1	2	4	2	2	1
$D_{calc.}$ (gm/cm^3)	4.488	4.527	4.227	4.329	5.062	4.253
Absorption Coefficient (mm^{-1})	29.073	29.515	27.666	27.139	32.846	27.240
F(000)	5569.0	5638.0	10932	8710.0	6286.5	8758.0
θ range for data collection	1.246 to 25.027	1.147 to 25.027	1.084 to 25.027	0.856 to 25.027	0.944 to 25.027	0.941 to 25.027
Completeness to θ_{max}	99.9%	99.7%	99.9%	99.8%	99.9%	99.8%
Index Ranges	-13≤h≤16, -23≤k≤23, -24≤l≤24	-16≤h≤16, -23≤k≤20, -21≤l≤24	-22≤h≤22, -44≤k≤44, -16≤l≤16	-17≤h≤17, -26≤k≤23, -29≤l≤29	-15≤h≤15, -21≤k≤17, -26≤l≤26	-13≤h≤15, -17≤k≤17, -51≤l≤51
Reflections Collected	176002	104110	134824	242764	107476	290609
Unique Reflections	16751	16817	17499	27051	17136	27733
Data/Restraints/ Parameters	16751/0/765	16817/0/760	17499/0/708	27051/0/1185	17136/30/757	27733/6/1186
Goodness of Fit on F^2	1.053	1.145	1.122	1.047	1.056	1.129
R_1[a] (I>2σ(I))	0.0556	0.0788	0.0849	0.0608	0.0719	0.0684
wR_2[b] (all data)	0.1546	0.1765	0.2038	0.1184	0.1716	0.1501

[a] $R_1=\Sigma\|F_0|-|F_c\|/\Sigma|F_0|$, [b] $wR_2=[\Sigma w(F_0^2-F_c^2)^2/\Sigma w(F_0^2)^2]^{1/}$

4.1.3 Results and Discussion

The syntheses of polyanions **1** and **2** were accomplished by one-pot synthetic procedures involving the reaction of $Bi(NO_3)_3 \cdot 5H_2O$ and the trilacunary POM precursors $Na_{10}[A\text{-}\alpha\text{-}SiW_9O_{34}] \cdot 18H_2O$ and $Na_2K_8[A\text{-}\alpha\text{-}GeW_9O_{34}] \cdot 25H_2O$ in 1 M KCl solution at 50 °C in 1:1.3 molar ratio (POM:Bi). The P-analogue **3** was also prepared in the same way but using the monolacunary $K_7[\alpha\text{-}PW_{11}O_{39}] \cdot 14H_2O$. The synthesis of the As- analogue **5** involved the addition of a solution of $BiCl_3 \cdot 6H_2O$ to a solution of $Na_9[A\text{-}\alpha\text{-}AsW_9O_{34}] \cdot 18H_2O$. The Wells-Dawson derivatives **4** and **6** were prepared by dissolving $K_{10}[\alpha_2\text{-}P_2W_{17}O_{61}] \cdot 20H_2O$ and $K_{10}[\alpha_2\text{-}As_2W_{17}O_{61}] \cdot 20H_2O$ in 1M KCl solution and adding solid $Bi(NO_3)_3 \cdot 5H_2O$.

The composition of polyanions **1**-**6** including counter cations and crystal waters were determined by a combination of single-crystal XRD, elemental and thermogravimetric analyses. (For **1-4**, all mentioned techniques were used.)

4.1.3.1 Infrared (IR) spectroscopy

Fourier transform infrared (IR) spectra were recorded for **NaK-1, NaK-2,K-3, K-4** and **CsNa-5** and **KRb-6**. For **NaK-1,** the band at 1006 cm^{-1} corresponds to Si-O stretching modes from the SiO_4 heterogroup. The vibration band around 810 cm^{-1} is assigned to Ge-O stretching vibrations of the GeO_4 heterogroup for **NaK-2.** For **CsNa-5** and **KRb-6,** the weak vibration bands at around 890 cm^{-1} corresponds to As-O stretching modes from the AsO_3 heterogroup. The vibration bands in the 1100-1050 cm^{-1} region are assigned to P-O stretching vibrations of the PO_4 heterogroup for **K-3 and K-4.** The $W\text{-}O_t$ and $W\text{-}O_b\text{-}W$ stretching bands appear in the 1000-760 cm^{-1} region of the spectra. The peaks around 717 cm^{-1} in all spectra can be assigned to Bi-O bond vibrations.
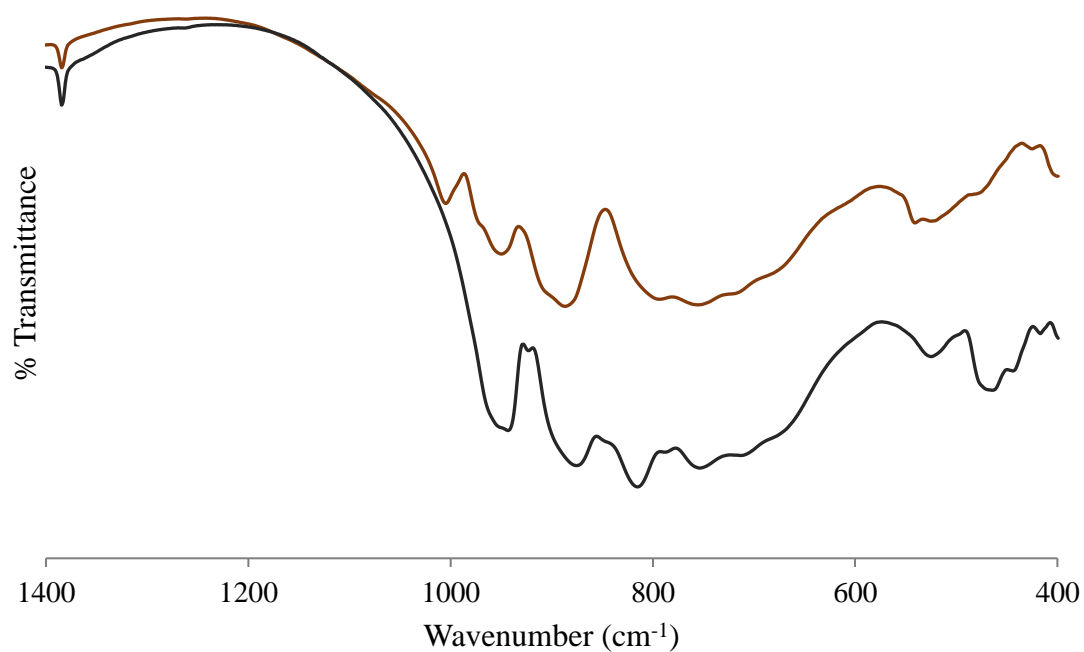
Figure 4.2. FT-IR spectra of **NaK-1** (dark brown) and **NaK-2** (black).
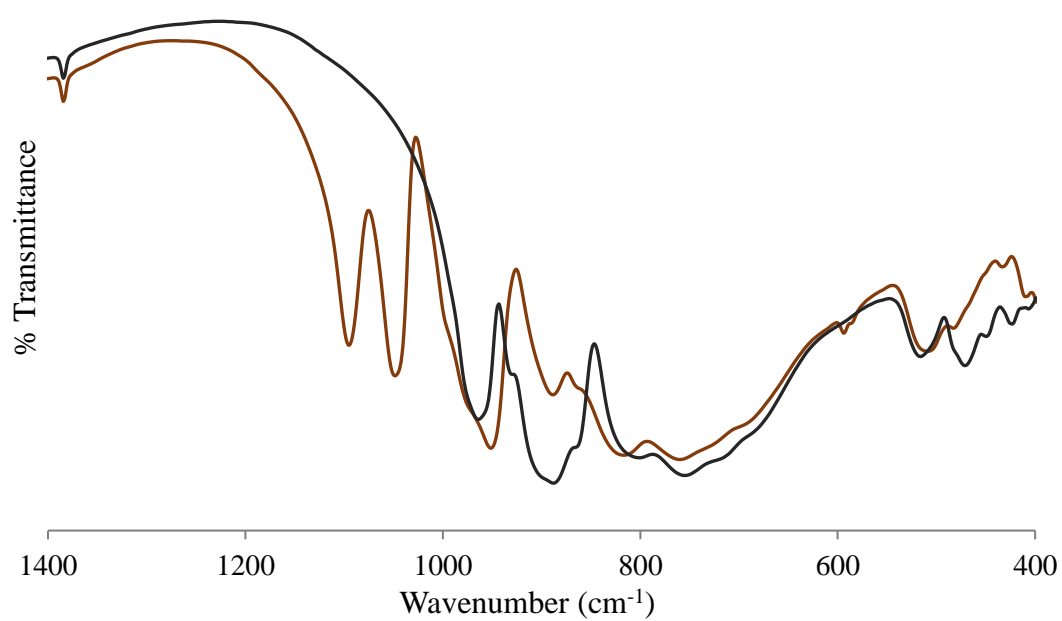
Figure 4.3. FT-IR spectra of **K-3** (dark brown) and **CsNa-5** (black).
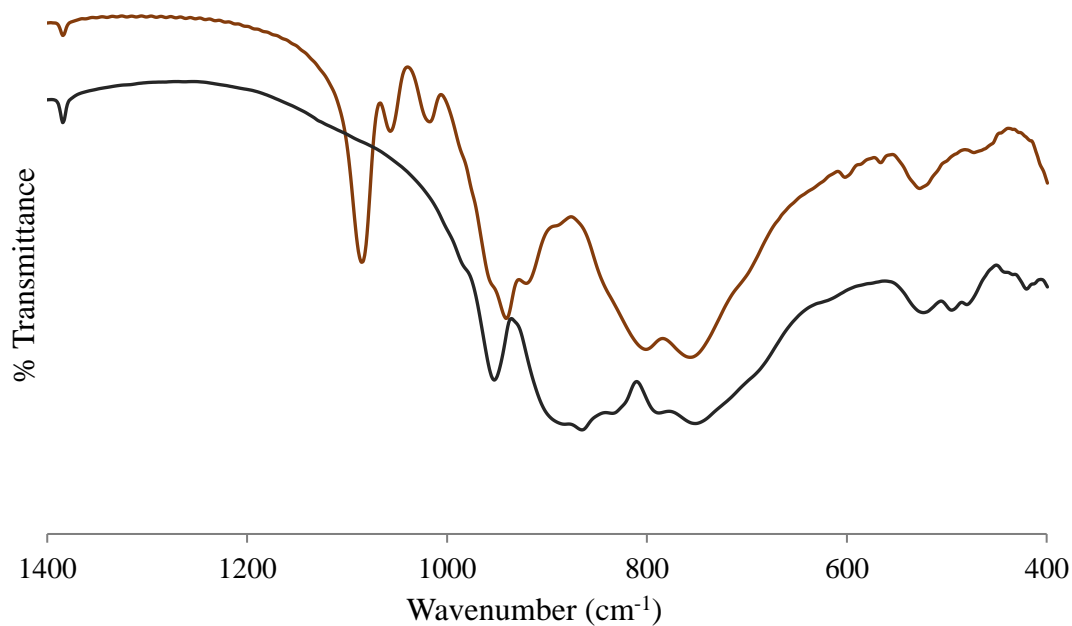
Figure 4.4. FT-IR spectra of **K-4** (dark brown) and **KRb-6** (black).

4.1.3.2 Thermogravimetric analyses

The thermal stabilities of the compounds **NaK-1, NaK-2, K-3, K-4** and **KRb-6** were monitored by thermogravimetric analysis (TGA). The first weight loss step for all four compounds from 20°C to around 200°C belongs to the loss of crystallization water. All five compounds are stable up to 500°C.
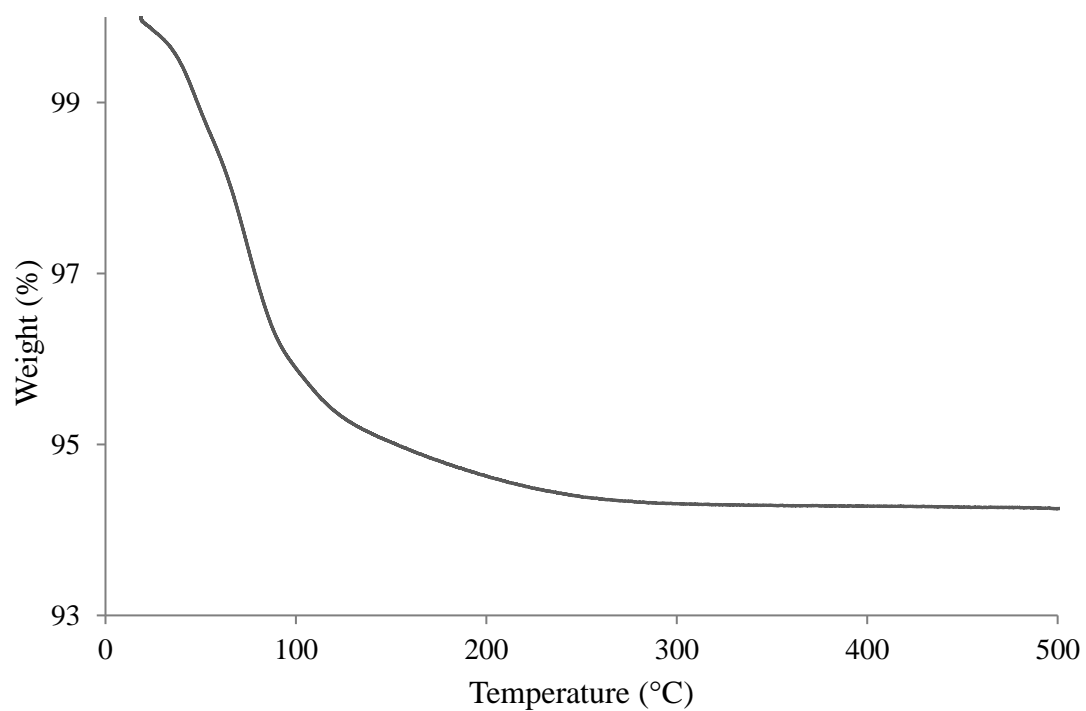
Figure 4.5. Thermogram of **NaK**-**1**.
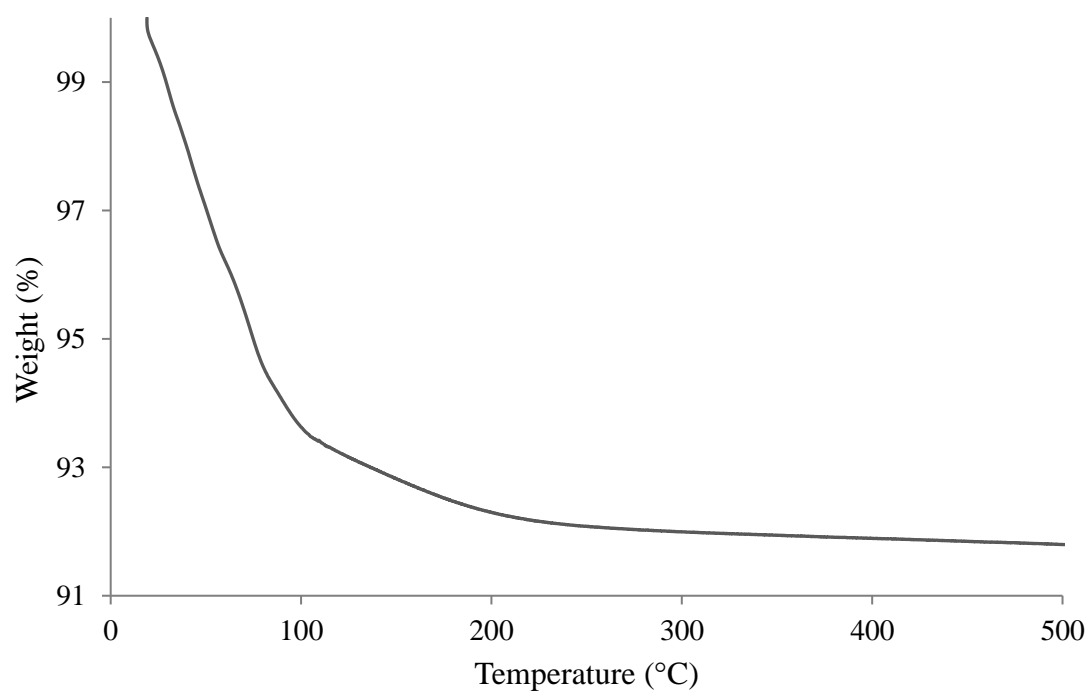
Figure 4.6. Thermogram of **NaK**-**2**.
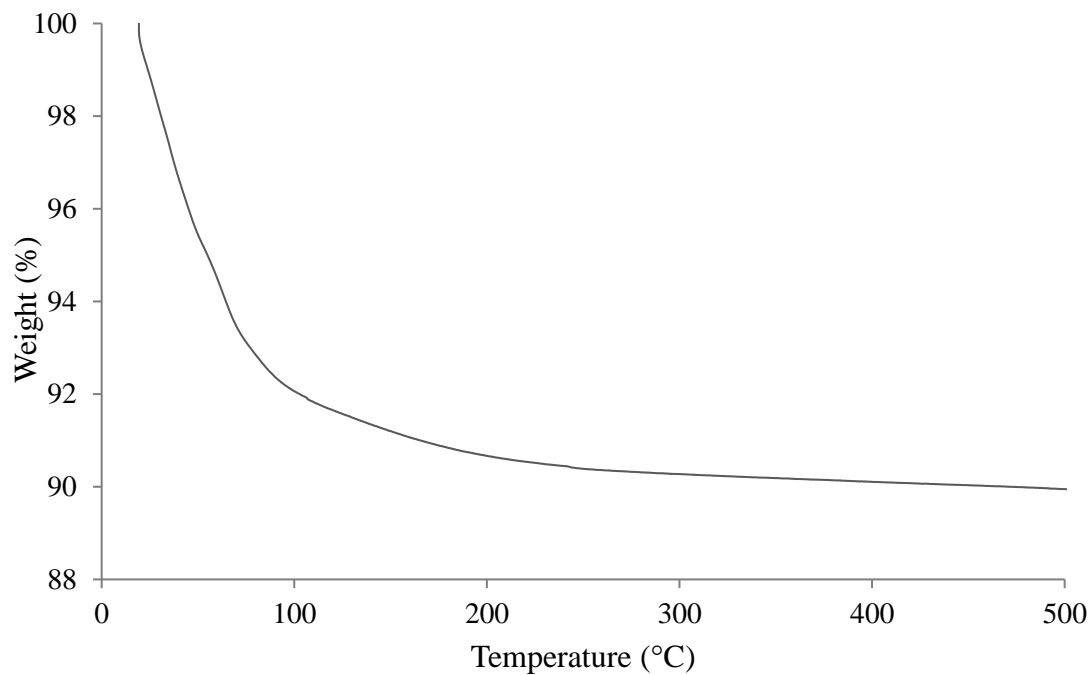
Figure 4.7. Thermogram of **K-3**.
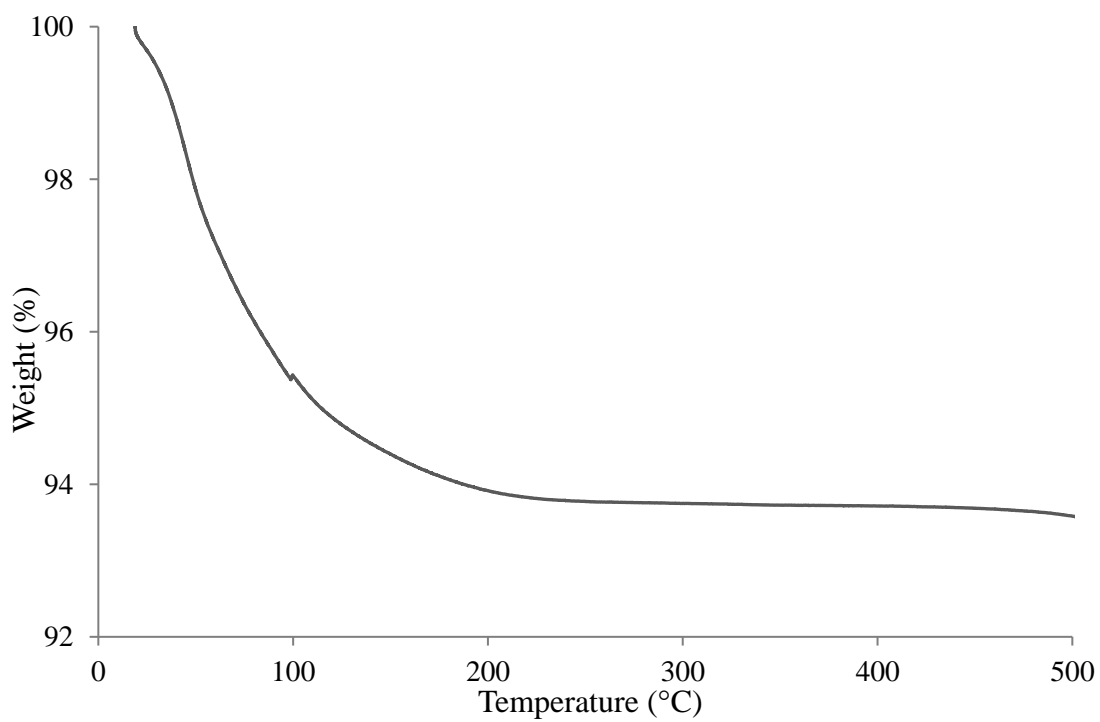
Figure 4.8. Thermogram of **K-4.**
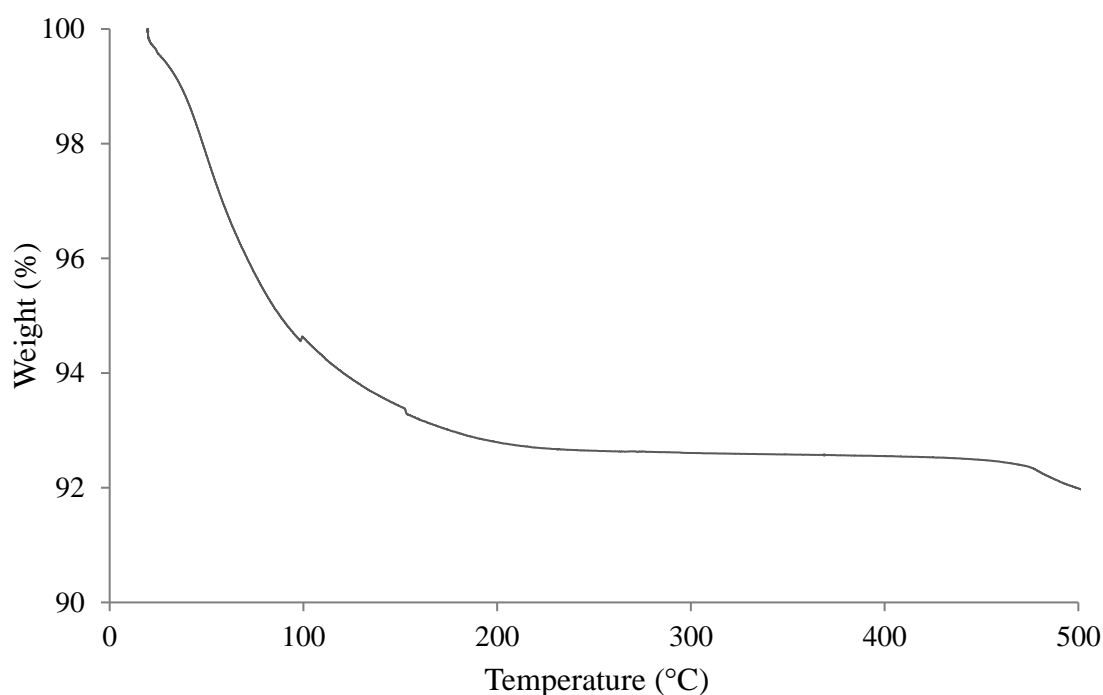
Figure 4.9. Thermogram of **KRb-6.**

4.1.3.3 Structural description

The isostructural Keggin-type polyanions **1-3** and **5** are composed of two monolacunary [α-$XW_{11}O_{39}$]$^{n-}$ anions sandwiching a Bi^{3+} ion with four Bi-O(W) bonds to each Keggin unit (**Figure 4.10**). The monolacunary Keggin units hence act as tetradentate ligands, resulting in 8-coordination of the Bi^{3+} ion. Bond valence sum (BVS) calculations show that Bi is in the +3-oxidation state (**Table 4.2**).[14]

Table 4.2. Bond valence sum (BVS) for the Bi^{3+} ion in **1-6**.

Compound	BVS
1	3.186
2	3.047
3	3.177
4	3.139
5	3.347
6	3.260

It should be noted that the synthesis of **NaK-1, NaK-2, K-3** and **CsNa-5** followed less rational procedures where the trilacunary Keggin precursors were used instead of the rational

monolacunary precursors. This observation is well-known in polyoxometalate chemistry and several cases of *in situ* isomerization accompanied by loss/gain of tungsten, and largely driven by pH are known.[15,16] However, **K-3** could also be synthesized following a rational procedure using the monolacunary Keggin precursor which resulted in a better yield. While crystals of **CsNa-5** and **KRb-6** could be harvested to afford a crystal structure of the two POMs, the yield for **CsNa-5** was very low that only single crystal XRD and FT-IR spectroscopy could be done. Although the yield for **KRb**-**6** was 15 mg, we were unable to verify the structure of the compound by elemental analysis.
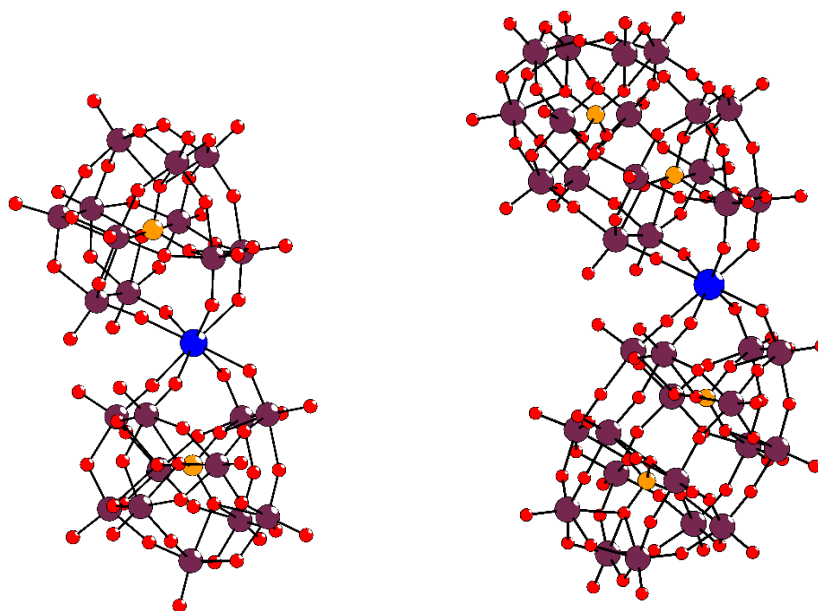
Figure 4.10. Ball-and-stick representations of $[Bi(\alpha\text{-}XW_{11}O_{39})_2]^{n-}$ (left) and $[Bi(\alpha_2\text{-}X_2W_{17}O_{61})_2]^{17-}$ (right). Colour code; W, dark-pink; Bi, blue; heteroatom (X = Si^{IV}, Ge^{IV}, P^V, As^V), orange; O, red.

Due to the isostructural nature of polyanions **1**-**3,** only polyanion **3** is described here in detail as a representative Keggin-based derivative. The coordination geometry of the Bi^{3+} ion in polyanion **3** is square-antiprismatic with Bi-O bond lengths from 2.41(3) Å to 2.50(3) Å (**Table 4.4**). The BiO_8 unit can be defined by four oxygens of each lacunary Keggin unit (O1, O2, O3, O4 and O5, O6, O7, O8). The average deviation of the oxygen atoms from the two idealized planes are 0.001 Å (top plane) and 0.014 Å (bottom plane), respectively, indicating that the

BiO_8 square-antiprism is quite regular. The distances of the Bi atom from the top and bottom planes are 1.28 Å and 1.32 Å, respectively (**Figure 4.11**).
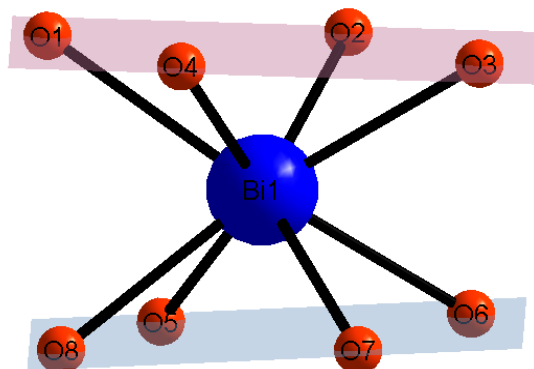
Figure 4.11. Ball-and-stick representation of BiO_8 showing the top plane (O1, O2, O3, O4) and bottom plane (O5, O6, O7, O8) for polyanions **1**-**4**.

Polyanions **4** and **6** are composed of two monolacunary $[\alpha_2\text{-}X_2W_{17}O_{61}]^{10-}$ Wells-Dawson fragments which are connected in a *syn* fashion by a Bi^{3+} ion. Both polyanions similarly have four Bi-O(W) bonds to each monolacunary Wells-Dawson unit and the Bi^{3+} ion has 8-coordination (square-antiprismatic).

A closer look at polyanion **4** shows that the Bi-O bond lengths range from 2.316(12) Å to 2.575(11) Å (**Table 4.4**). Two planes are formed by the four oxygens of each monolacunary Wells-Dawson unit: O1, O2, O3, O4 (top plane) and O5, O6, O7, O8 (bottom plane) and the oxygen atoms have an average deviation of 0.017 Å and 0.004 Å from their respective planes, indicating little distortion in the BiO_8 square-antiprism. The distances between the Bi atom and the top and bottom planes are 1.30 and 1.25 Å, respectively.

Table 4.3. Average deviation of oxygen atoms from two idealized planes of **BiO_8** square antiprism.

	Average d($\mathring{A}$)	
Polyanion	Top plane	Bottom plane
1	0.0045	0.020
2	0.0070	0.0045
3	0.00093	0.014
4	0.017	0.0040
5	0.0089	0.0044
6	0.017	0.0040

The square-antiprismatic geometry of the BiO_8 unit can be quantified using the twist angle θ, which our group defined earlier as the offset of the two O_4–based squares (*vide supra*) from the ideal eclipsed conformation. In other words, θ defines the angle of rotation or twist of the upper square with respect to the lower square. .[17] For example, the twist angles θ for polyanions **1**, **3** and **4** were determined by considering the offset (dihedral angle) of the two planes formed by the O2-Bi-O4 and O6-Bi-O8 atoms of the two monolacunary sites of each polyanion (**Figure 4.12**).
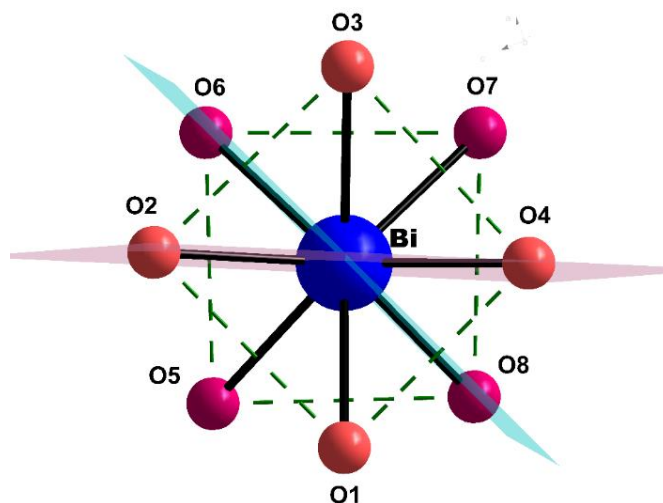
Figure 4.12. Ball-and-stick representation of BiO_8 showing how the twist angles for polyanions **1**, **3** and **4** are determined.

It can be seen that for polyanions **1-3** and **5** the twist angles increase with decreasing size of the heteroatoms. Comparing polyanions **1** and **3**, the twist angle increases from 38.5(4)° in **1** to 42.8(7)° in **3**. The same is true for polyanions **2** and **5**. The replacement of monolacunary Keggin by Wells-Dawson subunits and keeping the heteroelement the same does not have any significant effect on the coordination geometry of the Bi atom. For example, the twist angle of **3** is 42.8(7)° and that of **4** is 42.5 (3)°. Polyanions with P and As heteroelements exhibit Bi^{3+} in a coordination environment that is close to the ideal square-antiprismatic geometry (a twist angle of 45°). As the size of the heteroatom increases the X-O(W) bond length increases (Si *vs* Ge and P *vs* As) and consequently this leads to shorter *trans*-related (X)O-W bond lengths (**Table 4.4**).

Table 4.4. Average bond lengths and twist angles for $[Bi(\alpha\text{-}XW_{11}O_{39})_2]^{n-}$ (left) and $[Bi(\alpha_2\text{-}X_2W_{17}O_{61})_2]^{17-}$(right).

	$[Bi(\alpha\text{-}XW_{11}O_{39})_2]^{n-}$				$[Bi(\alpha_2\text{-}X_2W_{17}O_{39})_2]^{17-}$	
	Si(1)	**Ge(2)**	**P(3)**	**As(5)**	**P(4)**	**As(6)**
X-O-(W)	1.619(12) - 1.651(12)	1.708(18) - 1.750(19)	1.47(3) - 1.57(3)	1.652(17) - 1.694(18)	1.508(12) - 1.564(12)	1.647(14) - 1.716(15)
W-O(X)	2.213(11) - 2.422(11)	2.177(18) - 2.353(19)	2.27(3) - 2.51(3)	2.293(17) - 2.428(16)	2.265(11) - 2.406(11)	2.261(14) - 2.339(15)
Bi-O	2.319(12) - 2.507(11)	2.310(21) - 2.571(19)	2.41(3) - 2.50(3)	2.271(16) - 2.634(16)	2.316(12) - 2.575(11)	2.322(14) - 2.621(15)
Twist angle	38.48(4)	38.81(7)	42.78(7)	41.61(5)	42.49(3)	43.21(4)

Based on all the above observations, it appears that Bi^{3+} mimics the coordination chemistry of lanthanide ions. Lacunary heteropolytungstates are known to coordinate to lanthanide ions via oxygens in the vacant sites of the POM.[1–4] In the resulting compounds, a coordination number of 8 for the lanthanide ion is very common.[5] Classic examples are the Peacock and Weakley ion first reported in 1971. The sandwich-type heteropolyanions $[Ln(\alpha\text{-}XW_{11}O_{39})_2]^{n-}$ and $[Ln(\alpha_2\text{-}X_2W_{17}O_{61})_2]^{16-}$ consist of a $Ln^{3+/4+}$ centre connecting two monovacant Keggin $\{XW_{11}\}$ or

Wells-Dawson, $\{X_2W_{17}\}$ units, respectively. The central LnO_8 polyhedron adopts a square-antiprismatic coordination geometry.[6]

To date many compounds of these structural types have been studied and reported, including the different isomers of the monolacunary Keggin and Wells-Dawson subunits.[7-13] Hence we decided to compare polyanion **3** to its Ce^{3+} analogue $[Ce(\alpha\text{-}PW_{11}O_{39})_2]^{11-}$.[14] The average Bi-O and Ce-O bond lengths were found to be very similar, 2.438 Å vs 2.461 Å, respectively.

Table 4.5. Bi-O and Ce-O bond lengths in polyanion **3** and $[Ce^{III}(PW_{11}O_{39})_2]^{11-}$.[14]

Bi-O (Å)		Ce-O (Å)	
Bi-O1	2.45(3)	Ce-O32	2.453(12)
Bi-O2	2.41(3)	Ce-O31	2.524(11)
Bi-O3	2.44(3)	Ce-O34	2.447(13)
Bi-O4	2.41(3)	Ce-O33	2.384(14)
Bi-O5	2.50(3)	Ce-O38	2.495(14)
Bi-O6	2.43(3)	Ce-O37	2.454(12)
Bi-O7	2.43(3)	Ce-O36	2.495(12)
Bi-O8	2.43(3)	Ce-O35	2.433(11)
Average	**2.4375**	**Average**	**2.4610**

In both polyanions the central atom (Bi/Ce) has a square-antiprismatic coordination geometry and, as already described, the average deviation of the oxygen atoms from the top and bottom planes in polyanion **3** (0.001 Å and 0.014 Å) and $[Ce^{III}(\alpha\text{-}PW_{11}O_{39})_2]^{11-}$ (0.017 Å and 0.011 Å), indicates very little distortion (**Table 4.6**). The dihedral angles between the two planes of **3** and $[Ce^{III}(\alpha\text{-}PW_{11}O_{39})_2]^{11-}$ are 4.357° and 4.277°, respectively, and the distances between the Bi atom and the top and bottom planes are 1.29 Å and 1.32 Å, and for the Ce atom 1.32 Å and 1.31 Å, respectively.

Table 4.6. Distances of oxygen atoms from top and bottom planes of polyanion **3** and [Ce^{III}(α-PW$_{11}$O$_{39}$)$_2$]$^{11-}$.[14]

	[Ce^{III}(α-PW$_{11}$O$_{39}$)$_2$]$^{11-}$	d(Å)	mean(Å)	3	d(Å)	mean(Å)
Top	O32	0.015		O2	0.0009	
	O33	0.021		O3	0.0009	
	O31	0.014	0.017	O1	0.0009	0.00093
	O34	0.020		O4	0.001	
Bottom	O35	0.0095		O6	0.013	
	O38	0.012		O7	0.013	
	O36	0.0091	0.011	O5	0.017	0.014
	O37	0.012		O8	0.014	

In 2011, Naruke and co-workers published [La(α-PW$_{11}$O$_{39}$)$_2$]$^{11-}$[8] which can be compared to polyanion **3**. The rationale behind this comparison is the similarity in the electronic nature of Bi^{3+} and La^{3+}, which are both diamagnetic with [Xe]4f^{14}5d^{10}6s^2 *vs* [Xe] electronic configurations, respectively.

At a first glance, polyanion **3** resembles [La(α-PW$_{11}$O$_{39}$)$_2$]$^{11-}$, as both Bi^{3+} and La^{3+} are coordinated by eight oxygen atoms, four from each {PW$_{11}$} subunit. However, there are some structural differences in the coordination geometry around the Bi^{3+} and La^{3+} ions. The La^{3+} ion is in a pseudo-cubic coordination geometry as compared to the square-antiprismatic coordination of Bi^{3+} in **3**. The La-O distances of [La(a-PW$_{11}$O$_{39}$)$_2$]$^{11-}$ are in the range of 2.495(7) - 2.537(7) Å, as compared to the Bi-O distances from 2.41(3) to 2.50(3) Å for **3**.

Table 4.7. Bi-O and La-O bond lengths in **3** and [La^{III}(α-PW$_{11}$O$_{39}$)$_2$]$^{11-}$.[8]

Bi-O (Å)		La-O (Å)	
Bi-O1	2.45(3)	La-O16	2.50(6)
Bi-O2	2.41(3)	La-O17	2.54(7)
Bi-O3	2.44(3)	La-O18	2.53(6)
Bi-O4	2.41(3)	La-O19	2.49(7)
Bi-O5	2.50(3)	La-O16	2.50(6)
Bi-O6	2.43(3)	La-O17	2.54(7)
Bi-O7	2.43(3)	La-O18	2.53(6)
Bi-O8	2.43(3)	La-O19	2.49(7)
Average Bi-O	**2.44**	**Average Ce-O**	**2.52**

4.1.3.4 ^{31}P- and ^{183}W-NMR spectroscopy.

The ^{31}P NMR spectrum of **K-3** shows a singlet at -11.5 ppm which is attributed to the two equivalent phosphorous atoms in the polyanion. When compared to the ^{31}P NMR spectrum of $[La(a\text{-}PW_{11}O_{39})_2]^{11-}$, the exact same chemical shift of -11.5 ppm is also observed. However, for $[La(a\text{-}PW_{11}O_{39})_2]^{11-}$ two more peaks were present, which were assigned to free POM ligand $[a\text{-}PW_{11}O_{39}]^{7-}$ (-11.2 ppm) and the 1:1 dimer $[La(H_2O)_n(a\text{-}PW_{11}O_{39})]^{4-}$ (-11.7 ppm).
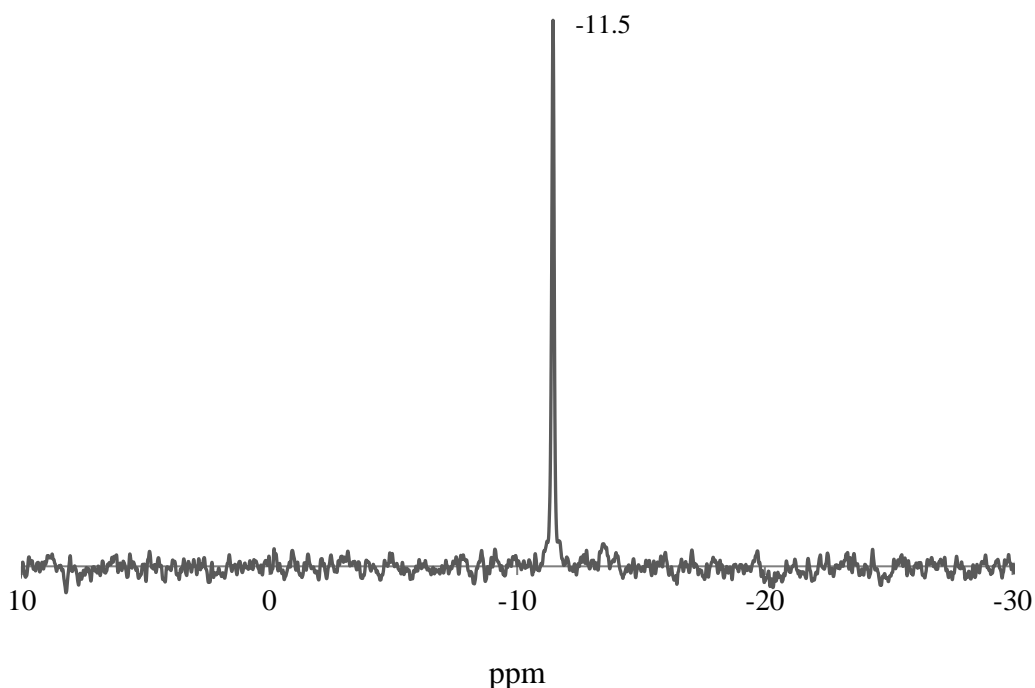
Figure 4.13. ^{31}P NMR spectra of **K-3** in H_2O/D_2O (pH 3.1) at room temperature.
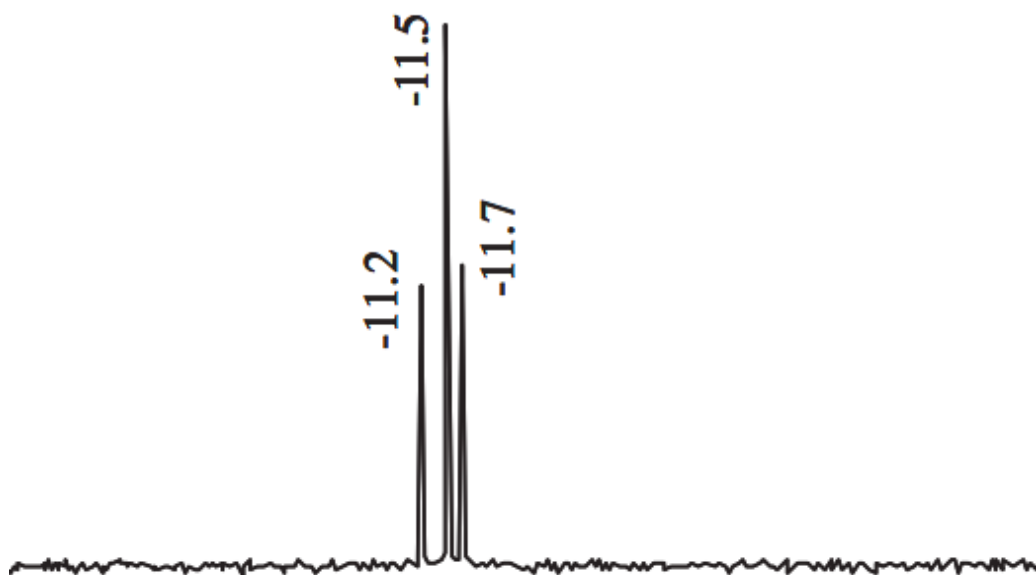
Figure 4.14. ^{31}P NMR spectrum of 35mM $[La(PW_{11}O_{39})_2]^{11-}$ in D_2O solution.[8]

With this information it can be suggested that $[La(a\text{-}PW_{11}O_{39})_2]^{11-}$ is less stable than polyanion **3**, for which a singlet was observed even after 24 hours of measurement. The higher stability of **3** compared to $[La(a\text{-}PW_{11}O_{39})_2]^{11-}$ is also reflected by shorter Bi-O bonds compared to the La-O bonds. Also, thermogravimetric analysis (TGA) studies showed that **K-3** is thermally stable until 500 °C.

The ^{31}P NMR spectrum of the Wells-Dawson derivative; **K-4** exhibits the expected two singlets at -7.8 and -13.4 ppm (**Figure 4.15**) that do not shift or change in intensity over a 24-hour measurement period; indicating that the polyanion is solution-stable. The signal at -7.8 ppm corresponds to the P atom that is closer to the lacunary site. This perturbed P atom is influenced by the insertion of Bi^{3+} in the lacunary site. The ^{31}P NMR of the free ligand (monolacunary species) $(P_2W_{17}O_{61})^{10-}$ shows two signals at -5.6 and -12.7 ppm, so based on this, the signal which shows the biggest shift must represent the P atom that shares an oxygen with Bi^{3+}. The peak at -12.7 ppm in the precursor remains almost the same in polyanion **4** suggesting that it is indeed the P atom that is furthest from the site of substitution.
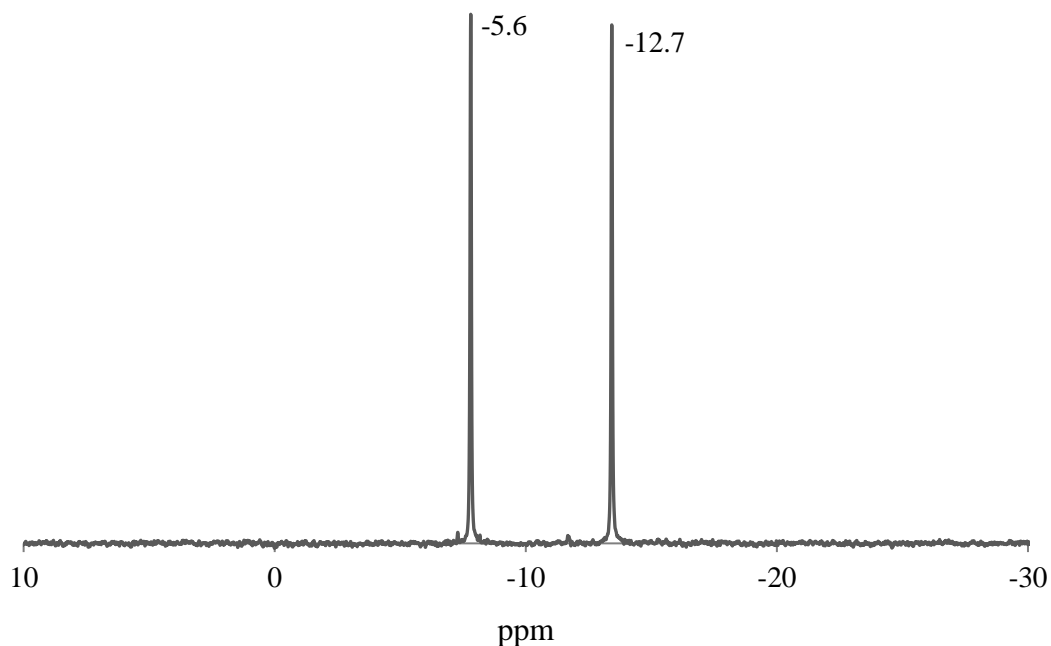
Figure 4.15. ^{31}P NMR spectra of **K-4** in H_2O/D_2O (pH 2.5) at room temperature.

We also measured ^{183}W NMR of **K-3** and the spectrum shows only four signals at -102.2, -108.3, -123.4, and -145.1 ppm (**Figure 4.16**), rather than the expected six. One reason is probably the fact that ^{209}Bi is quadrupolar (S = 9/2, 100%) and hence the two signals of the two pairs of tungsten at the POM lacunary site are wiped out. In fact, even the signal at -123.4 ppm is broadened. One of the complexes reported in 2019 by Sadakane and co-workers is the same as our $[Bi(PW_{11}O_{39})_2]^{11-}$ (polyanion **3**) for which they measured ^{183}W-NMR and obtained three sharp signals at −104.49, −110.83, and −147.98 ppm, and three broad signals at −85.68, −93.86, and −125.66 ppm. [15] Signal broadening has been explained by many groups. Francesconi et.al reported that some signals of the $[(SiW_{11}O_{39})_2Ln]^{13-}$ [Ln = La^{3+} (diamagnetic), Yb^{3+} (paramagnetic) and Lu^{3+} (diamagnetic)] were broad due to the rotation of the [α-SiW$_{11}$O$_{39}$]$^{8-}$ moiety. [16]Pope and co-workers described broadening of some signals for [Ce(α$_2$-P$_2$W$_{17}$O$_{61}$)$_2$]$^{17-}$ as well as the disappearance of a signal which the explained to be due to dynamic equilibrium between the 1:1 complex; [Ce(α$_2$-P$_2$W$_{17}$O$_{61}$)]$^{7-}$and the 1:2 complex; [{Ce(α$_2$-

$P_2W_{17}O_{61})\}_2]^{14-}$.[17] Therefore, the other reason for the broadening observed in the ^{183}W NMR spectrum of **K-3** could be due to dynamic rotation and/or equilibrium in D_2O between the 1:1 complex; $[Bi(PW_{11}O_{39})]^{4-}$ and the 1:2 complex; $[Bi(PW_{11}O_{39})_2]^{11-}$.
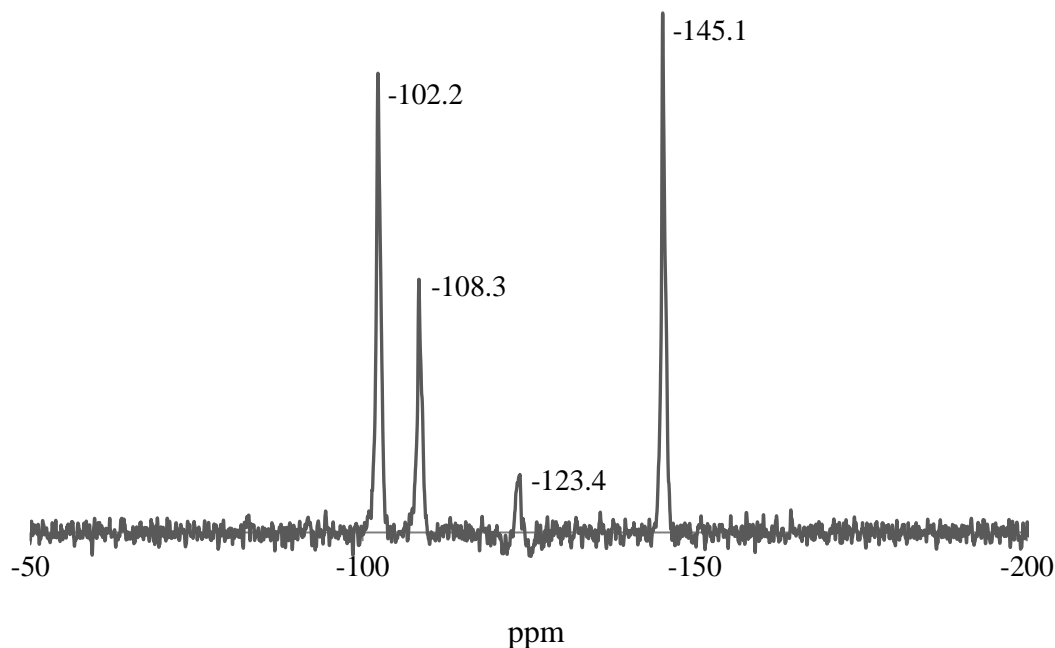
Figure 4.16. ^{183}W NMR spectrum of **3** in H_2O/D_2O (pH 3) at room temperature.

4.1.4 Conclusions

We have synthesized and structurally-characterized four novel Keggin-type heteropolytungstates $[[Bi(\alpha\text{-}XW_{11}O_{39})_2]^{n-}$ X = Si (**1**), Ge (**2**), n = 13; X = P (**3**), As (**5**), n = 11) and two Wells-Dawson-type ions $[Bi(\alpha_2\text{-}X_2W_{17}O_{61})_2]^{17-}$ X = P (**4**), As (**6**), n = 17. These were characterized in the solid state and in solution by standard analytical techniques. The polyanions comprise an 8-coordinated Bi^{3+}ion linking two monolacunary Keggin $\{XW_{11}\}$ or Wells-Dawson $\{X_2W_{17}\}$ units in a sandwich-type fashion. The Bi^{3+} ion is coordinated by four oxygens of each monolacunary unit, resulting in a square-antiprismatic coordination geometry. Such a coordination mode is rare for Bi^{3+} and is unprecedented in heteropolytungstate chemistry. Our work suggests that Bi^{3+} can mimic the structural chemistry of Ln^{3+} ions in POM chemistry.

4.2 Synthesis and structural characterization of $[(Bi(H_2O)SiW_{11}O_{39})_4]^{20-}$ and $\{[Bi(H_2O)SiW_{11}O_{39}]^{5-}\}_\infty$

In this section the syntheses and structural characterization of two novel 1:1 bismuth(III)-containing complexes are reported; namely $[(Bi(H_2O)SiW_{11}O_{39})_4]^{20-}$ (**7**) and $\{[Bi(H_2O)SiW_{11}O_{39}]^{5-}\}_\infty$ (**8**), an infinite one-dimensional structure in the solid state. The polyanions were synthesized via one-pot procedures in aqueous media and structurally characterized in the solid state and in solution by standard analytical techniques. The novel polyanions comprise a Bi^{3+} ion inserted in the lacunary site of $[\alpha\text{-}SiW_{11}O_{39}]^{8-}$ leading to different coordination numbers of Bi^{3+} (six and seven). Such coordination modes of Bi^{3+} in both polyanions is still rare in heteropolytungstate chemistry.

4.2.1 Synthesis

$K_{20}[(Bi(H_2O)SiW_{11}O_{39})_4]\cdot 40\ H_2O$ (K-7)

The synthesis was done as follows: A solution of the POM precursor $K_8[A\text{-}\alpha\text{-}SiW_{11}O_{39}]\cdot 13H_2O$ (0.303 g, 0.094 mmol) was prepared by dissolving it in 10ml IM KCl solution. To this solution was added $Bi(NO_3)_3\cdot 5H_2O$ (0.06 g, 0.124 mmol) under vigorous stirring. The resulting colourless solution was heated at 50°C for 1 h and filtered while hot. The pH of the solution was 2.1. The solution was left for evaporation open to the air and after 48 hrs, small, colorless, cube-shaped crystals of $K_{20}[(Bi(H_2O)SiW_{11}O_{39})_4]\cdot 40H_2O$ (**K-7**) were obtained. Yield: 100 mg, 32% (based on W). Elemental analysis; % calculated: K 5.97, Bi 6.38, W 61.71, Si 0.86; found: K 6.32, Bi 6.85, W 60.8, Si 0.78. The 40 waters of crystallization were determined by TGA (**Figure 4.18**).

$K_5[Bi(H_2O)SiW_{11}O_{39}]\cdot 12H_2O$ (K-8)

Procedure 1. The recrystallization of **K-7** in water resulted in the formation of needle-shaped crystals after 48 hours. Yield: 60 mg, 19% (based on W). Elemental analysis % calculated: K 5.90, Bi 6.31, W 61.04, Si 0.86; found: K 5.95, Bi 6.84, W 60.2, Si 1.18. The 12 waters of

crystallization were determined by (**Figure 4.19**).

Procedure 2. A solution of the POM precursor $K_8[\beta_2\text{-}SiW_{11}O_{39}]\cdot14H_2O$ (0.303 g, 0.094 mmol) was prepared by dissolving it in 10 ml 1 M KCl solution. To this solution solid $Bi(NO_3)_3\cdot5H_2O$ (0.06 g, 0.124 mmol) was added under vigorous stirring. The resulting solution was heated at 50 °C for 90 minutes and filtered while hot. The pH of the solution was 3.0. A few drops of IM RbCl were added and thin, colourless needle-shaped crystals formed upon cooling. The solution was left for evaporation open to the air and after a week the crystals of **KRb-8** were collected.

4.2.2 Single-Crystal X-Ray Diffraction

Table 4.8. Crystal data and structure refinement for **K-7 and K-8**.

Compound	**K-7**	**K-8**
Formula Weight (gm/mol)	13107.76	3312.97
Crystal System	Tetragonal	Triclinic
Space Group	I 4_1/a	P-1
a (Å)	18.3498(7)	11.6181(10)
b (Å)	18.3498(7)	11.9464(11)
c (Å)	53.982(2)	19.8601(18)
α (º)	90	96.122(2)
ß (º)	90	97.440(2)
γ (º)	90	118.642(2)
Volume (Å^3)	18176.5(16)	2353.3(4)
Z	4	2
$D_{calc.}$ (gm/cm^3)	4.733	4.716
Absorption Coefficient (mm^{-1})	37.849	31.168
F(000)	21600	2898
θ range for data collection	1.172 to 27.512	2.055 to 26.469
Completeness to θ_{max}	100%	99.7%
Index Ranges	-23<=h<=23, -23<=k<=23, -70<=l<=69	-14<=h<=13, -14<=k<=14, -24<=l<=24
Reflections Collected	86275	28828
Unique Reflections	10457	9668
Data/Restraints/Parameters	10457 / 14 / 275	9668 / 432 / 649
Goodness of Fit on F^2	3.761	1.059
R_1[a] (I>2σ(I))	0.3085	0.0639
wR_2[b] (all data)	0.7087	0.1832

[a] $R_1=\Sigma||F_0|-|F_c||/\Sigma|F_0|$, [b] $wR_2=[\Sigma w(F_0^2-F_c^2)^2/\Sigma w(F_0^2)^2]^{1/2}$

4.2.3   Results and Discussion

In section **4.1** of this dissertation, 1:2 complexes $[Bi(XW_{11}O_{39})_2]^{n-}$, X = Si (**1**), Ge (**2**), P (**3**) and

As (**5**) were reported where the syntheses of three of the complexes followed non-rational

procedures starting with trilacunary precursors. The phosphorus analogue $[Bi(PW_{11}O_{39})_2]^{11-}$ (**3**)

was reported to be synthesized following a rational procedure starting with the monolacunary

$[\alpha\text{-}PW_{11}O_{39}]^{7-}$.[18] We also attempted to prepare polyanions **1** and **2** starting with the respective

monolacunary precursors. The reaction of $[\alpha\text{-}SiW_{11}O_{39}]^{8-}$ with Bi^{3+} resulted in a 1:1 complex

$[(Bi(H_2O)SiW_{11}O_{39})_4]^{20-}$ (**7**), and not the expected 1:2 complex. Upon recrystallization of **7,**

$[Bi(H_2O)SiW_{11}O_{39}]^{5-}$ (**8**) was formed which exists as an infinite one-dimensional structure;

$\{[Bi(H_2O)SiW_{11}O_{39}]^{5-}\}_\infty$ in the solid state.

4.2.3.1 Infrared (IR) spectroscopy

Fourier transform infrared (IR) spectra were recorded for **K-7** and **K-8.**
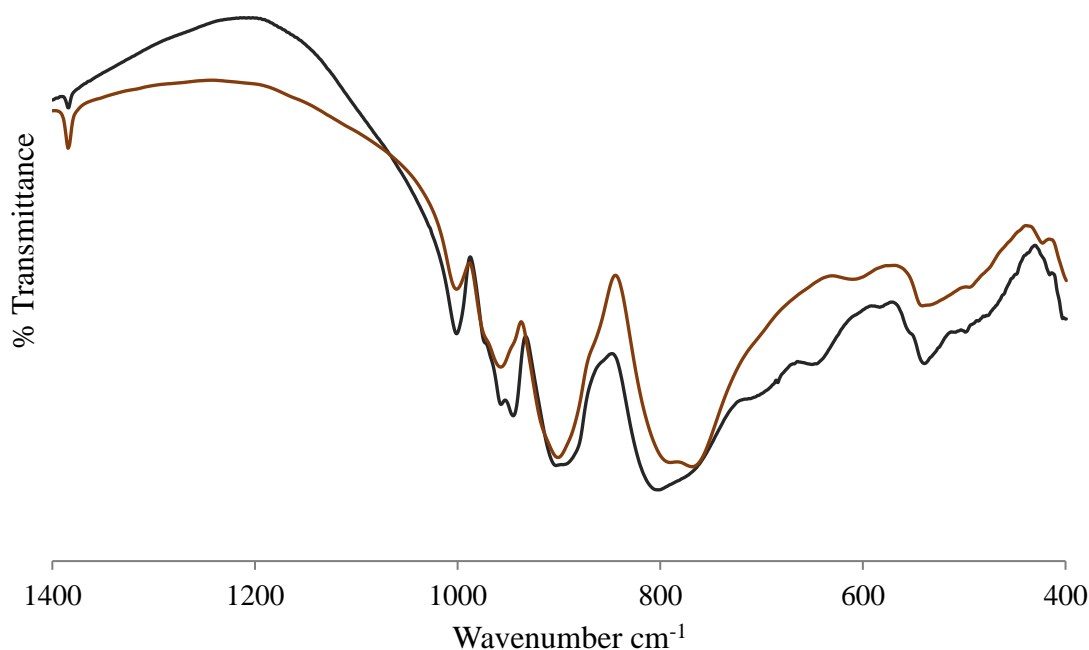
Figure 4.17. FT-IR spectra of **K-7** (dark orange) and the **K-8** (black).

In both spectra, the vibration band around 1000 cm^{-1} corresponds to Si-O stretching modes from the SiO$_4$ heterogroup. The W-O$_{terminal}$ and W-O$_{bridging}$-W stretching bands appear in the 1000-770 cm^{-1} region of the spectrum. The peaks around 711 cm^{-1} in all spectra can be assigned to Bi-O bond vibrations.

4.2.3.2 Thermogravimetric analyses

The thermal stabilities of **K-7** and **K-8** were monitored by thermogravimetric analysis (TGA). The weight loss from 20 ºC to around 200 ºC (6%) in the thermogram of **K-7** belongs to the loss of all 40 crystal water molecules and the covalently coordinated water molecules. Similarly, for **K-8**, the 6.5% weight loss from 25°C to about 200 °C is assigned to the loss of 12 crystal water molecules and the one coordination water molecule.
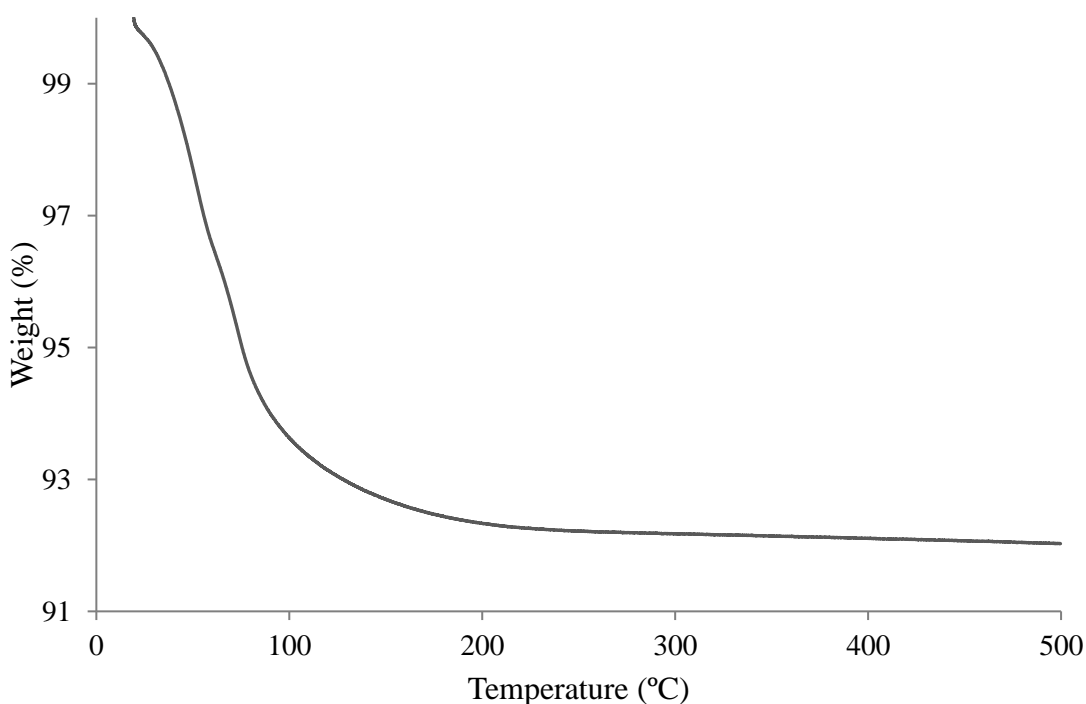
Figure 4.18. Thermogram of **K-7**.
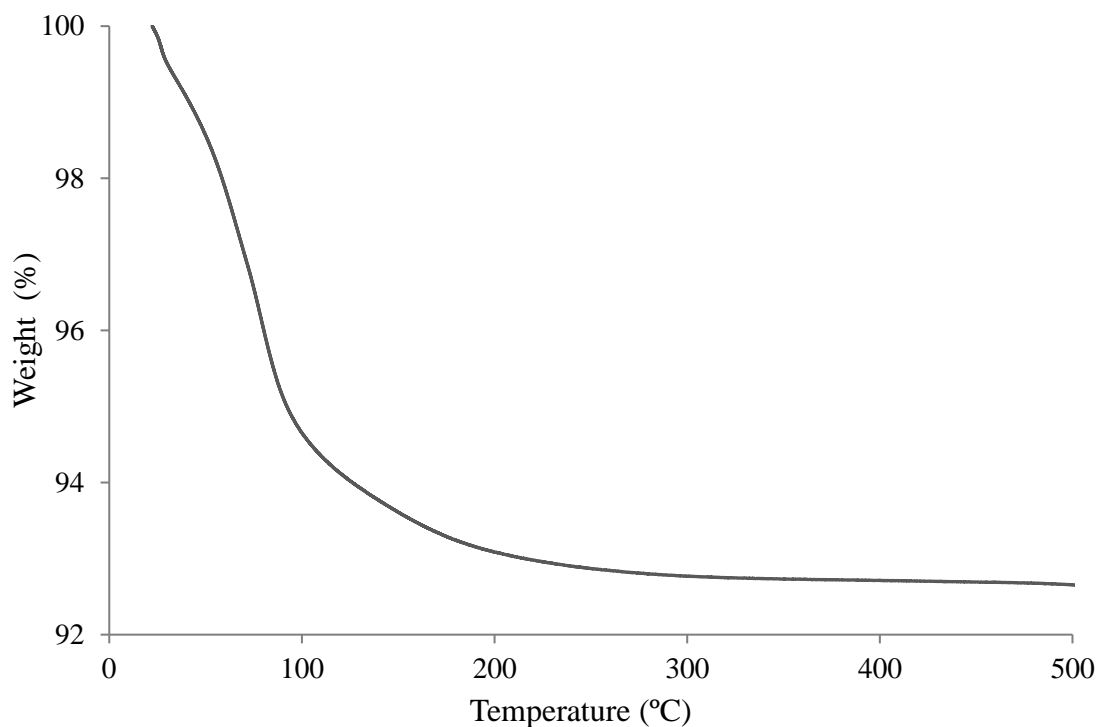
Figure 4.19. Thermogram of **K-8**.

4.2.3.3 UV-Visible spectroscopy

UV-Visible measurements of **K-7** in H_2O (4µg/ml, pH 5) were recorded at intervals for 24 hours in order to investigate the solution properties of the compound. The spectrum shows an absorption peak at 250 nm whose intensity/absorbance is unchanged for 24 hours but decreases by 16% after 48 hrs. This is consistent with the structural changes that take place when **K-7** is recrystallized in water forming **K-8**. Therefore polyanion **7** can be viewed as an intermediate product in the formation of polyanion **8**.
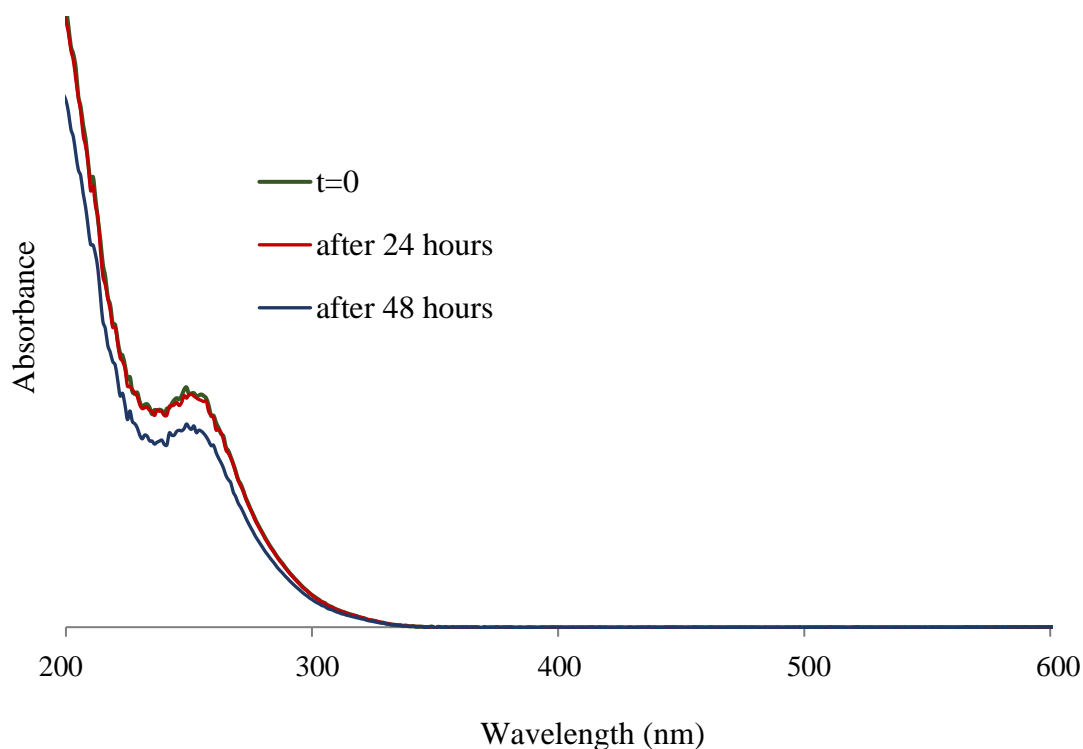
Figure 4.20. UV-Vis spectrum of **K-7** in H_2O (4µg/ml, pH 5) at different time intervals.

4.2.3.4 Structural description

Polyanion **7** crystallizes as the hydrated potassium salt $K_{20}[(Bi(H_2O)SiW_{11}O_{39})_4] \cdot 40H_2O$ in the tetragonal space group I 4_1/a. Single-crystal X-ray diffraction reveals that polyanion **7** is composed of four monolacunary Keggin units; $[\alpha\text{-SiW}_{11}O_{39}]^{8-}$ which are connected to each other by four Bi^{3+} ions to form a tetrameric structure. A Bi^{3+} ion fills the vacant position in $[\alpha\text{-SiW}_{11}O_{39}]^{8-}$ that would otherwise be occupied by a W-O unit leading to a complete Keggin structure. In the monolacunary fragments, all four Si atoms show a tetrahedral coordination environment, and all W centres exhibit an octahedral coordination geometry. Each Bi^{3+} ion is coordinated to six oxygen atoms resulting in a distorted octahedron. This coordination number of Bi^{3+} is unprecedented in POM chemistry. More precisely, Bi^{3+} connect to all the four O atoms from a $[\alpha\text{-SiW}_{11}O_{39}]^{8-}$ vacant site via three μ_2-O atoms leading to Bi-O bond lengths in the range of 2.082(1)- 2.246(1) Å and one μ_3-O atom with Bi-O distance of 2.152(1) Å. To achieve

the octahedral coordination geometry, Bi^{3+} connects to one μ_3-O atom from another $[\alpha$-$SiW_{11}O_{39}]^{8-}$ unit (Bi-O length is 2.810 Å) and to one free aqua ligand (Bi-OH$_2$) with a bond length of 2.667(2) Å.
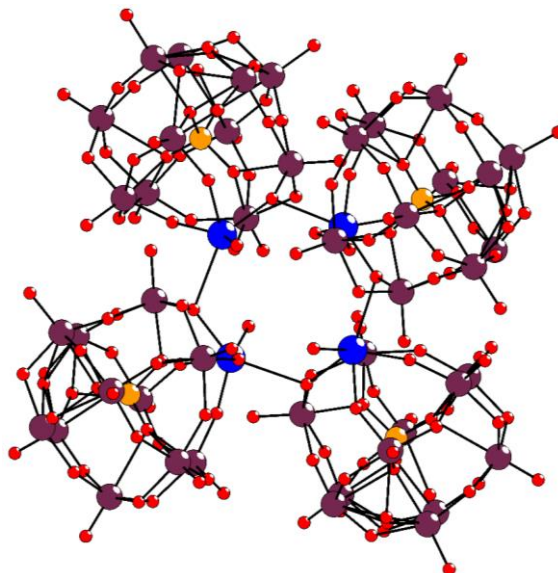
Figure 4.21. Ball-and-stick representation of $[(Bi(H_2O)SiW_{11}O_{39})_4]^{20-}$ (**7**). Colour code: W, dark-pink; Bi, blue; Si, orange; O, red.

When the cubic shaped crystals of **K**-**7** are dissolved in water, long needles of **K**-**8** form. The polyanion, $\{[Bi(H_2O)SiW_{11}O_{39}]^{5-}\}_\infty$ (**8**) consists of $[\alpha$-$SiW_{11}O_{39}]^{8-}$ units that are connected to each other via Bi^{3+} ions leading to an infinite one-dimensional zig-zag structure in the solid state. The Bi^{3+} ions are coordinated by seven oxygen atoms resulting in a distorted capped trigonal prism coordination environment. This coordination number of Bi^{3+} is unprecedented in POM chemistry.
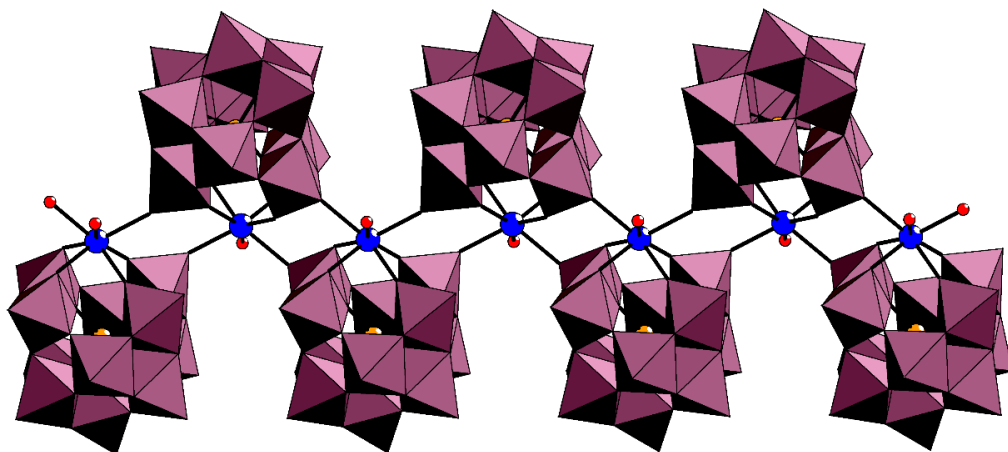
Figure 4.22. Combined polyhedral/ball-and-stick representation of $\{[Bi(H_2O)SiW_{11}O_{39}]^{5-}\}_\infty$ (**8**). Colour code: WO_6, dark-pink octahedra; Bi, blue; Si, orange; O, red.

Bi^{3+} connects to all the four O atoms of the $[\alpha\text{-}SiW_{11}O_{39}]^{8-}$ vacant site via four μ_2-O atoms leading to Bi-O bond lengths in the range of 2.320(11) - 2.381(12) Å and to two terminal oxygen atoms (μ_2-O), each from one tungsten centre of the lacunary site of two other $[\alpha\text{-}SiW_{11}O_{39}]^{8-}$ units (Bi-O length is 2.562(11) and 2.584(10) Å) and to one free aqua ligand (Bi-OH_2) with a bond length of 2.498(12) Å.
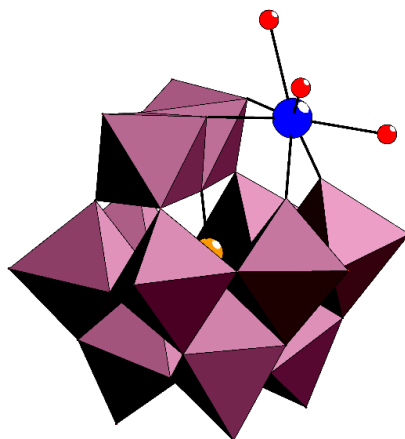
Figure 4.23. Combined polyhedral/ball-and-stick representation of the monomer $[Bi(H_2O)SiW_{11}O_{39}]^{5-}$ (**8**). showing the coordination environment of Bi^{3+}. Colour code: WO_6, dark-pink octahedra; Bi, blue; Si, orange; O, red.

The reactivity of monolacunary $[\alpha\text{-}XW_{11}O_{39}]^{n-}$ with several electrophiles has been well studied.

In 1971, Peacock and Weakley reported the first 1:1 and 1:2 complexes; $[Ln(\alpha\text{-}XW_{11}O_{39})]^{n-}$

and $[Ln(\alpha\text{-}XW_{11}O_{39})_2]^{n\text{-}}$.[6] Many 1:2 complexes have been isolated, but it was not until 2000 that a new series of 1:1 complexes $[Ln(\alpha\text{-}SiW_{11}O_{39})(H_2O)_3]^{5\text{-}}$ (Ln = Ce^{3+}, La^{3+}) was reported by Pope and co-workers. $[La(\alpha\text{-}SiW_{11}O_{39})(H_2O)_3]^{5\text{-}}$ is similar to the novel $[Bi(H_2O)SiW_{11}O_{39}]^{5\text{-}}$ in that they both exist as one-dimensional infinite chains in the solid state. However, La^{3+} is coordinated to nine oxygen atoms as compared to seven in polyanion **8**.[19]. Since then, several 1:1 complexes have been reported incorporating trivacant lanthanide ions such as Ce^{3+}, Nd^{3+}, Eu^{3+}, Gd^{3+} and Yb^{3+} leading to one dimensional infinite structures like our polyanion **8**.[20-21] This finding further reinforces our suggestion that Bi^{3+} can indeed mimic the chemistry of Ln^{3+} ions in POM chemistry

4.2.3.5 ^{183}W-NMR spectroscopy

We also performed ^{183}W-NMR spectroscopy of **K-8** dissolved in water and the spectrum obtained exhibits five signals at -69.6, -111.8, -114.8, -135.9 and -155.5 ppm (**Figure 4.23**) which is not in agreement with the structure of the polyanion as shown by single crystal XRD. If the structure of polyanion **8** is maintained in solution, we expect six signals which are characteristic of the $[\alpha\text{-}SiW_{11}O_{39}]^{8\text{-}}$ group with an intensity ratio are 2:2:1:2:2:2.[22] However, only five signals with apparent intensity ratio 1:4:1:1.5:1.5 were observed.

Table 4.9. Comparison of ^{183}W-NMR chemical shifts (ppm) of $[\alpha\text{-}SiW_{11}O_{39}]\cdot H_2O$ and polyanion **8**.

$[\alpha\text{-}SiW_{11}O_{39}]^{8\text{-}}$	-95.8, -113.1, -118.1, -124.9, -138.9, -172.9
$[Bi(H_2O)SiW_{11}O_{39}]^{5\text{-}}$ (**8**)	-69.6, -111.8, -114.8, -135.9, -155.5
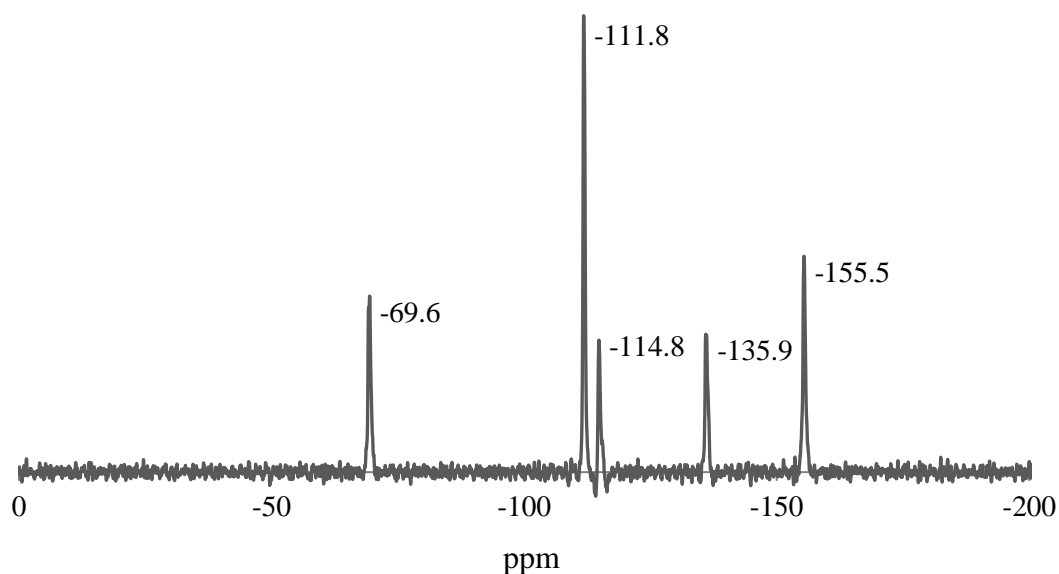
Figure 4.24. ^{183}W NMR spectrum of **K-8** dissolved in H_2O/D_2O (pH 3.4) at room temperature.

A comparison of the chemical shifts of the monolacunary precursor and polyanion **8** presented some questions about the identity of the species in solution when **K-8** is dissolved in water. The unjustifiable relative intensities of the signals (1:4:1:1.5:1.5), especially the signal at -111.8 ppm, raised questions about possible species responsible for it. As such, we performed a control experiment where an excess amount of $Na_4[SiW_{12}O_{40}]\cdot H_2O$ (the most probable species) was added to the NMR solution of **K-8** and then a ^{183}W NMR spectrum recorded.

Table 4.10. ^{183}W-NMR chemical shifts of **K-8** before and after the addition of solid $Na_4[SiW_{12}O_{40}]\cdot H_2O$.

Polyanion **8**	Polyanion **8** + $[SiW_{12}O_{40}]^{4-}$
-69.6	-72.1
	-101.8
-111.8	-112.9
-114.8	-116.4
-135.9	-137.5
-155.5	-157.5

From the resulting spectrum in **Figure 4.24**, we could rule out the assumption that the signal at -111.8 ppm could be $[SiW_{12}O_{40}]^{4-}$ since this polyanion has a distinct chemical shift of -101.8 ppm which is seen as the new additional signal observed in the spectrum of **K-8**. At this point, it is not clear which species is responsible for the signal at ~ 112 ppm. It cannot be excluded that this signal actually corresponds to two overlapping signals, but further studies are needed to shed more light on this issue.
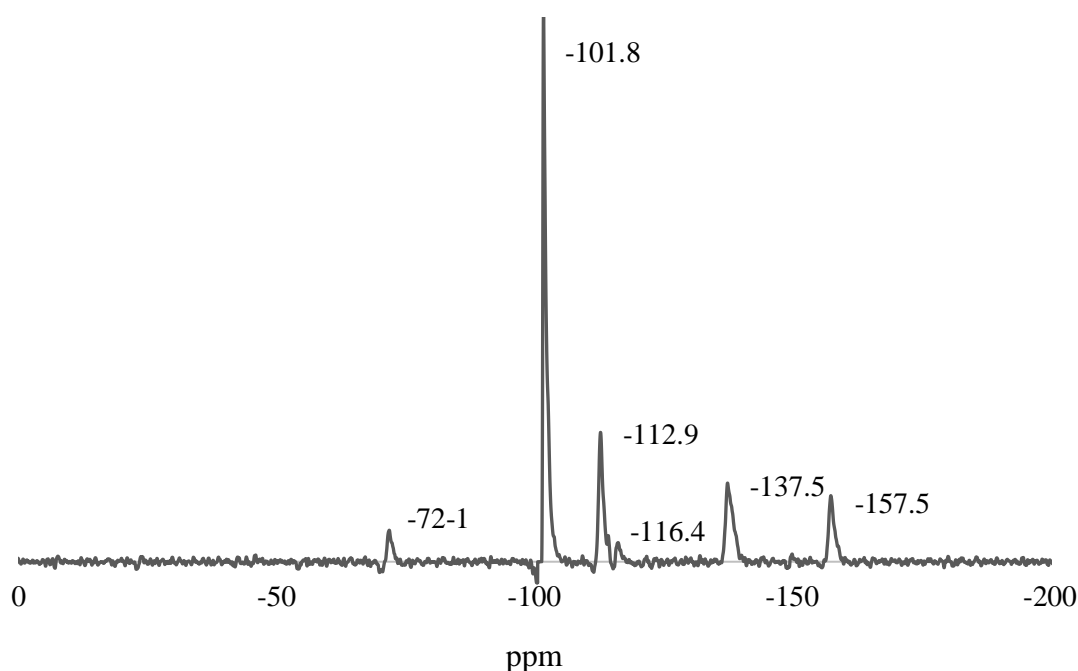
Figure 4.24. ^{183}W NMR spectrum of **K-8** after the addition of $Na_4[SiW_{12}O_{40}]\cdot H_2O$ in H_2O/D_2O ((pH 2.6) at room temperature.

4.2.4   Conclusions

We have synthesized and structurally-characterized two novel 1:1 Keggin-type heteropolytungstates; $[(Bi(H_2O)SiW_{11}O_{39})_4]^{20-}$ (**7**) and $\{[Bi(H_2O)SiW_{11}O_{39}]^{5-}\}_\infty$ (**8**). The tetramer and the infinite one-dimensional complexes were synthesized via one-pot procedure in aqueous media and structurally characterized in the solid state and in solution by standard analytical techniques. The novel polyanions comprise a Bi^{3+} ion inserted in the lacunary site of $\{SiW_{11}\}$ leading to different coordination numbers of Bi^{3+} (six and seven). Such coordination

modes are still rare for Bi^{3+}. Polyanion **7** is composed of four monolacunary Keggin units, $[\alpha\text{-}SiW_{11}O_{39}]^{8-}$ which are connected to each other by four Bi^{3+} ions to form a tetrameric structure. The 6-coordinated Bi^{3+} ions connect to all the four O atoms from a $[\alpha\text{-}SiW_{11}O_{39}]^{8-}$ vacant site, to one μ_3-O atom from another $[\alpha\text{-}SiW_{11}O_{39}]^{8-}$ unit and to a free aqua ligand. In polyanion **8**, Bi^{3+} connects to all the four O atoms from a $[\alpha\text{-}SiW_{11}O_{39}]^{8-}$ vacant site via four μ_2-O atoms and to two terminal oxygen atoms (μ_2-O), each from one tungsten centre of two $[\alpha\text{-}SiW_{11}O_{39}]^{8-}$ subunits. Such a coordination mode (coordination number 7) is still rare for Bi^{3+} and is unprecedented in heteropolytungstate chemistry and suggest that Bi^{3+} mimics the chemistry of lanthanides.

4.3 References

[1]   C. Boglio, G. Lenoble, C. Duhayon, B. Hasenknopf, R. Thouvenot, C. Zhang, R. C. Howell, B. P. Burton-Pye, L. C. Francesconi, E. Lacôte, S. Thorimbert, M. Malacria, C. Afonso, J. Tabetet, *Inorg. Chem.* **2006**, *45*, 1389–1398.

[2]   U. Kortz, C. Holzapfel, M. Reicke, *J. Mol. Struct.* **2003**, *656*, 93–100.

[3]   M. A. Fedotov, B. Z. Pertsikov, D. K. Danovich, *Polyhedron* **1990**, *9*, 1249–1256.

[4]   C. Zhang, R. C. Howell, D. McGregor, L. Bensaid, S. Rahyab, M. Nayshtut, S. Lekperic, L. C. Francesconi, *Compt. Rend. Chim.* **2005**, *8*, 1035–1044.

[5]   B. S. Bassil, U. Kortz, *Z. Anorg. Allg. Chem.* **2010**, *636*, 2222–2231.

[6]   R. D. Peacock, T. J. R. Weakley, *J. Chem. Soc. (A).* **1971**, 1836–1839.

[7]   S. A. Zubairi, S. M. Ifzal, A. Malik, *Inorg. Chim. Acta.* **1977**, *22*, L29–L30.

[8]   J. Iijima, H. Naruke, *Inorg. Chim. Acta.* **2011**, *379*, 95–99.

[9]   C. Rong, J. Liu, X. Chen, E. Wang, *Inorg. Chim. Acta.* **1987**, *130*, 265–269.

[10]   Q. Lunyu, W. Shouguo, P. Jun, C. Yaguang, W. Guang, *Polyhedron.* **1992**, *11*, 2645–

2649.

[11]   N. Haraguchi, Y. Okaue, T. Isobe, Y. Matsuda, *Inorg. Chem.* **1994**, *33*, 1015–1020.

[12]   J. Bartis, M. Dankova, J. J. Lessmann, Q. Luo, W. D. Horrocks,, L. C. Francesconi, *Inorg. Chem.* **1999**, *38*, 1042–1053.

[13]   B. S. Bassil, M. H. Dickman, B. von der Kammer, U. Kortz, *Inorg. Chem.* **2007**, *46*, 2452–2458.

[14]   J. Iijima, E. Ishikawa, Y. Nakamura, H. Naruke, *Inorg. Chim. Acta* **2010**, *363*, 1500–1506.

[15]   M. N. K. Wihadi, A. Hayashi, K. Ichihashi, H. Ota, S. Nishihara, K. Inoue, N. Tsunoji, T. Sano, M. Sadakane, *Eur. J. Inorg. Chem.* **2019**, *2019*, 357–362.

[16]   J. Bartis, S. Sukal, M. Dankova, E. Kraft, R. Kronzon, M. Blumenstein, L. C. Francesconi, *Dalton. Trans.* **1997**, 1937–1944.

[17]   M. Sadakane, A. Ostuni, M. T. Pop, *Dalton. Trans.* **2002**, *2*, 63–67.

[18]   N. Ncube, S. Bhattacharya, D. Thiam, J. Goura, A. S. Mougharbel, U. Kortz, *Eur. J. Inorg. Chem.* **2019**, 363–366.

[19]   M. Sadakane, M. H. Dickman, M. T. Pope, *Angew. Chem. Int. Ed.* **2000**, *39*, 2914–2916.

[20]   H. T. Evans, T. J. R. Weakley, G. B. Jameson, *Dalton. Trans.* **1996**, 2537–2540.

[21]   P. Mialane, L. Lisnard, A. Mallard, J. Marrot, E. Antic-Fidancev, P. Aschehoug, D. Vivien, F. Sécheresse, *Inorg. Chem.* **2003**, *42*, 2102–2108.

[22]   R. Acerete, C. F. Hammer, L. C. W. Baker, *J. Am. Chem. Soc.* **1982**, *104*, 5384–5390.

CHAPTER 5. LEAD-CONTAINING POLYOXOMETALATES

5.1 Synthesis and Characterization of Lead(II)-Containing Heteropolytungstates, $\{[Pb(\alpha\text{-}XW_{11}O_{39})]^{6-}\}_{\infty}$ (X = Si , Ge)

In this section we report the results of the interaction of Pb^{2+} ions with mono-lacunary Keggin polyanions. The novel polyanions; $[Pb(\alpha\text{-}XW_{11}O_{39})]^{6-}$ X = Si (**9**) and Ge(**10**) that exist in the solid state as infinite one-dimensional structures, were synthesized following one-pot procedures in aqueous media and structurally characterized in the solid state and in solution by standard analytical techniques. The novel polyanions comprise a Pb^{2+} ion that is connected to the lacunary site of $[\alpha\text{-}XW_{11}O_{39}]^{8-}$ through its four oxygen atoms and to three oxygens of a neighbouring $[\alpha\text{-}XW_{11}O_{39}]^{8-}$ leading to an infinite one-dimensional structure;$\{[Pb(\alpha\text{-}XW_{11}O_{39})]^{6-}\}_{\infty}$. Polyanions **9** and **10** are structural analogues of $[PbGaW_{11}O_{39}]^{7-}$ which was reported 38 years ago. Our work suggests that Pb^{2+} can mimic the structural chemistry of Ln^{3+} ions in POM chemistry.
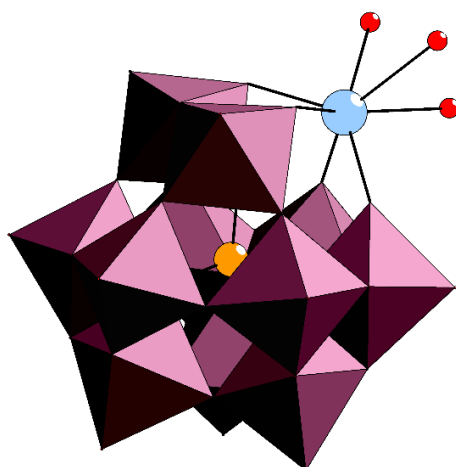
Figure 5.1. Combined polyhedral/ball-and-stick representations of $[Pb(\alpha\text{-}XW_{11}O_{39})]^{6-}$ (X = Si, Ge). Colour code: WO_6, dark-pink octahedra; Pb, light-blue; X, orange; O, red.

5.1.1   Synthesis

$K_6[Pb(\alpha\text{-}SiW_{11}O_{39})]\cdot 12H_2O$ (K-9)

Procedure 1: A solution of the POM precursor $K_8[\beta_2\text{-}SiW_{11}O_{39}]\cdot 14H_2O$ (0.305 g, 0.094 mmol) was prepared by dissolving it in 10 ml 1 M KCl solution. To this solution solid $PbCl_2$ (0.042 g, 0.151 mmol) was added under vigorous stirring. The resulting solution was heated at 50 °C for 90 minutes and filtered while hot. The pH of the solution was 4.9. Thin, colourless needle-shaped crystals formed upon cooling and the solution was left for evaporation open to the air and after a week the crystals of **K-9** were collected. Yield: 73 mg, 23% (based on W). The 12 waters of crystallization were determined by TGA (**Figure 5.5**). *The product of this reaction was utilized for IR spectroscopy, XRD crystallography and TGA.*

Procedure 2: A solution of the POM precursor $K_8[\alpha\text{-}SiW_{11}O_{39}]\cdot 13H_2O$ (0.303 g, 0.094 mmol) was prepared by dissolving it in 10 ml 1 M KCl solution. To this solution solid $Pb(NO_3)_2$ (0.05 g, 0.151 mmol) was added under vigorous stirring. The resulting solution was heated at 50 °C for 90 minutes and filtered while hot. The pH of the solution was 4.24. Thin, colourless needle-shaped crystals formed upon cooling. Yield: 165 mg, 51% (based on W and assuming same formulae as **K-9**).

$K_6[Pb(\alpha\text{-}GeW_{11}O_{39})]\cdot 16H_2O$ (K-10).

Procedure 1: A solution of the POM precursor $K_8[\beta_2\text{-}GeW_{11}O_{39}]\cdot 14H_2O$ (0.309 g, 0.094 mmol) was prepared by dissolving it in 10 ml 1 M KCl solution. To this solution solid $PbCl_2$ (0.042 g, 0.151 mmol) was added under vigorous stirring. The resulting clear solution was heated at 50 °C for 1 hour and filtered while hot. The pH of the solution was 4.5. Colourless needle-shaped crystals of **K-10** formed upon cooling. Yield: 35 mg, 11% (based on W). The 16 waters of crystallization were determined by TGA (**Figure 5.6**). *The product of this reaction was utilized for IR spectroscopy, XRD crystallography and TGA.*

Procedure 2: Solid $Pb(NO_3)_2$ (0.05 g, 0.151 mmol) was added (with vigorous stirring) to a 10 ml solution of [α-$GeW_{11}O_{39}$] (0.304 g, 0.094 mmol) in 1M KCl. The resulting solution was heated at 50 °C for 90 minutes and filtered while hot. The pH of the solution was 4.67. Thin, colourless needle-shaped crystals formed upon cooling. Yield: 93 mg, 29% (based on W and assuming same formulae as **K-10**). *The product of this reaction was utilized for IR spectroscopy, XRD crystallography and TGA.*

5.1.2   Single-Crystal X-Ray Diffraction

Table 5.1. Crystal data and structure refinement for **K-9 and K-10.**

Compound	**K-9**	**K-10**
Formula Weight (gm/mol)	6517.28	6651.34
Crystal System	Orthorhombic	Orthorhombic
Space Group	Pna2$_1$	Pna2$_1$
a (Å)	17.6667(14)	17.6892(4)
b (Å)	20.5563(16)	20.5706(6)
c (Å)	13.7032(11)	13.6707(4)
α (º)	90	90
ß (º)	90	90
γ (º)	90	90
Volume (Å^3)	4976.5(7)	4974.5(2)
Z	2	2
D$_{calc.}$ (gm/cm^3)	5.966	4.321
Absorption Coefficient (mm^{-1})	58.386	31.236
F(000)	7317	5532
θ range for data collection	1.520 to 25.100	2.733 to 25.074
Completeness to θ$_{max}$	99.7%	99.6%
Index Ranges	-21<=h<=21, -24<=k<=24, -16<=l<=16	-21<=h<=20, -24<=k<=23, -16<=l<=15
Reflections Collected	74316	30422
Unique Reflections	8837	8281
Data/Restraints/Parameters	8837 / 1 / 301	8281 / 283 / 570
Goodness of Fit on F^2	1.531	1.033
R$_1$[a] (I>2σ(I))	0.0539	0.0736
wR$_2$[b] (all data)	0.1932	0.1437

[a] $R_1 = \Sigma ||F_0| - |F_c|| / \Sigma |F_0|$, [b] $wR_2 = [\Sigma w(F_0^2 - F_c^2)^2 / \Sigma w(F_0^2)^2]^{1/2}$

5.1.3   Results and Discussion

Despite the great progress achieved in POM chemistry there are still some areas that remain less explored. POMs containing heavier post-transition metals such as bismuth and lead are still rare. This is especially true when considering complexes where bismuth or lead play the role of secondary heteroatoms vs primary (central) heteroatoms (for example, in [BiW$_9$O$_{33}$]$^{9-}$). The reaction of [β_2-SiW$_{11}$O$_{39}$]$^{8-}$ with Bi^{3+} in Chapter 5 of this dissertation resulted in the formation of [Bi(H$_2$O)SiW$_{11}$O$_{39}$]$^{5-}$ (**8**). We were thus motivated to explore reactions of the β_2-

monolacunary POM precursors with Pb^{2+} since it is isoelectronic to Bi^{3+} ([Xe] $6s^2 4f^{14} 5d^{10}$). If Bi^{3+} can mimic the chemistry of lanthanide ions in POM chemistry, then based on the similar structural properties of Pb^{2+}, we expected that it would behave like Bi^{3+} and Ln^{3+} ions.

5.1.3.1 Infrared (IR) spectroscopy

Fourier transform infrared (IR) spectra were recorded for **K-9** and **K-10**.. The spectrum of **K-9** shows a vibration band at 993 cm^{-1} which is characteristic of Si-O stretching modes from the SiO_4 heterogroup. In the spectrum of **K-10**, the vibration band around 803 cm^{-1} correspond to Ge-O stretching modes from the GeO_4 heterogroup. The $W-O_t$ and $W-O_b-W$ stretching bands appear in the 950-700 cm^{-1} region of the spectrum.
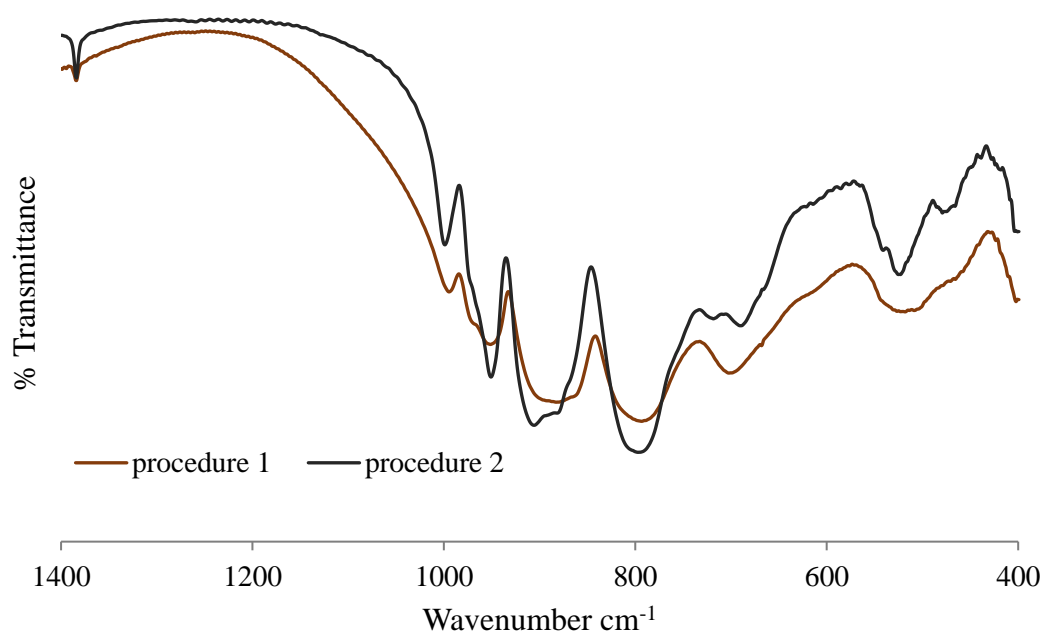
Figure 5.2. FT-IR spectrum of **K-9**.
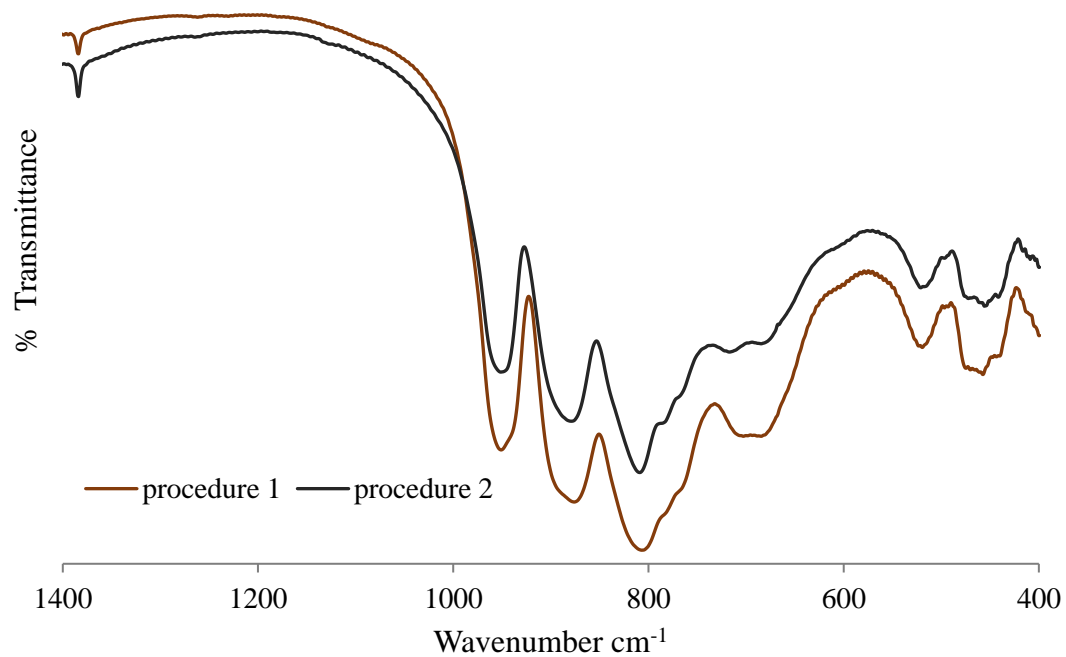
Figure 5.3. FT-IR spectra of **K-10**.
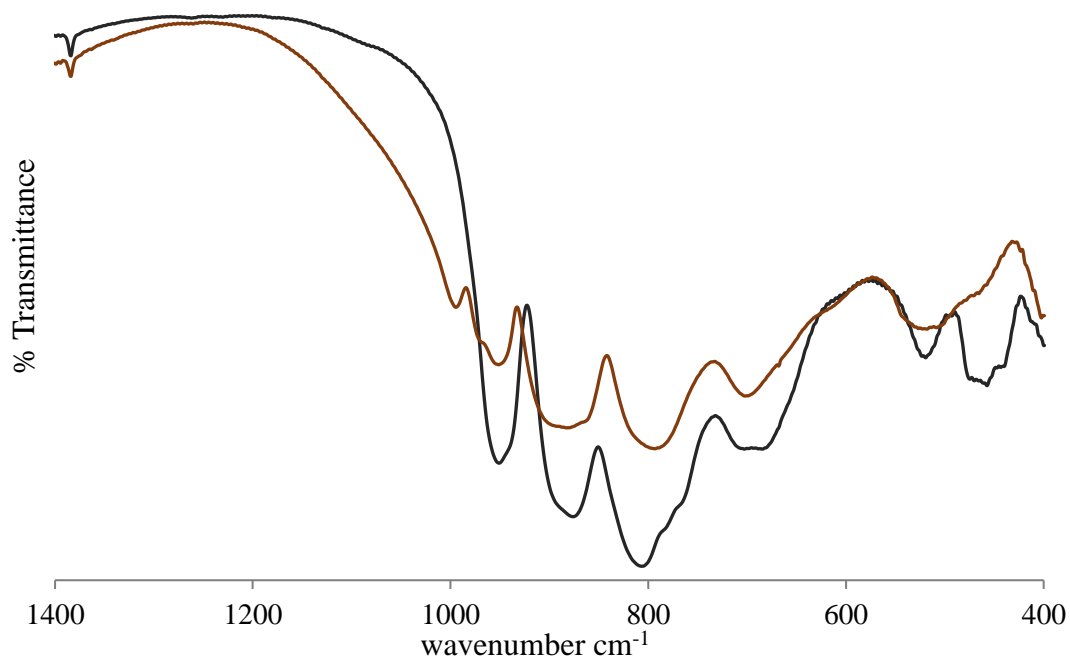
Figure 5.4. FT-IR spectra of **K-9** (dark orange) and **K-10** (black).

5.1.3.2 Thermogravimetric analysis

The thermal stability and amount of crystal water molecules of **K-9** and **K-10** were monitored

by thermogravimetric analysis (TGA). All the 12 crystallization waters in **K-9** were lost from

room temperature to 200 ℃. This accounts for 6.4 % total weight loss. The 16 waters of

crystallization of **K-10** were lost from room temperature to 200 ℃ and this accounts for an

8.3% total weight loss.
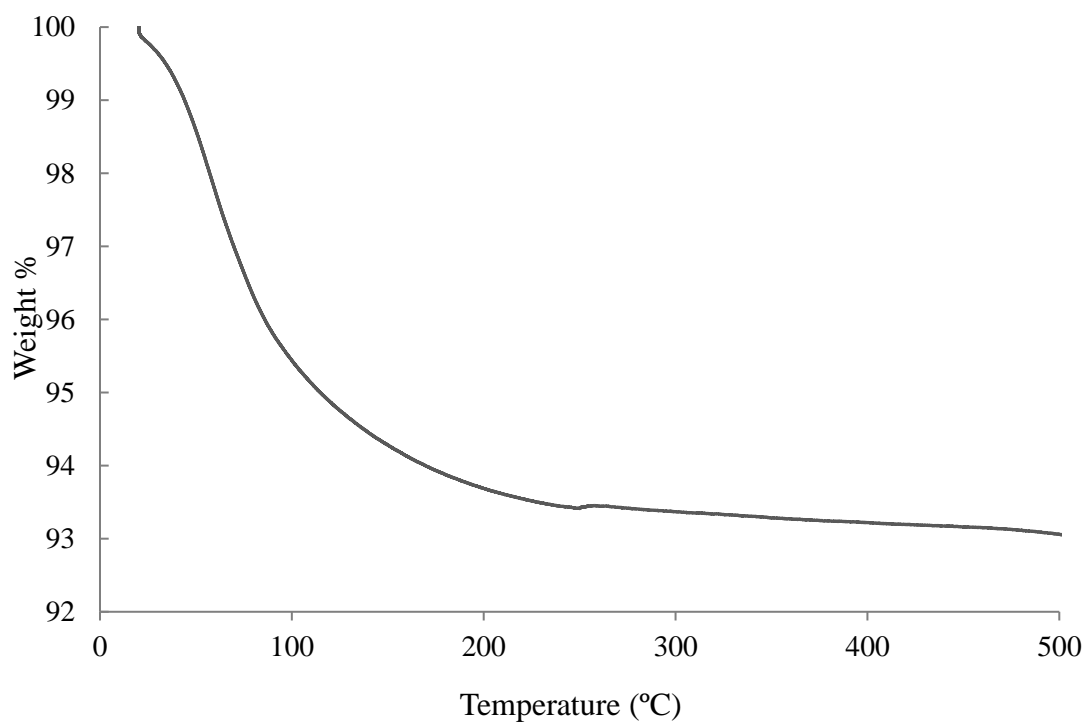
Figure 5.5. Thermogram of **K-9**.
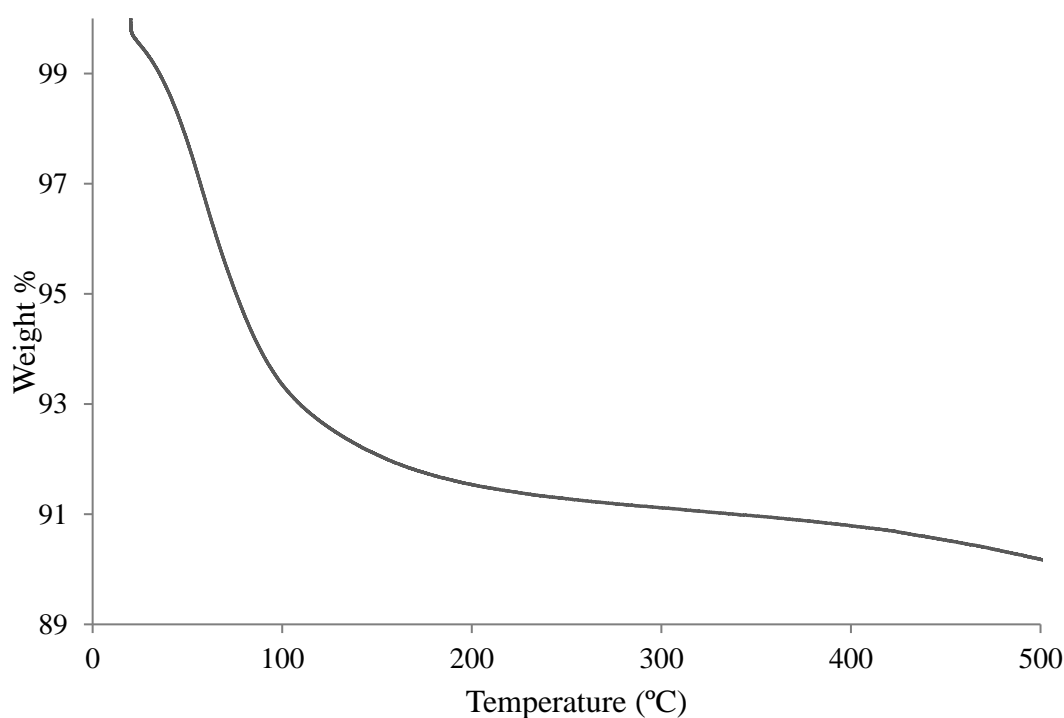
Figure 5.6. Thermogram of **K-10**.

5.1.3.3 Structural description

The two 1:1 lead(II)-substituted Keggin-type polyoxotungstates **K-9** and **K-10** both crystallize as isomorphous K salts in the Orthorhombic space group Pna2$_1$. Single-crystal X-ray diffraction reveals that both polyanion **9** and **10** exhibit an infinite one-dimensional structure $\{[Pb(\alpha\text{-}XW_{11}O_{39})]^{6-}\}_{\infty}$ where the monomeric unit: $[Pb(\alpha\text{-}XW_{11}O_{39})]^{6-}$ (X = Si, Ge) consists of a monolacunary Keggin unit; $[\alpha\text{-}XW_{11}O_{39}]^{8-}$ where a Pb^{2+} ion occupies the vacant position leading to a complete Keggin structure. As expected, the less stable $[\beta_2\text{-}SiW_{11}O_{39}]^{8-}$ isomerized in an aqueous acidic medium to the more stable α-isomer $[\alpha\text{-}SiW_{11}O_{39}]^{8-}$.[1]
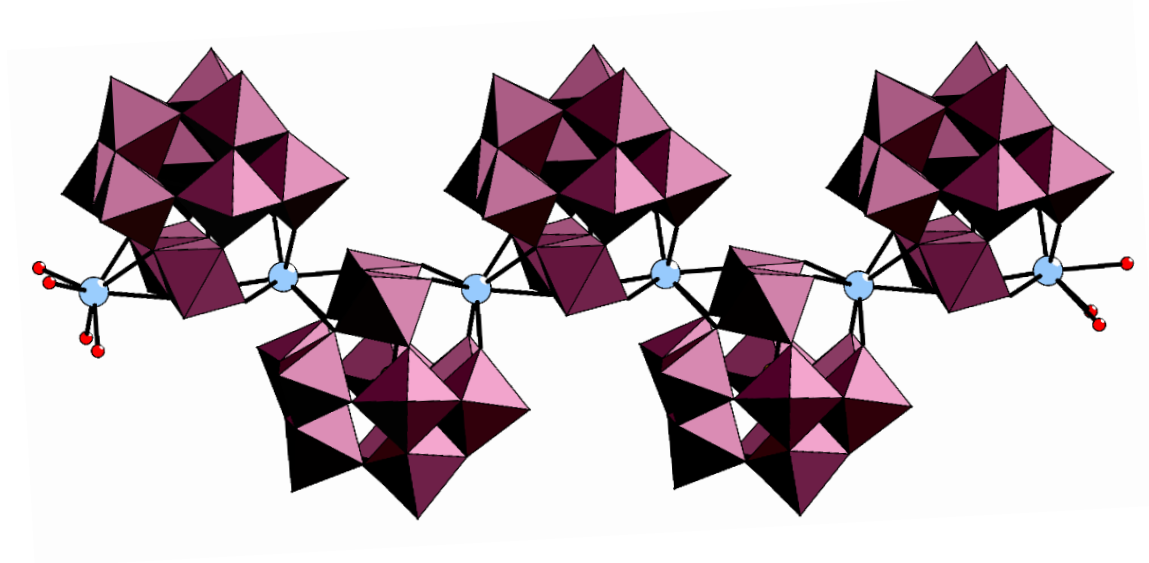
Figure 5.7. Combined polyhedral/ball-and-stick representations of $\{[Pb(\alpha\text{-}XW_{11}O_{39})]^{6\text{-}}\}_\infty$, X = Si (**9**), Ge (**10**) Colour code: WO_6, dark-pink octahedra; Pb, light blue; X, orange; O, red.

Due to the isostructural nature of **9** and **10**, only polyanion **10** is described here in detail as a representative of the two polyanions. The addenda atoms in polyanion **10** are arranged in 4 different groups: three W_3O_{13} triads; W(9)-W(10)-W(11), W(6)-W(7)-W(8) and W(3)-W(4)-W(5), as well as another group of two edge shared tungsten atoms; W(1)-W(2) (what remains of the fourth triad after the removal of a W-O unit). Pb^{2+} atom is located in the lacunary site therefore completing the triad. A closer look at the W-W distances in each W-W-W triad as well as in W-W-Pb triad shows that the W(1)-W(2) distance in the W-W-Pb triad is 3.335(24) Å while the W(9)-W(10), W(9)-W(11) and W(10)-W(11) distances in one W-W-W triad are 3.363(23) Å, 3.365(26) Å and 3.371(26) Å, respectively. From this, it can be seen that the insertion of Pb^{2+} into the lacunary site leads to the shortening of the W-W distances in the W-W-Pb triad.
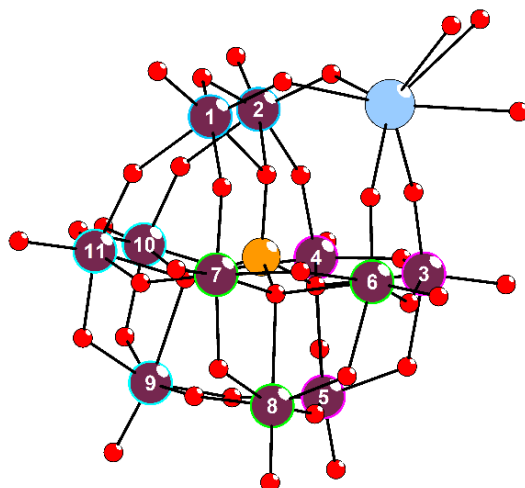
Figure 5.8. Ball-and-stick representations of $[Pb(\alpha\text{-}GeW_{11}O_{39})]^{6-}$ (**10**). Colour code: W, dark-pink (W atoms in the same triad have the same borders); Pb, light blue; Ge, orange; O, red.

The distances of W(1) and W(2) to the neighbouring W atoms e.g., W(1)-W(11) and W(2)-W(10) is 3.823(23) Å and 3.816(24) Å, respectively. When compared to the distances of W(8)-W(9) and W(7)-W(11) which are 3.726 (27) Å and 3.714 (28) Å respectively, it can be seen that there is an elongation of the distance between W(1) and W(2) with its neighbouring addenda atoms. The W(1)-Pb(1) and W(2)-Pb(1) distances are 3.801(24) Å and 3.821(24) Å respectively meaning that Pb^{2+} is greatly displaced from the position of the missing tungsten by ~ +0.45 Å for both W(1)-Pb and W(2)-Pb and this agrees with the large size of the Pb^{2+} ion (1.43 Å vs 0.6 Å for W^{6+}).

All tungsten atoms have a distorted octahedral coordination geometry which is well known for all Keggin based species. The oxidation state of +6 was confirmed by bond valence sum calculations)[2] where the average bond valence sum (BVS) of the tungsten atoms is 6.053.

Table 5.2. W-O bond lengths (Å) and bond valence sum (BVS) for W^{6+} ions in polyanion **10**.

W(1) BVS =6.210	O5	1.696(29)	W(2) BVS = 6.043	O10	1.717(27)
	O1	1.738(25)		O2	1.798(28)
	O8	1.948(25)		O6	1.928(27)
	O6	1.979(28)		O11	1.950(26)
	O9	2.142(28)		O12	2.081(27)
	O7	2.206(29)		O7	2.239(26)
W(3) BVS = 6.008	O13	1.736(41)	W(4) BVS = 6.061	O18	1.761(35)
	O3	1.768(26)		O14	1.876(26)
	O17	1.907(25)		O11	1.890(26)
	O14	1.996(26)		O20	1.91525)
	O16	2.061(32)		O19	1.921(29)
	O15	2.285(26)		O15	2.310(26)
W(5) BVS = 6.164	O21	1.687(29)	W(6) BVS = 5.605	O24	1.771(41)
	O16	1.883(28)		O4	1.804(29)
	O23	1.917(28)		O17	1.941(27)
	O22	1.927(28)		O25	2.007(31)
	O19	1.931(29)		O27	2.047(30)
	O15	2.408(26)		O26	2.316(28)
W(7) BVS = 6.148	O28	1.676(35)	W(8) BVS = 6.126	O31	1.689(32)
	O25	1.868(27)		O27	1.865(28)
	O8	1.914(25)		O22	1.903(29)
	O29	1.975(36)		O32	1.946(28)
	O30	1.987(28)		O29	1.970(39)
	O26	2.259(29)		O26	2.367(25)
W(9) BVS = 6.153	O33	1.681(27)	W(10) BVS = 5.912	O37	1.727(28)
	O34	1.897(29)		O12	1.860(27)
	O32	1.899(30)		O20	1.926(26)
	O36	1.936(38)		O38	1.955(28)
	O23	1.966(28)		O34	1.983(29)
	O35	2.332(24)		O35	2.295(24)
W(11) BVS = 6.154	O39	1.766(29)			
	O9	1.821(29)			
	O30	1.878(29)			
	O36	1.934(35)			
	O38	1.936(28)			
	O35	2.317(25)			

The oxidation state of the Pb atom is confirmed to be +2 by bond valence sum calculations[2]. The Pb^{2+} cation in both polyanions **9** and **10** can be described as being coordinated to 7 oxygen atoms resulting in a capped trigonal prismatic molecular geometry. Pb^{2+} ion is coordinated to the four available oxygen atoms belonging to the lacunary site of $[\alpha\text{-}XW_{11}O_{39}]^{8-}$ resulting in Pb-O bond lengths ranging from 2.354(20)- 2.454(10) Å for **9** and 2.382(29) to 2.502(26) Å for **10**. The remaining Pb-O bonds connect two $[\alpha\text{-}XW_{11}O_{39}]^{8-}$ subunits. The binding mode is different in that the oxygen atoms utilized are not from the vacant site of the polyanion. Pb^{2+} binds to one μ_2-O atom connecting tungsten atoms belonging to the same W_3O_{13} triad (edge sharing) and to two μ_2-O that connect two tungsten atoms from different triads (corner sharing). The resulting Pb-O bond lengths in **9** and **10** are in the ranges of 2.741(10) - 2.858(20) Å and 2.747(27) - 2.860(29) Å, respectively.

The structures of the polyanion $[Pb(\alpha\text{-}XW_{11}O_{39})]^{6-}$ (X = Si (**9**), Ge (**10**)) resemble the structure of the first structurally characterized Pb(II)-containing heteropolytungstate, $[PbGaW_{11}O_{39}]^{7-}$ which was described by Tourné *et al.* 40 years ago. The structure is a monolacunary tungstogallate where Pb^{2+} occupies the vacant site. The resulting coordination number of Pb^{2+} to $[\alpha\text{-}GaW_{11}O_{39}]^{9-}$ was four. [3] A careful look at the structure show that the Pb^{2+} ion in $[PbGaW_{11}O_{39}]^{7-}$ further coordinates with oxygen atoms from another monolacunary tungstogallate resulting in 6 coordination. The Pb-O bond lengths range from 2.37(4) - 2.86(4) Å as compared to 2.35(2) - 2.86(3) Å in polyanions $[Pb(\alpha\text{-}XW_{11}O_{39})]^{6-}$ (X = Si (**9**), Ge (**10**)). Such long bond lengths have been reported in Pb(II)-containing POMs for example in $[Pb(\gamma\text{-}SiW_{10}O_{32})_2(\mu\text{-}O)_4]^{6-}$ where Pb-O bond lengths range from 2.60 -2.90 Å.[4]

Table 5.3. Pb-O bond lengths (Å) for polyanions **9**, **10** and **[PbGaW₁₁O₃₉]⁷⁻**.[3]

Pb-O bond lengths (Å)		
9	**10**	**[PbGaW$_{11}$O$_{39}$]$^{7-}$**
2.354(20)	2.382(29)	2.37 (4)
2.358(10)	2.436(26)	2.37(4)
2.403(10)	2.453(29)	2.50(4)
2.454(10)	2.502(26)	2.50(4)
2.741(10)	2.747(27)	2.86(4)
2.762(20)	2.780(28)	2.86(4)
2.858(20)	2.860(29)	
Bond Valence Sum (BVS)		
2.236	2.246	1.966

The reactivity of $[\alpha\text{-XW}_{11}\text{O}_{39}]^{n-}$ has been extensively studied with several elements including trivacant lanthanides such as Ce^{3+}, La^{3+}, Nd^{3+}, Eu^{3+}, Gd^{3+} and Yb^{3+} leading to one dimensional infinite structures. [5-7] An example is $[Yb(H_2O)_2SiW_{11}O_{39}]^{5-}$ which consists of Yb^{3+} coordinated to four oxygen atoms of the lacunary site. The coordination sphere of the ion is completed by two water molecules, and one terminal-oxo ligand connecting two $[\alpha\text{-XW}_{11}\text{O}_{39}]^{8-}$ subunits resulting in a coordination number of 7.[7] In this dissertation we report that the reaction of $[\alpha\text{-XW}_{11}\text{O}_{39}]^{8-}$ with Bi^{3+} leads to the polyanion $[Bi(H_2O)SiW_{11}O_{39}]^{5-}$ (**8**) where the Bi^{3+} ion is inserted in the lacunary site of $[\alpha\text{-XW}_{11}\text{O}_{39}]^{8-}$ leading to a coordination numbers of seven. This coordination number of Yb^{3+} in $[Yb(H_2O)_2SiW_{11}O_{39}]^{5-}$ and Bi^{3+} in $[Bi(H_2O)SiW_{11}O_{39}]^{5-}$ suggests that both Bi^{3+} and Pb^{2+} ions, which behave similarly in their reaction with monovacant heteropolytungstates could mimic the chemistry of Ln^{3+} ions in POM chemistry.

5.1.4   Conclusions

We have synthesized and structurally characterized two novel Keggin-type lead(II)-containing heteropolytungstates: $[Pb(\alpha\text{-}XW_{11}O_{39})]^{6-}$ (X = Si , Ge). Both compounds were characterized in the solid state by standard analytical techniques. The novel polyanions **9** and **10** exist in the solid state as infinite one-dimensional structures built from the plenary Keggin ion $[\alpha\text{-}XW_{12}O_{40}]^{4-}$ (X=Si , Ge) which has lost one of the terminal W - O units. The monomeric unit: $[Pb(\alpha\text{-}XW_{11}O_{39})]^{6-}$ (X = Si , Ge) comprises a monolacunary Keggin unit; $[\alpha\text{-}XW_{11}O_{39}]^{8-}$ where a Pb^{2+} ion occupies the vacant position leading to a complete Keggin structure. The Pb^{2+} ion is coordinated by four oxygens of the monolacunary Keggin and three oxygens of a neighbouring $[\alpha\text{-}XW_{11}O_{39}]^{8-}$ resulting in a coordination number of 7. Polyanions **9** and **10** are structural analogues of $[PbGaW_{11}O_{39}]^{7-}$ reported 38 years ago. Our work suggests that Pb^{2+} can mimic the structural chemistry of Ln^{3+} ions in POM chemistry.

5.2 References

[1]   M. T. Pope, *Heteropoly and Isopoly Oxometalates*, Springer-Verlag, 1983.

[2]   K. Y. Matsumoto, A. Kobayashi, Y. Sasaki, *Bull. Chem. Soc. Jpn.* **1975**, *48*, 3146–3151.

[3]   G. F. Tourné, C. M. Tourné, A. Schouten, *Acta Crystallogr. B.* **1982**, *38*, 1414–1418.

[4]   A. Yoshida, Y. Nakagawa, K. Uehara, S. Hikichi, N. Mizuno, *Angew. Chem.* **2009**, *121*, 7189–7192.

[5]   H. T. Evans, T. J. R. Weakley, G. B. Jameson, *Dalton. Trans.* **1996**, 2537–2540.

[6]   M. Sadakane, M. H. Dickman, M. T. Pope, *Angew. Chem. Int. Ed.* **2000**, *39*, 2914–2916.

[7]   P. Mialane, L. Lisnard, A. Mallard, J. Marrot, E. Antic-Fidancev, P. Aschehoug, D. Vivien, F. Sécheresse, *Inorg. Chem.* **2003**, *42*, 2102–2108.

CHAPTER 6. SCANDIUM-CONTAINING POLYOXOMETALATES

6.1 Synthesis and Characterization of Di-Scandium(III)-30-Tungsto-4-Phosphate, $[(Na(H_2O))_2Sc_2(P_2W_{15}O_{56})_2]^{16-}$

This section presents the synthesis and structural characterization of a novel disubstituted scandium-30-tungsto-4-phosphate $[(Na(H_2O))_2Sc_2(P_2W_{15}O_{56})_2]^{16-}$ (**11**). This compound was synthesized as an aqueous-soluble sodium salt following a one pot procedure and characterized in solid state and solution by standard analytical techniques. The polyanion consists of two $[\alpha-P_2W_{15}O_{56}]^{12-}$ units that sandwich two Sc^{3+} and Na^+ ions. This is the first crystal structure of a scandium-containing tungstophosphate based on Wells-Dawson building blocks to be added to the small library of Sc-containing heteropolytungstates.
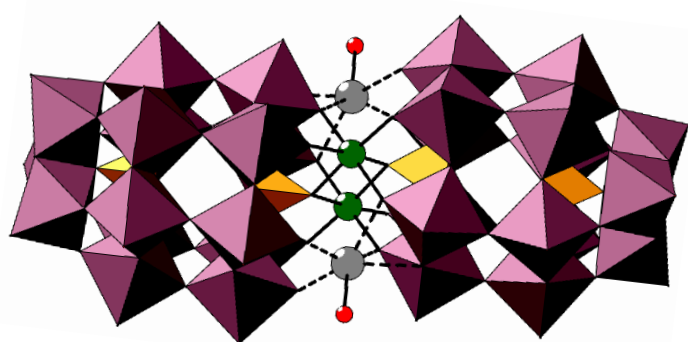
Figure 6.1. Combined polyhedral/ ball-and-stick representation of $[(Na(H_2O))_2Sc_2(P_2W_{15}O_{56})_2]^{16-}$ (**11**). Colour code: WO_6, dark-pink octahedra; PO_4, orange tetrahedra; Sc, green; Na, grey; O, red.

6.1.1 Synthesis

$Na_{16}[(Na_2(H_2O)_2Sc_2(P_2W_{15}O_{56})_2]\cdot 20H_2O$ (Na-11).

The synthesis of polyanion **11** was done via a one-pot procedure as follows:

$$2[P_2W_{15}O_{56}]^{12-} + 2H_2O + 2Sc^{3+} + 2Na^+ \rightarrow [Sc_2Na_2(H_2O)_2(P_2W_{15}O_{56})_2]^{16-} \quad (\textbf{1})$$
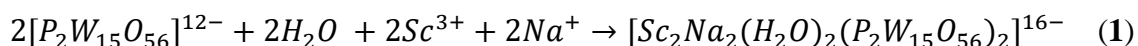
To a 10 ml solution of $Sc(NO_3)_3\cdot 6H_2O$ (0.061 g, 0.180 mmol); prepared by dissolving the scandium salt in sodium acetate/acetic acid buffer (0.5M, pH 4.6); solid

$Na_{12}[P_2W_{15}O_{56}] \cdot 24H_2O$ (0.889 g, 0.201 mmol) was added. The resulting solution was vigorously stirred at 70 °C for 24 hours and the final pH of the solution was 5.7. This solution was stored in a refrigerator at 4°C for two weeks after which colourless, rhombic shaped crystals of the title compound were collected and air-dried. Yield: 0.29 g, 38.7 % (based on Sc).

The composition of **Na-11** including countercations and crystal waters was determined by a combination of single-crystal XRD, elemental and thermogravimetric analyses. Elemental analysis (%) found (calculated): Na 4.67 (4.97); Sc 1.22 (1.08); P 1.50 (1.47); W 66.77 (66.29). The 20 waters of crystallization were determined by TGA.

6.1.2   Single-Crystal X-ray Diffraction

Table 6.1. Crystal data and structure refinement for **Na-11**.

Compound	Na-11
Formula Weight (g/mol)	8331.09
Crystal System	*Triclinic*
Space Group	*P*-1
a (Å)	12.8392(13)
b (Å)	14.0414(14)
c (Å)	23.637(2)
α (°)	79.668(3)
β (°)	78.834(3)
γ (°)	80.324(3)
Volume (Å^3)	4073.3(7)
Z	1
$D_{calc.}$ (gm/cm^3)	3.740
Absorption Coefficient (mm^{-1})	21.385
F(000)	4035
θ range for data collection	2.486 to 27.530
Completeness to θ_{max}	99.9%
Index Ranges	-16≤h≤16,
	-18≤k≤18,
	-30≤l≤30
Reflections Collected	103893
Unique Reflections	18739
Data/Restraints/ Parameters	18739/0/616
Goodness of Fit on F^2	1.034
R_1[a] ($I>2\sigma(I)$)	0.0518
wR_2[b] (all data)	0.0875

[a] $R_1=\Sigma\|F_0\|-|F_c\|/\Sigma|F_0|$, [b] $wR_2=[\Sigma w(F_0^2-F_c^2)^2/\Sigma w(F_0^2)^2]^{1/2}$

6.1.3   Results and Discussion

General. The synthesis of **Na-11** was achieved after several syntheses attempts involving varying temperature, pH, molar ratios of the starting reagents, countercations, solvents, reaction time as well as crystallization temperature. We report that favourable results were obtained only when the reaction took place in sodium acetate/acetic acid buffer (0.5M, pH 4.6) and when

the ratio of Sc:W was 1:1.11 and crystallization at 4°C. We tried to incorporate additional Sc^{3+} ions into the already formed polyanion framework in aqueous solution but the results were undesirable.

6.1.3.1 Infrared (IR) spectroscopy

The compound was also characterized in the solid state by FT-IR spectroscopy (KBr pellet, cm^{-1}) with vibration bands at 1089(s), 1055(m), 941(m), 903(m), 827(w), 727(s), 600(w), 521(m), 450(w) (**Figure 6.2**). The spectrum shows characteristic bands of the trivacant lacunary starting material $Na_{12}[P_2W_{15}O_{56}] \cdot 24H_2O$. The bands corresponding to the P-O bonds in P_2W_{15} are 1087 cm^{-1}, 1009 cm^{-1} (corresponding to the P-O bond in the PW_9 unit) as well as 1130 cm^{-1} which is assigned to the P-O_t bond of PW_6.[1] In the spectrum of **Na-11**, the P-O_t vibration band shows a shift from 1130 cm^{-1} to 1055 cm^{-1}. This shift to a lower vibrational frequency can be ascribed to the newly formed P-O-Sc bond. Since the P_2W_{15} unit contains two unidentical P atoms, the one that is not perturbed still shows the vibration band at 1089 cm^{-1} while the perturbed one results in the new vibration band. The W-O_t and W-O_b-W stretching bands appear in the 950-720 cm^{-1} region of the spectrum.
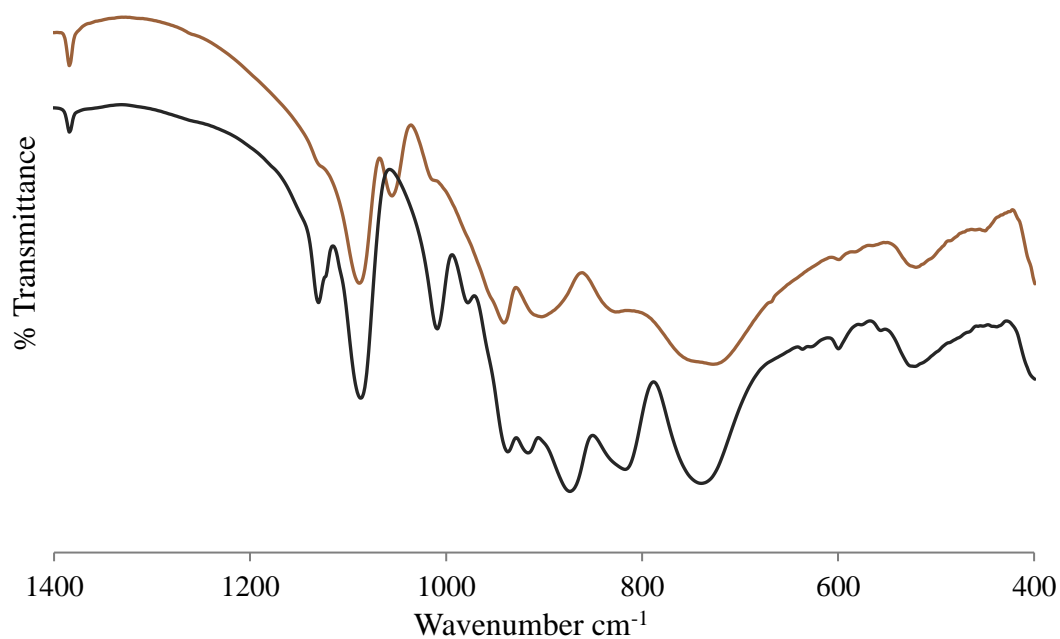
Figure 6.2. IR spectra of compound **Na-11** (dark brown) and the trilacunary Na$_{12}$[P$_2$W$_{15}$O$_{56}$]·24H$_2$O precursor (black).

6.1.3.2 Thermogravimetric analysis
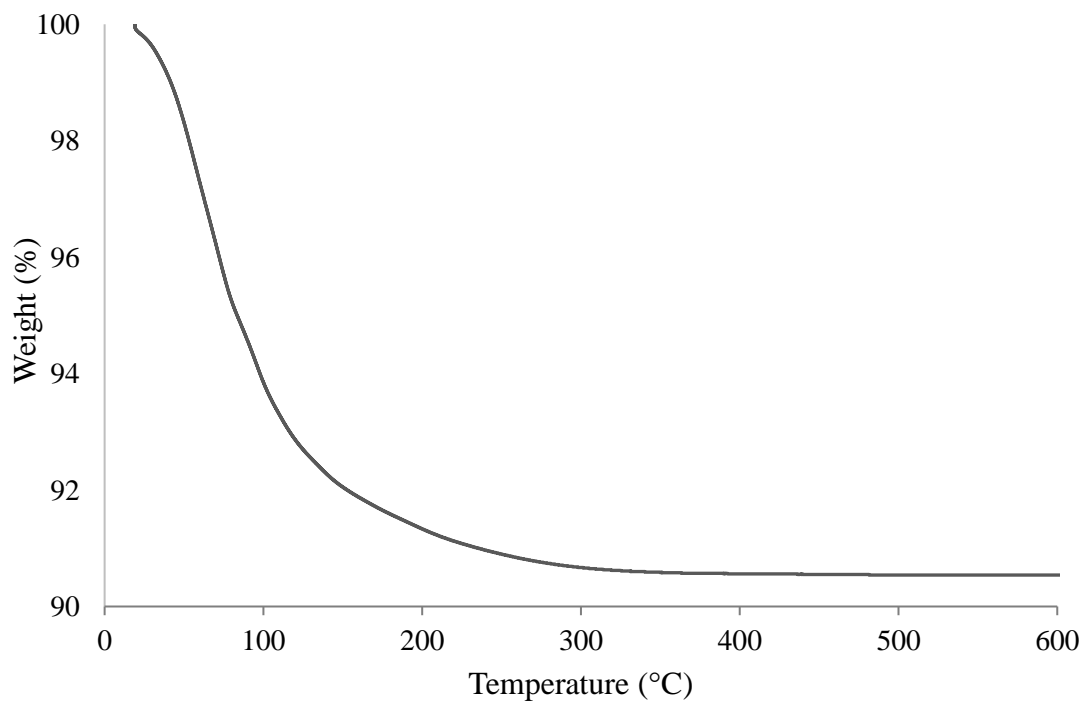
Figure 6.3. Thermogram of **Na-11**.

Thermogravimetric analysis of **Na-11** was performed between 20 and 600°C to determine the amount of crystal water molecules. The loss of all 20 crystal waters and two water molecules bound to the polyanion through Na^+ centres corresponds to a weight loss of about 4.6%.

6.1.3.3 Structural description

The structure of polyanion **11**, is formed by the fusion of two trilacunary $[\alpha\text{-}P_2W_{15}O_{56}]^{12-}$ (P_2W_{15}) units via two Sc^{3+} and two Na^+ ions in a centrosymmetric arrangement with an idealized C_{2h} symmetry. The title compound was synthesized by the reaction of $Na_{12}[P_2W_{15}O_{56}]\cdot24H_2O$ with $Sc(NO_3)_3\cdot6H_2O$. The trilacunary precursor $[P_2W_{15}O_{56}]^{12-}$ is formed via base degradation of the parent $[\alpha\text{-}P_2W_{18}O_{62}]^{6-}$ at pH 9,[2] where one edge-sharing capping triad W_3O_{13} is removed, resulting in the exposure of 7 nucleophilic oxygen atoms. The $\{Na_2(OH_2)_2Sc_2\}$ unit fills the gap left by the missing W_3O_{13} units in each P_2W_{15} unit.
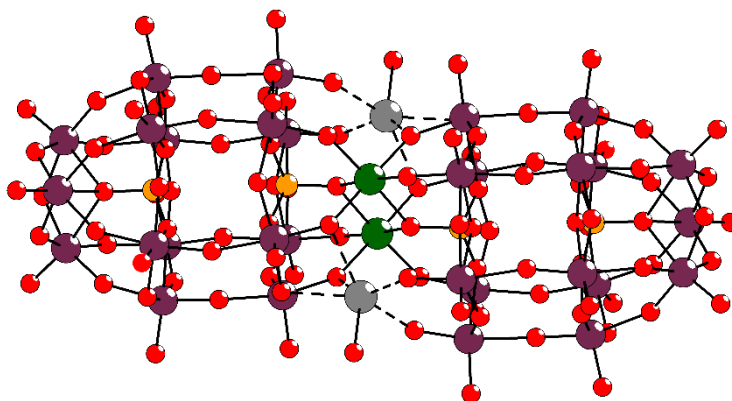
Figure 6.4. Ball and stick representation of $[(Na(H_2O))_2Sc_2(P_2W_{15}O_{56})_2]^{16-}$ (**11**). Colour code: W, dark-pink; Sc, green; P, orange; Na, grey; O, red.

The tetranuclear central core of polyanion **11**, is composed of two internal ScO_6 and two external $NaO_5(H_2O)$ octahedra. The four metal atoms resemble a rhombus with sides of 3.741(4) and 3.749(4) Å and a short and long diagonal of 3.325(3) and 6.710(9) Å.
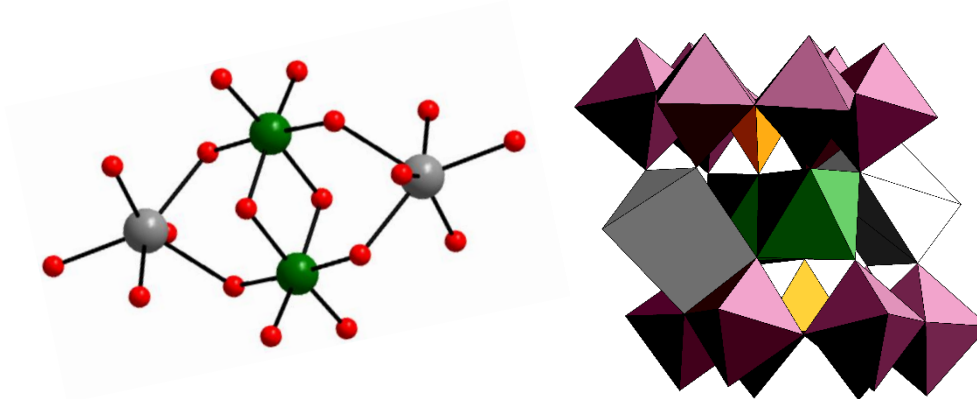
Figure 6.5. Ball-and-stick representation of the central tetranuclear $Na_2(OH_2)_2Sc_2O_{14}$ unit (left) and polyhedral representation of the belt-M_4 junction showing $\alpha\alpha\alpha\alpha$ configuration (right) of $[(Na(H_2O))_2Sc_2(P_2W_{15}O_{56})_2]^{16-}$ (**11**). Colour code: WO_6, dark-pink octahedra; PO_4, orange tetrahedra; ScO_6, green octahedra; $NaO_5(H_2O)$, grey octahedra, Sc, green; Na, grey; O, red.

Each Sc^{3+} centre adopts an octahedral geometry formed by one μ_2-O from a WO_6 octahedron (Sc(1)-O(3): 2.077(6) Å), one μ_3-O from another WO_6 octahedron (Sc(1)-O(2): 2.058(6) Å) and one μ_3-O from the central PO_4 tetrahedron (Sc(1)-O(1): 2.177(7) -2.197(6) Å) on each P_2W_{15} unit. In other words, each Sc^{3+} ion is linked to the two P_2W_{15} sub-units via four Sc-O-(W) bonds and two Sc-O-(P) bonds. The Sc-O bond lengths are in the range of 2.031(7)-2.197(6) Å (an average of 2.012 (6) Å) and the Sc-Sc distance is 3.325(3) Å. The O-Sc-O angles range from 81.0(2) to 96(3)° (**Table 6.2**) A bond valence sum of +3 was calculated for each Sc centre.

Table 6.2 Selected bond lengths (Å) and angles (°) for **11**.

Sc-O (Å)		Na-O (Å)		O–Na-O bond angles (°)	
Sc(1)-O(4)#1	2.031(7)	Na(1)-O10	2.252(8)	O(18)-Na(1)-O(23)	86.9(3)
Sc(1)-O(2)	2.058(6)	Na(1)-O14	2.267(7)	O(18)-Na(1)-O(57)	79.1(3)
Sc(1)-O(27)#1	2.074(6)	Na(1)-O(57	2.339(10)	O(23)-Na(1)-O(57)	91.0(3)
Sc(1)-O(3)	2.077(6)	Na(1)-O(27#1	2.463(8)	O(18)-Na(1)-O(2)#1	141.1(3)
Sc(1)-O(1)	2.177(7)	Na(1)-O(3)#1	2.523(7)	O(23)-Na(1)-O(2)#1	85.7(3)
Sc(1)-O(1)#1	2.197(6)	Na(1)-O(23)#1	2.527(7)	O(57)-Na(1)-O(2)#1	139.1(3)
O-Sc-O bond angles (°)		O(4)#1-Sc(1)-O(2)	94.2(3)	O(18)-Na(1)-O(5)#1	84.5(3)
O(4)#1-Sc(1)-O(2)	94.2(3)	O(4)#1-Sc(1)-O(27)#1	86.7(3)	O(23)-Na(1)-O(5)#1	143.3(3)
O(4)#1-Sc(1)-O(27)#1	86.7(3)	O(2)-Sc(1)-O(27)#1	96.5(3)	O(57)-Na(1)-O(5)#1	122.0(3)
O(2)-Sc(1)-O(27)#1	96.5(3)	O(4)#1-Sc(1)-O(3)	96.3(3)	O(2)#1-Na(1)-O(5)#1	79.2(2)
O(4)#1-Sc(1)-O(3)	96.3(3)	O(2)-Sc(1)-O(3)	86.1(2)	O(18)-Na(1)-O(8)#1	135.6(3)
O(2)-Sc(1)-O(3)	86.1(2)	O(27)#1-Sc(1)-O(3)	175.9(3)	O(23)-Na(1)-O(8)#1	136.8(3)
O(27)#1-Sc(1)-O(3)	175.9(3)	O(4)#1-Sc(1)-O(1)	172.4(3)	O(57)-Na(1)-O(8)#1	90.9(3)
O(4)#1-Sc(1)-O(1)	172.4(3)	O(2)-Sc(1)-O(1)	93.1(3)	O(2)#1-Na(1)-O(8)#1	65.7(2)
O(2)-Sc(1)-O(1)	93.1(3)	O(27)#1-Sc(1)-O(1)	90.5(2)	O(5)#1-Na(1)-O(8)#1	64.4(2)
O(27)#1-Sc(1)-O(1)	90.5(2)	O(3)-Sc(1)-O(1)	86.1(2)	O(18)-Na(1)-O(1)	74.7(2)
O(3)-Sc(1)-O(1)	86.1(2)	O(4)#1-Sc(1)-O(1)#1	91.7(3)	O(23)-Na(1)-O(1)	76.1(2)
O(4)#1-Sc(1)-O(1)#1	91.7(3)	O(2)-Sc(1)-O(1)#1	174.0(3)	O(57)-Na(1)-O(1)	151.2(3)
O(2)-Sc(1)-O(1)#1	174.0(3)	O(27)#1-Sc(1)-O(1)#1	85.0(2)	O(2)#1-Na(1)-O(1)	66.5(2)
O(27)#1-Sc(1)-O(1)#1	85.0(2)	O(3)-Sc(1)-O(1)#1	92.1(2)	O(5)#1-Na(1)-O(1)	67.3(2)
O(3)-Sc(1)-O(1)#1	92.1(2)	O(1)-Sc(1)-O(1)#1	81.0(3)	O(8)#1-Na(1)-O(1)	116.2(2)
O(1)-Sc(1)-O(1)#1	81.0(3)				

The two externally positioned Na^+ ions each adopt a distorted octahedral geometry. Each Na^+ ion is connected to one P_2W_{15} (**A**), via two μ_2-O (Na-O-(W) bonds; Na(1)-O(10) and Na(1)-O(14): 2.252(8) and 2.267(7) Å) and to the other P_2W_{15} unit (**B**) via two μ_3-O (Na(1)-O(27) and Na(1)-O(3): 2.463(8) and 2.523(7) Å) and one μ_3-O [Na(1)-O(23): 2.527(7) Å] which does not belong to the lacunary sites of (**B**). This triply bridging oxygen atom of the two-edge shared WO_6 octahedra connects each Na^+ to (**B**). Lastly Na^+ is connected to a free aqua ligand [Na(1)-O (23): 2.339(1) Å]. Therefore, Na-O bond lengths range from 2.252(8) to 2.527(7) Å (an average of 2.395(8) Å) and the corresponding O−Na−O angles vary from 64.4(2) to 90.9(3)° (**Table 6.2**).

(B)

(A)
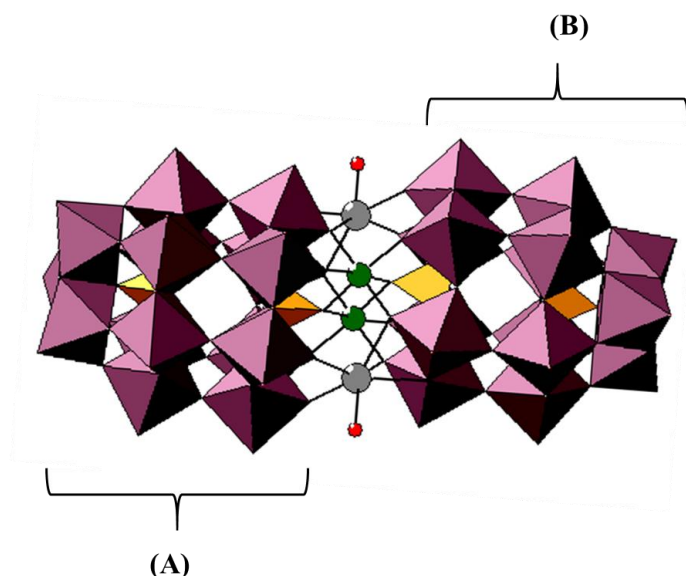
Figure 6.6. Combined polyhedral/ball-and stick-representation of the two lacunary {P_2W_{15}} units of [(Na(H_2O))_2Sc_2(P_2W_{15}O_{56})_2]^{16-} (**11**). Colour code: WO_6, dark-pink octahedra; P, orange tetrahedra; Sc, green; Na, grey; O, red.

The first reported heteropolytungstate derived from P_2W_{15} was the tetranuclear sandwich-type POM, [M_4(H_2O)_2(P_2W_{15}O_{56})_2]^{16-} (M = Co^{2+}, Cu^{2+}, Zn^{2+}) reported by Finke and co-workers. These compounds consist of a central tetrameric metal core that connects two P_2W_{15} units.[3-5] Since then a vast library of the Finke ion has been reported mostly incorporating 3d-transition

metal ions including Mn^{2+} and Ni^{2+}, Cd^{2+} and Fe^{3+} and all these complexes present the well-known $\alpha\beta\beta\alpha$ configuration with β connectivities between the two P_2W_{15} units and the central tetrameric metal core. [1, 6-8]

Polyanion **11** is a structural analogue of $[Fe^{III}_2Na_2(H_2O)_2(P_2W_{15}O_{56})_2]^{16-}$ reported by Hill and co-workers. This sandwich type is different from the classical Wells-Dawson tetranuclear sandwich complexes in that the tetrametallic core has two central Fe^{3+} ions and the two other positions are occupied by two external Na^+ ions. In this complex, the connectivity between the two P_2W_{15} units and the central Fe_2Na_2 core is rotated by 60° relative to the classical sandwich complexes.[9] Polyanion **11** exhibits the $\alpha\alpha\alpha\alpha$ configuration (with α connectivities between the two P_2W_{15} units and the central tetranuclear $Na_2(OH_2)_2Sc_2O_{14}$ unit). This means that the two internal ScO_6 and two external $NaO_5(H_2O)$ octahedra each share corners with two WO_6 octahedra at the belt position of P_2W_{15} that are connected to each other via a corner (see **Figure 6.5**). According to Hill and co-workers when the first cap-belt, the first belt-M_4, the second belt-M_4 as well as the second belt-cap junctions of $[Na_2M^{III}_2(H_2O)_2(P_2W_{15}O_{56})_2]^{16-}$ display α connectivities, then the complex has an $\alpha\alpha\alpha\alpha$ configuration.[9]

Other researchers reported di- and trimetallic sandwich derivatives such as ($[Co_2Na_2(H_2O)_2(P_2W_{15}O_{56})_2]^{18-}$ and $[M_3Na(H_2O)_2(P_2W_{15}O_{56})_2]^{17-}$ (M = Co^{2+}, Mn^{2+}, Ni^{2+}) respectively, as well as mixed-metal sandwich complexes such as $[MCo_3(H_2O)_2(P_2W_{15}O_{56})_2]^{16-}$ (M = Mn^{2+}, Ni^{2+}, Zn^{2+}, Cd^{2+}) and $[CoNi_3(H_2O)_2(P_2W_{15}O_{56})_2]^{16-}$ among others.[10-16] Our group has reported $[Ti_2(P_2W_{15}O_{55}OH)_2]^{14-}$, $[Ni_2Na_2(H_2O)_2(P_2W_{15}O_{56})_2]^{18-}$ and a dithallium(III)-containing polyanion $[Na_2Tl^{III}_2(H_2O)_2(P_2W_{15}O_{56})_2]^{16-}$ based on the Hill structure [17-19]

6.1.3.4 ^{31}P- and ^{183}W-NMR spectroscopy.

The ^{31}P NMR spectrum of **Na-11** exhibits two major signals at -4.5 and -14.3 ppm relative to the reference 85% H_3PO_4. The expected intensity ratio of the two signals is 1:1. However, we

observe an intensity of 0.85:1 with the signal further downfield with a slightly lower intensity

in relation to the upfield signal. The peak at -14.3 ppm is assigned to the phosphorus atom (in

the PW_9 unit of P_2W_{15}) that is furthest from the $Na_2(OH_2)_2Sc_2O_{14}$ unit. The other signal at -4.5

ppm is assigned to the phosphorus atom that is affected by the substitution (in the PW_6 unit). In

other words, this signal represents the phosphorus atom that is directly bound to scandium and

sodium ions. This phosphorus atom is deshielded hence it is positioned further downfield as

compared to the more upfield atom that is not interacting with the $Na_2(OH_2)_2Sc_2O_{14}$ unit.
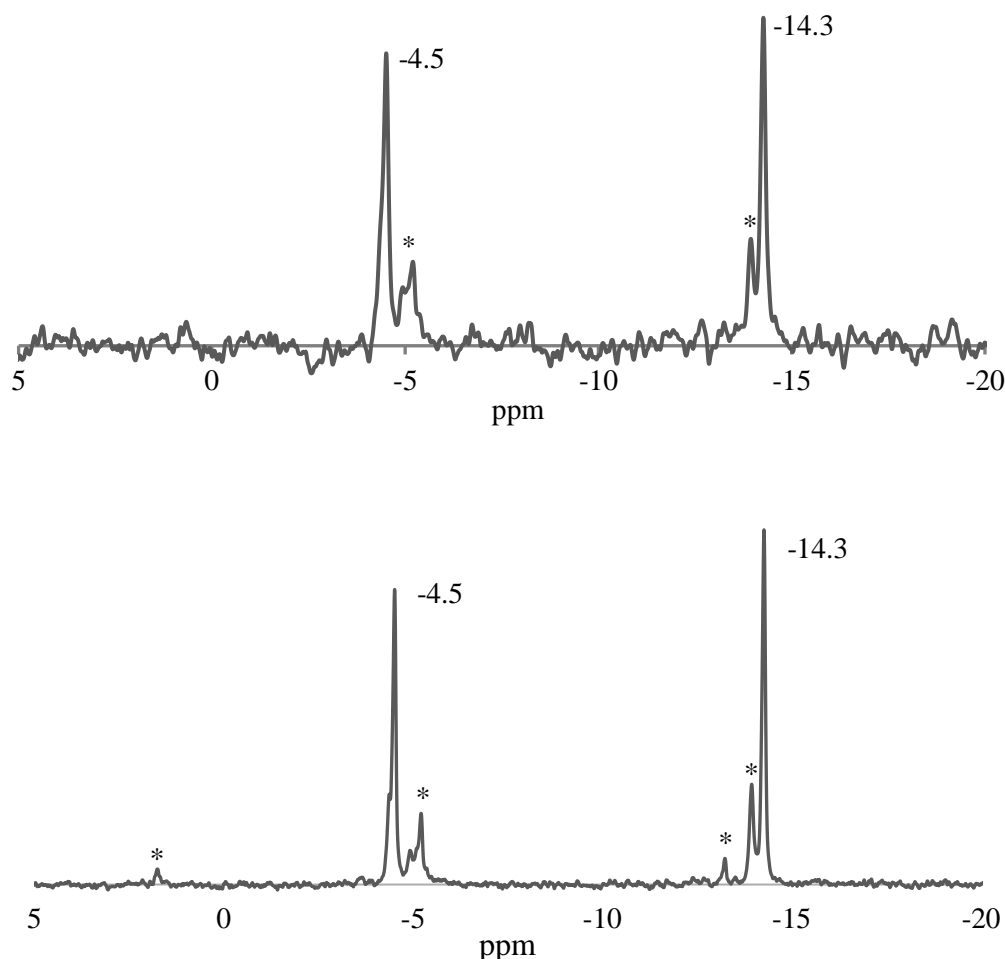
Figure 6.7. ^{31}P NMR spectra of **Na-11** in NaOAc/HOAc buffer/D_2O (pH 5.2) after 55 scans (top) and 4500 scans (bottom).
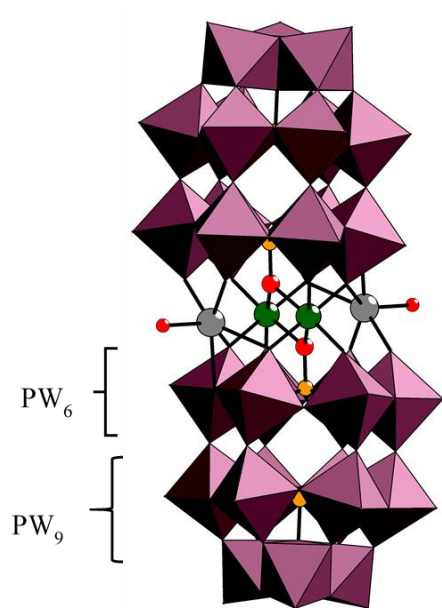
Figure   6.8.   Combined   polyhedral/ball-and-stick   representation   of $[(Na(H_2O))_2Sc_2(P_2W_{15}O_{56})_2]^{16-}$ (**11**) showing the two PW_6 and PW_9 subunits. Colour code: WO_6, dark-pink octahedra; P, orange tetrahedra; Sc, green; Na, grey; O, red.

Although **Na-11** is bulk pure as determined by elemental analysis we were unable to prove the purity of the compound in solution as shown in **Figure 6.7**. In addition to the two major signals, we observed several additional weaker/minor signals whose intensities remain largely the same from the onset until the end of the measurement (24 hours), indicating the presence of by-products at pH 6.83 and 5.20 (in H_2O and NaOAc/HOAc buffer) respectively. We propose that possible by-products could exist due the fact that Na^+ cations are weakly bound to the P_2W_{15} units (Na-O bond distances from 2.252(8) to 2.527(7) Å) and as such are labile, meaning that at one particular time, in the structure there could be one, two or no Na^+ cation(s) attached. It is well known that P_2W_{15} units and the tetrametallic core can arrange in a *αββα* configuration where the two cap-belt junctions display *α* connectivities and the two belt-M_4 junctions display *β* connectivities. As such, the possibility of rotational isomers of polyanion **11** cannot be ruled out. We propose that the solution of **Na-11**, is a cocktail of species, with polyanion **11** being the predominant one.

To try and understand the formation mechanism of polyanion **11**, ^{31}P-NMR spectra of (**i**) the starting precursor $Na_{12}[P_2W_{15}O_{56}]\cdot24H_2O$, (**ii**) the solution after mixing $Na_{12}[P_2W_{15}O_{56}]\cdot24H_2O$ with $Sc(NO_3)_3\cdot6H_2O$ in HOAc/NaOAc (t=0), (**iii**) this solution at the end of the reaction (t = 24 hrs) and (**iv**) the crystals of **Na-11** redissolved in NaOAc/HOAc buffer were recorded. The ^{31}P-NMR spectrum of (**ii**) exhibits the two major signals that also present in (**i**) but there are additional (minor) peaks at -14.1, -5.4 and -4.1 pm. In the spectrum of (**iii**) the signals at -4.5 and -14.2 ppm are more intense as compare to (**ii**) suggesting that polyanion **11** is present in the solution at the end of the reaction, alongside other species (see signals with asterisks in **Figure 6.9**). The ^{31}P-NMR spectrum of the crystals of **Na-11** (**iv**) exhibits two major signals at -4.5 and -14.3 ppm which are the same major signals observed in the spectrum of (**iii**). Some of the minor signals/impurities seen in this spectrum (**iii**) are observed in the spectrum of the crystals of **Na-11** suggesting that these signals are indeed by-products of the reaction and that they are not products of the decomposition of polyanion **11**.
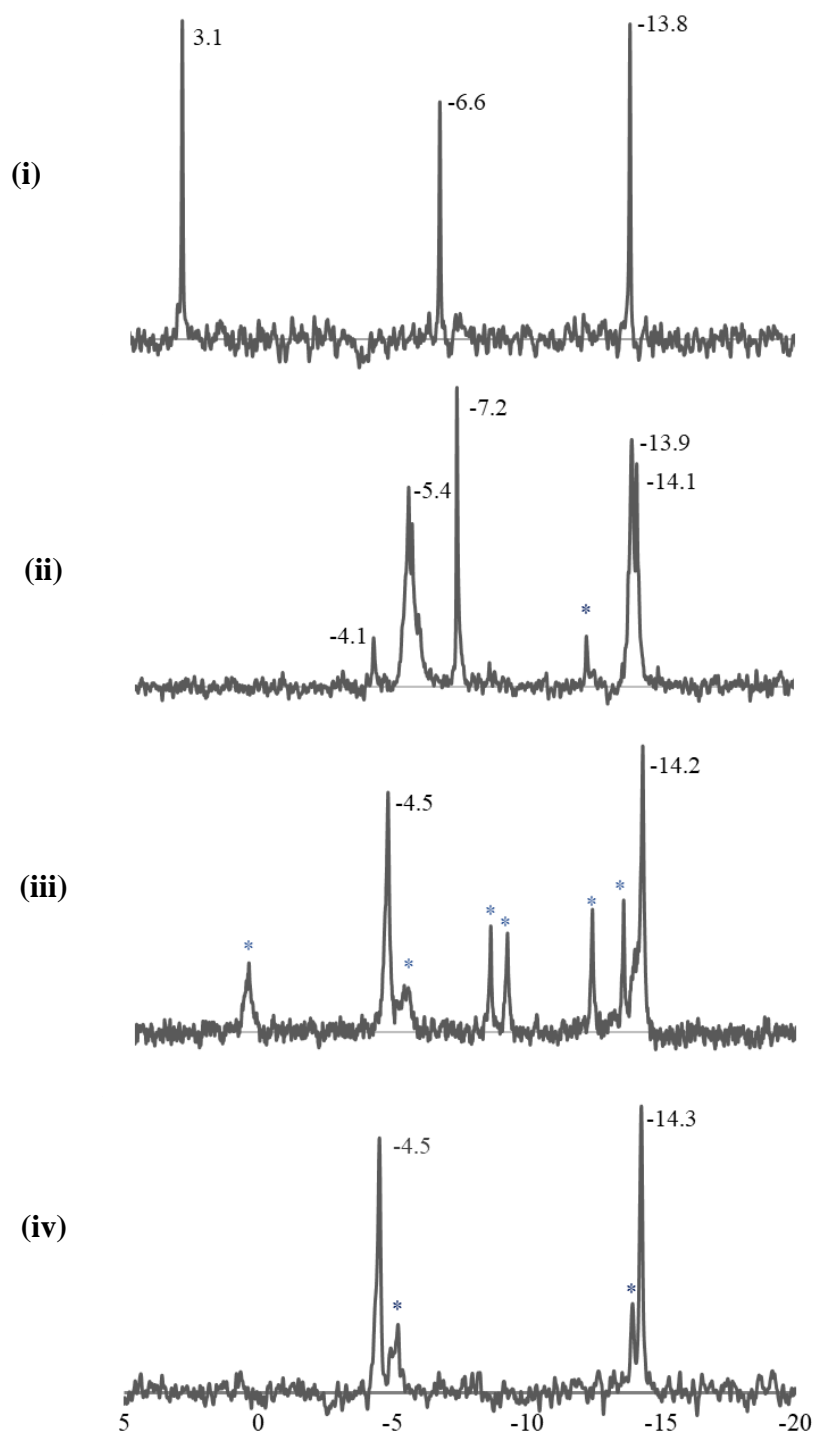
Figure 6.9. Formation of **Na-11** followed by ^{31}P-NMR spectroscopy; (**i**) the starting precursor $Na_{12}[P_2W_{15}O_{56}] \cdot 24H_2O$, (**ii**) the solution after mixing $Na_{12}[P_2W_{15}O_{56}] \cdot 24H_2O$ with $Sc(NO_3)_3 \cdot 6H_2O$ in HOAc/NaOAc (t = 0), (**iii**) this solution at the end of the reaction (t = 24 hrs) and (**iv**) the crystals of **Na-11** redissolved in NaOAc/HOAc buffer.

An attempt was made to further investigate the solution properties of **Na-11** by ^{183}W-NMR spectroscopy. For a polyanion exhibiting C_{2h} symmetry, eight signals with relative intensities 1:2:2:2:2:2:2:2 are expected but the spectrum of **Na-11** exhibits only seven signals at -142.3, -172.6, -177.5, -192.1, -225.6, -233.1, -241.8 ppm with relative intensities of 1:2:2:2:2:2:2 (**Figure 6.10**).

ppm
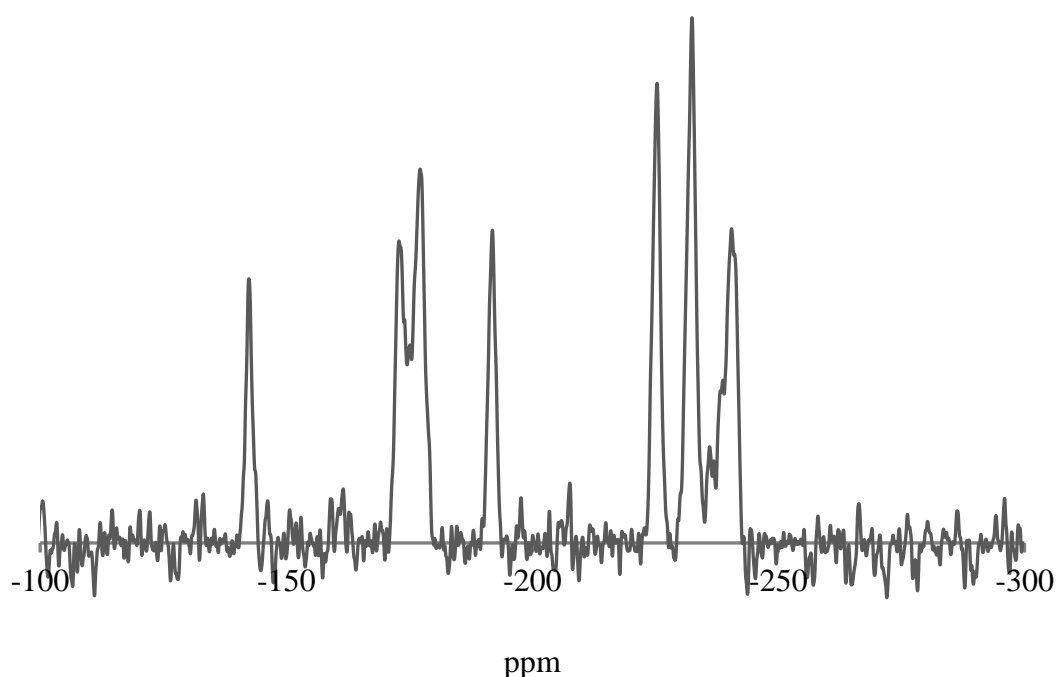
Figure 6.10. ^{183}W-NMR spectrum of **Na-11** in NaOAc/HOAc buffer /D$_2$O.

6.1.4   Conclusions

We have synthesized and structurally characterized a novel discrete di-scandium-30-tungsto-4-phosphate [(Na(H$_2$O))$_2$Sc$_2$(P$_2$W$_{15}$O$_{56}$)$_2$]$^{16-}$. The compound was studied in solid state and solution by single crystal XRD, IR, TGA, elemental analysis, ^{31}P and ^{183}W NMR. The compound consists of two P$_2$W$_{15}$ units that sandwich four metal ions resulting in a central tetranuclear core which is composed of two internal ScO$_6$ and two external NaO$_5$(H$_2$O) octahedra. This is the first structurally characterized scandium-containing tungstophosphate based on Wells-Dawson building blocks.

6.2 Synthesis and Structural Characterization of Scandium(III)-Containing 14-

Tungsto-2-Phosphate, [Sc(HPW$_7$O$_{28}$)$_2$]$^{8-}$

In this section the synthesis and structural characterization of a scandium(III)-containing 14-tungsto-2-phosphate is reported. The discrete polyoxometalate, [Sc(HPW$_7$O$_{28}$)$_2$]$^{13-}$ (**12**) was synthesized following several one pot procedures of the composing elements at pH 8. The compound was studied in solid state and solution by single crystal XRD, IR, TGA, elemental analysis and ^{31}P-NMR. The compound consists of two equivalent pentalacunary, heptatungstate Keggin based subunits [HPW$_7$O$_{28}$]$^{8-}$, which are connected to each other by one Sc^{3+} ion through four Sc-O-W and two Sc-O-P bridges.
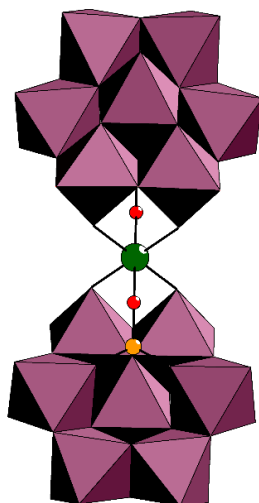
Figure 6.11. Combined polyhedral/ball-and-stick representation of [Sc(HPW$_7$O$_{28}$)$_2$]$^{13-}$ (**12**). Colour code: WO$_6$, dark-pink octahedra; Sc, green; P, orange; O, red.

6.2.1 Synthesis

Na$_{13}$[Sc(HPW$_7$O$_{28}$)$_2$]·27H$_2$O (Na-12)

Procedure 1: Sc(NO$_3$)$_3$·H$_2$O (0.063 g, 0.25 mmol) was dissolved in 20 mL of sodium acetate solution (1M, pH 6) followed by the addition of 85% H$_3$PO$_4$ (33.125 μl, 0.5 mmol). To the resulting solution was added Na$_2$WO$_4$·2H$_2$O (1.32 g, 4.0 mmol). The mixture was then stirred

for 1 h at 80°C. And filtered after cooling to room temperature, and pH was measured as 7.9. The colourless solution was stored in a refrigerator at 4°C for about a week after which rod shaped crystals of $Na_{13}[Sc(HPW_7O_{28})_2]\cdot27H_2O$ (**Na-12**) were collected and air-dried. (yield 0.16 g, 15% based on Sc). The composition of **Na-12** including countercations and crystal waters was determined by a combination of single-crystal XRD, elemental and thermogravimetric analyses. Elemental analysis (%) found (calculated): Na 6.55 (6.50); Sc 0.92 (0.98); P 1.35 (1.35); W 55.90 (55.97). The 27 waters of crystallization were determined by TGA. *The product of this reaction was utilized for IR spectroscopy, XRD crystallography and TGA.*

Procedure 2: $Sc(NO_3)_3\cdot H_2O$ (0.063 g, 0.25 mmol) was dissolved in 20 ml of sodium acetate solution (1M, pH 6) followed by the addition of solid P_2O_5 (0.071 g, 0.5 mmol). To the resulting solution was added $Na_2WO_4\cdot2H_2O$ (1.32 g, 5.0 mmol). The mixture was then stirred for 1 h at 80°C. And filtered after cooling to room temperature, and pH was measured as 7.8. The colourless solution was stored in a refrigerator at 4°C for about a week after which rod shaped crystals of $Na_{13}[Sc(HPW_7O_{28})_2]\cdot xH_2O$ (**Na-27**) were collected and air-dried.

Procedure 3. $Sc(NO_3)_3\cdot4H_2O$ (0.061 g, 0.2 mmol), $Na_2WO_4\cdot2H_2O$ (0.066 g, 0.2 mmol) and $K_{12}[P_2W_{15}O_{56}]\cdot24H_2O$ (0.889 g, 0.2 mmol) were dissolved in 10 ml sodium acetate/acetic acid buffer (0.5M, pH 4.60). The resulting solution was transferred into a teflon tube for hydrothermal reaction at 100 °C for 24 hrs. This solution was stored in a refrigerator at 4°C for about a month after which a small number of crystals of **Na-12** were collected and air-dried.

6.2.2   Single-Crystal X-Ray Diffraction

Table 6.3. Crystal data and structure refinement for **Na-12**.

Compound	**Na-12**
Formula Weight (g/mol)	4328.12
Crystal System	Triclinic
Space Group	P-1
a (Å)	11.8462(9)
b (Å)	12.0866(9)
c (Å)	17.8650(14)
α (°)	94.962(2)
ß (°)	94.582(2)
γ (°)	119.339(2)
Volume (Å^3)	2199.3(3)
Z	1
$D_{calc.}$ (gm/cm^3)	3.475
Absorption Coefficient (mm^{-1})	18.535
F(000)	2041
θ range for data collection	2.803 to 27.571
Completeness to θ_{max}	99.8%
Index Ranges	-15<=h<=15, -15<=k<=15, -23<=l<=23
Reflections Collected	55650
Unique Reflections	10131
Data/Restraints/Parameters	10131 / 306 / 595
Goodness of Fit on F^2	1.079
R_1[a] (I>2σ(I))	0.0292
wR_2[b] (all data)	0.0658

[a] $R_1=\Sigma\|F_0|-|F_c\|/\Sigma|F_0|$, [b] $wR_2=[\Sigma w(F_0^2-F_c^2)^2/\Sigma w(F_0^2)^2]^{1/2}$

6.2.3   Results and Discussion

The novel compound **Na-12** was prepared following three different procedures in a one-pot procedure under conventional and hydrothermal conditions, through the interaction of the source of heteroatom: H_3PO_4, P_2O_5 and $K_{12}[\alpha\text{-}P_2W_{15}O_{56}]\cdot24H_2O$ with different salts of Sc^{3+} and $Na_2WO_4\cdot2H_2O$ in an aqueous solution of 1M NaOAc (pH 8) at 80°C. The polyanion was

first isolated following the hydrothermal procedure where we believe $[\alpha\text{-}P_2W_{15}O_{56}]^{12-}$ broke down and rearranged into the $\{PW_7\}$ subunit. This phenomenon is well known in POM chemistry, but it should be noted that in addition to the undeniable effect of pH, the presence of additional tungstate ions in solution also had an influence because when the reaction was done in the absence of tungstate, the title compound could not be isolated.

The successful synthesis of **Na-12** depends on the ideal final pH of 7.7 - 8.0. Using water did not lead to the title compound - emphasizing the importance of choosing the right solvent in the synthesis of POMs. It is necessary that the temperature of the reaction be kept at 80°C. Performing the reaction at room temperature and at 50°C led to an undesirable precipitate. The optimum ratios of $Sc^{3+}/PO_4^{3-}/WO_4^{2-}$ is 1:2:16 which is close to the polyanion's stoichiometric ratio as indicated by the equation:

$$Sc^{3+} + 2PO_4^{3-} + 7WO_4^{3-} + 18H^+ \rightarrow [Sc(HPW_7O_{28})_2]^{13-} + 8H_2O \quad (\mathbf{2})$$
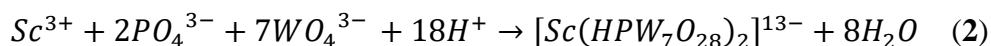
6.2.3.1 Infrared (IR) spectroscopy

A FT-IR spectrum of **Na-12** was recorded. The bands at 1081 and 1014 cm^{-1} correspond to the P-O stretching mode. The stretching modes of the terminal (W-O$_t$) and bridging (W-O$_b$-W) bonds appear below 950 cm^{-1}. The broad bands at 3421 cm^{-1} and 1656 cm^{-1} are assigned to the asymmetric vibrations of crystallized water molecules.
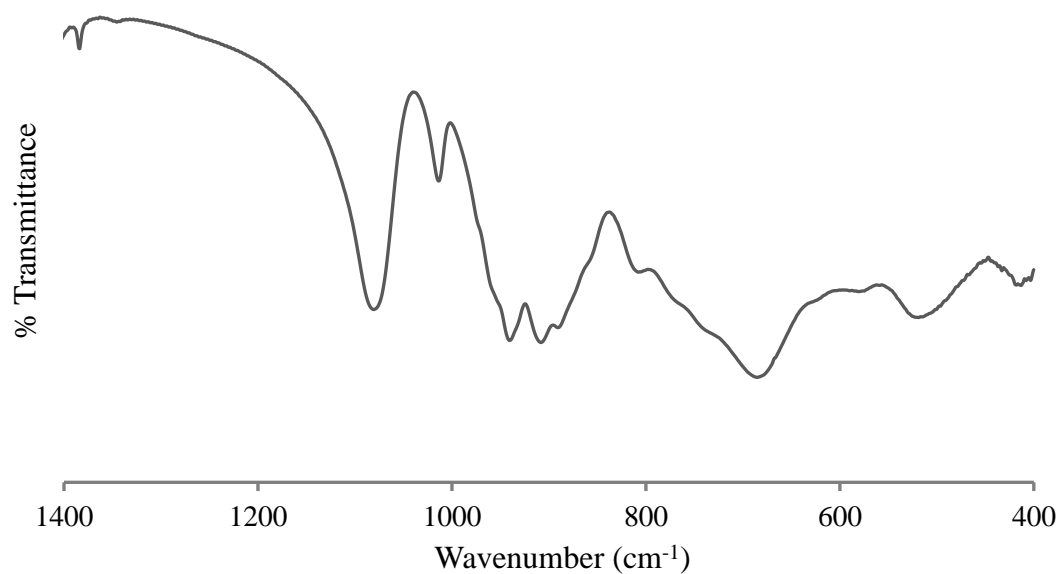
Figure 6.12. FT-IR spectrum of **Na-12**.

6.2.3.2 Thermogravimetric analysis

The thermal analysis of **Na-12** shows a multi-step weight loss which starts at room temperature and ends at 440 ºC. The first two dehydration steps are attributed to the loss of 25 crystal waters. This accounts for a 10.1 % weight loss. The third weight loss of ca. 1.1 % between 200 and 450 °C is probably the result of the loss of two H_2O molecule, derived from the combination of H and O atoms in $[(HPW_7O_{28})_2]^{8-}$. The whole weight loss is 11.18%.
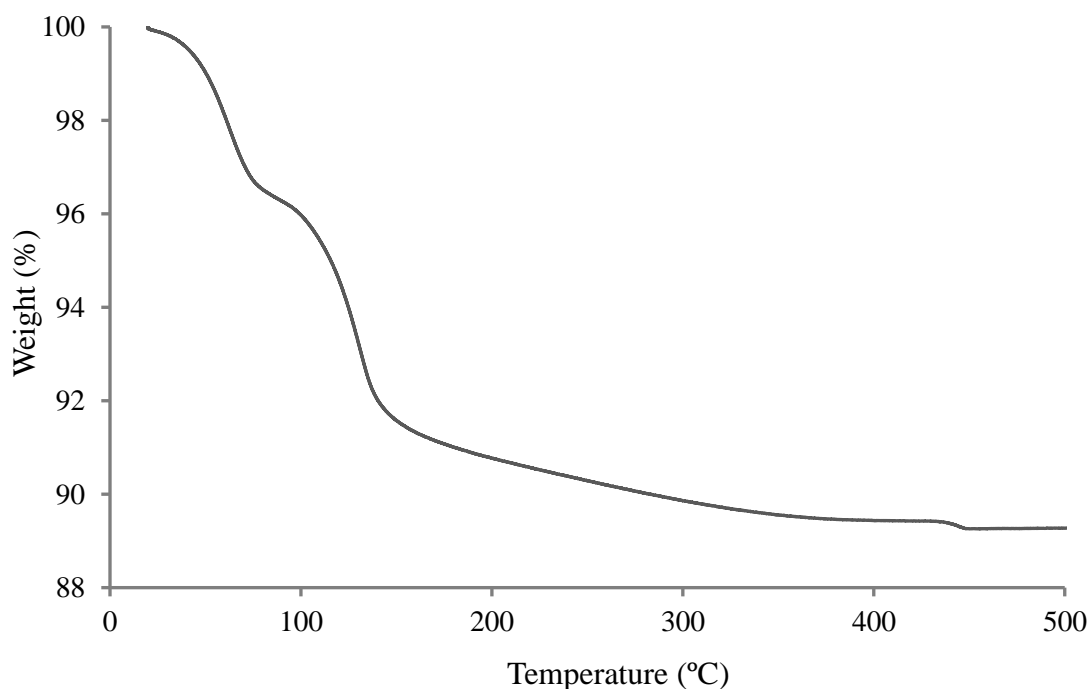
Figure 6.13. Thermogram of **Na-12**.

6.2.3.4 Structural description

Single crystal X-ray diffraction analysis revealed that $[Sc(HPW_7O_{28})_2]^{13-}$ (**12**) crystallizes in a triclinic space group *P-1*. The polyanion consists of two equivalent pentalacunary, heptatungstate Keggin based subunits $[HPW_7O_{28}]^{8-}$, which are connected to each other by one Sc^{3+} ion through four Sc-O-W and two Sc-O-P bridges. Each heptatungstate subunit is made up of an edge-shared W_3O_{13} triad that is connected to a half ring made of four edge-shared WO_6 octahedra. The half-ring and the triad connect *via* corner-sharing (two W-μ_2-O and two W-μ_3-O) and both subunits are stabilized by a central PO_4 unit. The resulting C_{2h} point-group symmetry is as a result of the twofold symmetry axis (*C2*) passing through the Sc^{3+} ion.
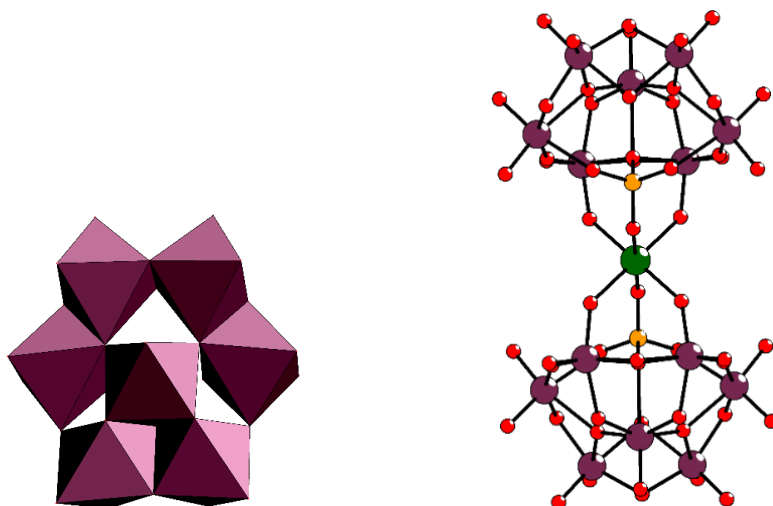
Figure 6.14. Polyhedral and ball-and-stick representations of the half-ring and triad in each $[HPW_7O_{28})_2]^{8-}$ unit (left) and $[Sc(HPW_7O_{28})_2]^{13-}$ (**12**) (right). Colour code: WO_6, dark-pink octahedra; W, dark-pink; Sc, green; P, orange tetrahedra; O, red.

The tungsten atoms in the edge-shared W_3O_{13} triad have one terminal oxo ligand whereas the four tungsten atoms from the half-ring have two terminal oxo groups. Polyanion **12,** like all the other reported compounds based on $[HXW_7O_{28}]^{8-}$ does not violate the Lipscomb principle which states that no heteropoly or isopolyanion can contain three or more terminal oxo groups due to the strong *trans* influence of the terminal metal–oxygen bonds that would facilitate dissociation of the cluster.[20] All the tungsten cations are hexacoordinated coordinated resulting in a distorted octahedral geometry with each tungsten centre having a bond valence sum of 6.[21] The W-O bonds can be categorised in 4 different groups:

1. the shortest terminal bonds (W-O_t): 1.717(4) -1.761(4)Å,

2. the double-bridging oxygen bonds (W-μ_2-O_b): 1.731(4)- 2.289(4) Å,

3. the triple-bridging oxygen bonds (W-μ_3-O_b): 1.905(4)- 2.211(4) Å, and

4. the longest bonds of the central bridging oxygen atoms (W-O_c): 2.343(4)-2.383(4) Å.

The central Sc^{3+} ion also adopts a six-coordinate octahedral geometry formed by four μ_2-O_b from four WO_6 octahedra of two edge-shared W_3O_{13} triads (2.109(4)-2.116(4) Å) and two more

μ_2-O$_b$ from two central PO$_4$ tetrahedra (2.088(7) Å).(**Table 6.4**). The PO$_4$ tetrahedron has three

P-μ_2-O bond and one the P-μ_4-O (where P is connected to the central O atom of the edge shared

triad) leading to bond lengths of 1.518(4)–1.541(4) Å and 1.586(4) Å respectively. One of the

P-μ_2-O oxygen atoms is connected to the Sc^{3+} ion.

Table 6.4. Selected bond lengths (Å) for **12**.

Sc-O			
Sc(1)-O(2)#1	2.088(4)	W(3)-O(15)	1.964(4)
Sc(1)-O(2)	2.088(4)	W(3)-O(14)	2.205(4)
Sc(1)-O(1)#1	2.109(4)	W(3)-O(16)	2.227(4)
Sc(1)-O(1)	2.109(4)	W(4)-O(17)	1.717(4)
Sc(1)-O(3)#1	2.116(4)	W(4)-O(18)	1.910(4)
Sc(1)-O(3)	2.116(4)	W(4)-O(14)	1.915(4)
P-O		W(4)-O(7)	1.928(4)
P(1)-O(2)	1.518(4)	W(4)-O(11)	1.939(4)
P(1)-O(16)	1.524(4)	W(4)-O(6)	2.383(4)
P(1)-O(22)	1.541(4)	W(5)-O(20)	1.743(4)
P(1)-O(6)	1.586(4)	W(5)-O(19)	1.754(4)
W-O		W(5)-O(8)	1.923(4)
W(1)-O(4)	1.731(4)	W(5)-O(21)	1.933(4)
W(1)-O(1)	1.795(4)	W(5)-O(22)	2.198(4)
W(1)-O(8)	1.905(4)	W(5)-O(18)	2.211(4)
W(1)-O(5)	1.943(4)	W(6)-O(23)	1.746(4)
W(1)-O(7)	1.994(4)	W(6)-O(24)	1.750(4)
W(1)-O(6)	2.343(4)	W(6)-O(15)	1.912(4)
W(2)-O(9)	1.721(4)	W(6)-O(25)	1.935(4)
W(2)-O(3)	1.819(4)	W(6)-O(26)	2.144(4)
W(2)-O(10)	1.912(4)	W(6)-O(14)	2.289(4)
W(2)-O(5)	1.936(4)	W(7)-O(28)	1.740(4)
W(2)-O(11)	1.976(4)	W(7)-O(27)	1.761(4)
W(2)-O(6)	2.378(4)	W(7)-O(21)	1.923(4)
W(3)-O(13)	1.731(4)	W(7)-O(25)	1.929(4)
W(3)-O(12)	1.736(4)	W(7)-O(26)	2.153(4)
W(3)-O(10)	1.927(4)	W(7)-O(18)	2.265(4)

In the formula there are two protons, each from one $\{HPW_7O_{28}\}$ subunit. They are located on the bridging oxygen O(26). The length of the W(7)–O(26) bond is 2.153(4) Å and the BVS of this bridging oxygen is 1.07, which is a characteristic value for a hydroxo group. (**Table 6.5**).
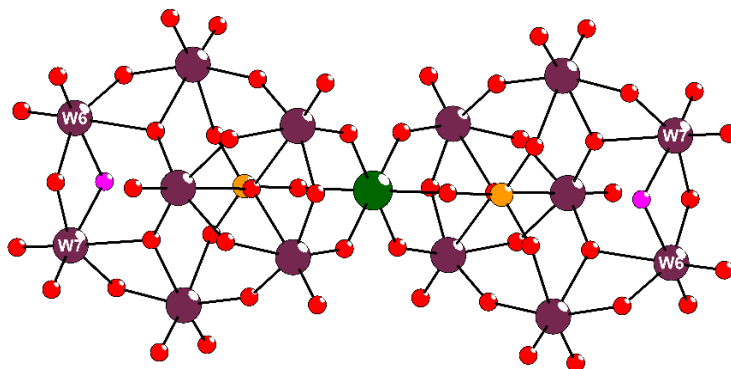
Figure 6.15. Ball-and-stick representations of $[Sc(HPW_7O_{28})_2]^{13-}$ (**12**) showing the O atoms belonging to the hydroxo groups. Colour code: WO_6, dark-pink octahedra; W, dark-pink; Sc, green; P, orange tetrahedra; O, red.

Table 6.5. Bond valence sum values of the different bridging oxygen atoms in **12**.

Bridging oxygen	BVS value
$\mu2$-O	
O(1)	1.950
O(3)	1.852
O(5)	1.882
O(7)	1.783
O(8)	2.017
O(10)	1.987
O(11)	1.795
O(15)	1.894
O(16)	1.718
O(21)	1.942
O(22)	1.696
O(25)	1.921
O(26)	1.069
$\mu3$-O	
O(14)	1.830
O(18)	1.861
$\mu4$-O	
O(6)	1.975

6.2.3.5 ^{31}P-NMR spectroscopy.

The ^{31}P-NMR study of the solution of **Na-12** in H_2O/D_2O exhibits the expected one signal at -2.3 ppm which is consistent with the crystal structure where there is only one phosphorus atom per $[HPW_7O_{28}]^{8-}$ unit.
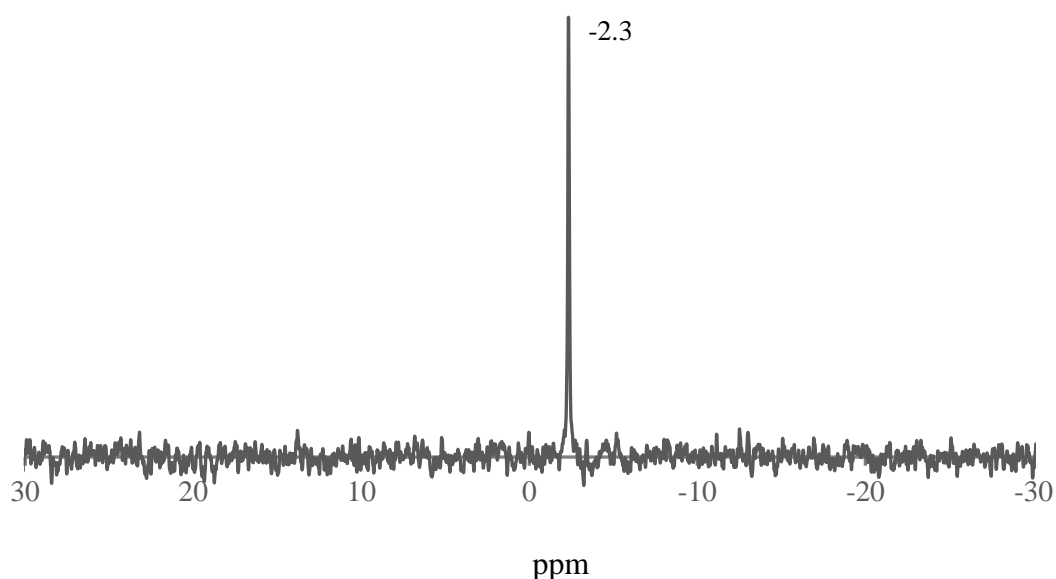
Figure 6.16. ^{31}P NMR spectrum of **Na-12** in H_2O/D_2O.

This sandwich type structure is the first to be reported in scandium POM chemistry but the heptatungstate subunit is well known. In fact, our group was the first to report two polyanions containing the then unprecedented heptatungstate fragment ($[HXW_7O_{28}Ru(dmso)_3]^{6-})$[22] However the first sandwich-type POM constructed by the pentalacunary heptatungstophosphate $[HPW_7O_{28}]^{8-}$ fragment was published in 2010 by Wang and co-workers when they reported $[Mn(HPW_7O_{28})_2]^{13-}$.[23] In the same year Wu et al. reported $[HVW_7O_{28}Ru(dmso)_3]^{6-}$ [24] and the Boskovic group reported POMs based on the Te-containing lacunary Keggin ions $[Te_2W_{16}O_{58}(OH)_2]^{14-}$ and $[Te_2W_{18}O_{62}(OH)_2]^{10-}$ which contain a novel lacunary Keggin

building block $[A\text{-}\alpha\text{-TeW}_7\text{O}_{28}]^{10-}$.[24] In 2012, more mono-transition metal containing sandwich compounds with the same structure $[M(HPW_7O_{28})_2]^{n-}$ ($n = 13$, M = Fe^{3+}, Mn^{3+}; and n = 14, M = Co^{2+}, Cd^{2+}, Mn^{2+}), were reported by Niu and co-workers.[25] Our group reported $[Cr(HX^VW_7O_{28})_2]^{13-}$ (X = P, As) in 2014 adding to the small library of POMs containing the heptatungstophosphate $[HPW_7O_{28}]^{8-}$ fragment.[26]

The fact that only a handful of polyoxometalates based on high-lacunary fragments are known indicates the difficulty in obtaining these compounds. However, our work and the work described in literature suggests that finding the right combination of reaction conditions such pH, concentration and ratio of starting materials, ionic strengths, makes the design and synthesis of polyanion Sc(HPW_7O_{28})_2]^{13-}$ (**12**) possible.

6.2.4   Conclusions

We have synthesized the first example of a discrete scandium-containing heteropolytungstate based on the $[HPW_7O_{28}]^{8-}$ subunt, $[Sc(HPW_7O_{28})_2]^{13-}$ (**12**) by several one pot procedures of the composing elements at pH 8. The compound was studied in solid state by single crystal XRD, IR, TGA and elemental analysis and in solution by ^{31}P-NMR spectroscopy. The compound consists of two equivalent pentalacunary, heptatungstate Keggin-based subunits $[HPW_7O_{28}]^{8-}$, which are connected to each other by one Sc^{3+} ion through four Sc-O-W and two Sc-O-P bridges.

6.3 References

[1]   L. Ruhlmann, L. Nadjo, J. Canny, R. Contant, R. Thouvenot, *Eur. J. Inorg. Chem.* **2002**, *2002*, 975–986.

[2]   A.P. Ginsberg, Ed., *Inorganic Syntheses*, John Wiley & Sons, Inc., Hoboken, NJ, USA, 1990, *27*, 108.

[3]   R. G. Finke, M. W. Droege, *Inorg. Chem.* **1983**, *22*, 1006–1008.

[4]   R. G. Finke, M. W. Droege, P. J. Domaille, *Inorg. Chem.* **1987**, *26*, 3886–3896.

[5]   T. J. R. Weakley, R. G. Finke, *Inorg. Chem.* **1990**, *29*, 1235–1241.

[6]   C. J. Gómez-García, J. J. Borrás-Almenar, E. Coronado, L. Ouahab, *Inorg. Chem.* **1994**, *33*, 4016–4022.

[7]   J. F. Kirby, L. C. W. Baker, *J. Am. Chem. Soc.* **1995**, *117*, 10010–10016.

[8]   X. Zhang, Q. Chen, D. C. Duncan, C. F. Campana, C. L. Hill, *Inorg. Chem.* **1997**, *36*, 4208–4215.

[9]   X. Zhang, T. M. Anderson, Q. Chen, C. L. Hill, *Inorg. Chem.* **2001**, *40*, 418–419.

[10]   L. Ruhlmann, J. Canny, R. Contant, R. Thouvenot, *Inorg. Chem.* **2002**, *41*, 3811–3819.

[11]   A. Flambard, L. Ruhlmann, J. Canny, R. Thouvenot, *Comptes Rendus Chim.* **2008**, *11*, 415–422.

[12]   L. Ruhlmann, C. Costa-Coquelard, J. Canny, R. Thouvenot, *J. Electroanal. Chem.* **2007**, *603*, 260–268.

[13]   D. Schaming, J. Canny, K. Boubekeur, R. Thouvenot, L. Ruhlmann, *Eur. J. Inorg. Chem.* **2009**, 5004–5009.

[14]   L. Ruhlmann, C. Costa-Coquelard, J. Canny, R. Thouvenot, *Eur. J. Inorg. Chem.* **2007**, 1493–1500.

[15]   T. M. Anderson, K. I. Hardcastle, N. Okun, C. L. Hill, *Inorg. Chem.* **2001**, *40*, 6418–6425.

[16]   T. M. Anderson, X. Zhang, K. I. Hardcastle, C. L. Hill, *Inorg. Chem.* **2002**, *41*, 2477–

2488.

[17]   U. Kortz, S. S. Hamzeh, N. A. Nasser, *Chem. - A Eur. J.* **2003**, *9*, 2945–2952.

[18]   B. S. Bassil, A. M. Bossoh, M. Ibrahim, B. A. Bile, A. S. Mougharbel, Z. Lin, P. de Oliveira, I.-M. Mbomekalle, U. Kortz, *Curr. Inorg. Chem.* **2017**, *7*, 21–27.

[19]   W. W. Ayass, T. Fodor, E. Farkas, Z. Lin, H. M. Qasim, S. Bhattacharya, A. S. Mougharbel, K. Abdallah, M. S. Ullrich, S. Zaib, et al., *Inorg. Chem.* **2018**, *57*, 7168–7179.

[20]   M. T. Pope, *Heteropoly and Isopoly Oxometalates*, Springer-Verlag, 1983.

[21]   I. D. Brown, D. Altermatt, *Acta Cryst. Sect. B.* **1985**, *41*, 244–247.

[22]   L. H. Bi, M. H. Dickman, U. Kortz, I. Dix, *Chem. Commun.* **2005**, 3962–3964.

[23]   Q. Wu, Y. G. Li, Y. H. Wang, Z. M. Zhang, E. B. Wang, *Inorg. Chem. Commun.* **2010**, *13*, 66–69.

[24]   L. H. Bi, B. Wang, G. F. Hou, B. Li, L. X. Wu, *Cryst. Eng. Comm.* **2010**, *12*, 3511–3514.

[25]   D. Zhang, Y. Zhang, J. Zhao, P. Ma, J. Wang, J. Niu, *Eur. J. Inorg. Chem.* **2013**, *2013*, 1672–1680.

[26]   W. Liu, J. H. Christian, R. Al-Oweini, B. S. Bassil, J. Van Tol, M. Atanasov, F. Neese, N. S. Dalal, U. Kortz, *Inorg. Chem.* **2014**, *53*, 9274–9283.

CHAPTER 7. SUMMARY AND OUTLOOK

This thesis is based on three research projects: bismuth(III)-, lead(II) and scandium(III)-containing heteropolytungstates. 12 novel compounds have been studied extensively using solid state and solution analytical techniques. Additionally, synthetic procedures of 8 novel compounds are reported in the appendix. The highlights are as follows:

- Successful insertion of Bi^{3+} into $\{XW_{11}\}$ and $\{X_2W_{17}\}$ units resulting in four isostructural Keggin-type ions $[Bi(\alpha-XW_{11}O_{39})_2]^{n-}$ (X = Si (**1**), Ge (**2**), n = 13; X = P (**3**), As (**4**), n = 11)and two Wells-Dawson-type ion $[Bi(\alpha_2-X_2W_{17}O_{61})_2]^{17-}$ (X = P (**5**), As (**6**), n = 17). In each of the 1:2 sandwich complexes, the Bi^{3+} is in 8-coordination with square-antiprismatic geometry. This coordination mode is typical of $Ln^{2+/3+}$ in POM chemistry. Therefore, we suggest that Bi^{3+} mimics the chemistry of Ln ions in POM chemistry.

- Synthesis of the two 1:1 complexes; $[(Bi(H_2O)SiW_{11}O_{39})_4]^{20-}$ (**7**) with Bi^{3+} in 6 coordination and $[Bi(H_2O)SiW_{11}O_{39}]^{5-}$ (**8**) which exists as an infinite one-dimensional chain with Bi^{3+} has a coordination number of 7. Such coordination modes of Bi^{3+} are still rare in POM chemistry.

- Incorporation of Pb^{2+} ions into mono-lacunary Keggin polyanions resulting in two polyanions $[Pb(\alpha-XW_{11}O_{39})]^{6-}$ (X = Si (**9**) and Ge(**10**)) where Pb^{2+} occupies the vacant position in $[\alpha-XW_{11}O_{39}]^{8-}$ leading to a complete Keggin structure. Polyanion **9** and **10** are derivatives of the $[Pb(GaW_{11}O_{39})]^{7-}$ reported 38 years ago.

- Synthesis and structural characterization of a novel disubstituted scandium-30-tungsto-4-phosphate $[(Na(H_2O))_2Sc_2(P_2W_{15}O_{56})_2]^{16-}$ (**11**) This is the first crystal structure of a scandium containing tungstophosphate based on Wells-Dawson building blocks.

- Synthesis of a discrete mono-scandium-containing polyoxometalate, $[Sc(HPW_7O_{28})_2]^{13-}$ (**12**) by several one pot procedures.

- Polyanions **13**–**19** (**see Chapter 8**) present several open questions where some synthetic procedures are not clear.

Based on the results reported in this dissertation and the inconclusive results reported in Chapter 8, several follow-up experiments to further develop this research field will be done.

- Since the field of bismuth(III), lead(II) and scandium(III)-containing heteropolytungstates has not been extensively explored and we have shown that Bi^{3+} and Pb^{2+} can mimic the chemistry of Ln^{3+} ions in POM chemistry, we can assume that these two cations can lead to very large POM complexes when reacted with lone pair-containing lacunary species such as $[B\text{-}\alpha\text{-}X^{III}W_9O_{33}]^{9-}$, X = As, Sb, Bi and $[B\text{-}\alpha\text{-}TeW_9O_{33}]^{8-}$ as is the case with lanthanide ions.

- The fact that there is a large number of combinatorial possibilities for POM synthesis and the ability of POMs to adopt a wide range of potential isomers implies that the entire arsenal of lacunary heteropolyanions such as $[\alpha\text{-}PW_{11}O_{39}]^{7-}$, $[A\text{-}\alpha\text{-}PW_9O_{34}]^{9-}$, $[B\text{-}\alpha\text{-}PW_9O_{34}]^{9-}$, $[\alpha\text{-}P_2W_{15}O_{56}]^{12-}$, $[H_2P_2W_{12}O_{48}]^{12-}$, $[P_2W_{19}O_{69}(H_2O)]^{14-}$, $[\alpha_2\text{-}P_2W_{17}O_{61}]^{10-}$, $[H_6P_4W_{24}O_{94}]^{18-}$, $[H_7P_8W_{48}O_{184}]^{33-}$, $[H_4PW_{17}O_{61}]^{11-}$, $[\beta_1\text{-}SiW_{11}O_{39}]^{8-}$, $[\beta_2\text{-}SiW_{11}O_{39}]^{8-}$, $[\beta_3\text{-}SiW_{11}O_{39}]^{8-}$, $[\alpha\text{-}SiW_{11}O_{39}]^{8-}$, $[\gamma\text{-}SiW_{10}O_{36}]^{8-}$, $[\alpha\text{-}SiW_9O_{34}]^{10-}$, $[\beta\text{-}SiW_9O_{34}H]^{9-}$, $[\beta_2\text{-}GeW_{11}O_{39}]^{7-}$, $[\gamma\text{-}GeW_{10}O_{36}]^{8-}$ $[A\text{-}\alpha\text{-}GeW_9O_{34}]^{10-}$, $[B\text{-}\alpha\text{-}AsW_9O_{33}]^{9-}$, $[A\text{-}\alpha\text{-}As^VW_9O_{34}]^{9-}$, $[B\text{-}\alpha\text{-}As_2W_{15}O_{56}]^{12-}$, $[B\text{-}\alpha\text{-}Sb^{III}W_9O_{33}]^{9-}$, $[Te_2W_{17}O_{61}]^{12-}$, $[Te_2W_{16}O_{58}(OH)_2]^{14-}$ and $[B\text{-}\alpha\text{-}BiW_9O_{33}]^{9-}$ can be reacted with Bi^{3+} and Pb^{2+} salts.

- Rather than only performing experiments using preformed tungsten lacunary precursors for the synthesis of Bi^{3+}-, Pb^{2+}- and Sc^{3+}-containing heteropolytungstates it is necessary

to employ an *in-situ* synthesis approach where salts of constituting elements in predetermined ratios are used.

- The on-going challenge in the synthesis of the trilacunary precursor: $[B\text{-}\alpha\text{-}BiW_9O_{33}]^{9-}$ needs to be tackled. We plan to investigate the use of different cations in order to avoid undesirable side-products such as paratungstate-B. It is well known that the product that is isolated in crystalline form may not necessarily be the one with the highest abundance in solution.[37] As such we would like to continue studying the reactions of $[B\text{-}\alpha\text{-}BiW_9O_{33}]^{9-}$ by controlling different variables in hopes of isolating a bulk pure material.

CHAPTER 8: INCONCLUSIVE AND INCOMPLETE RESULTS.

During the course of my studies, several compounds were synthesized but not reported in the main sections of this thesis because of the difficulty in reproduction, isolation of a pure compound and very low yields. Some challenges faced are listed below:

- The difficulty in reproducing novel tetra-scandium-polyanions (**13** and **14**) was witnessed after changing the commercial source of scandium(III) nitrate. The salt initially used was $Sc(NO_3)_3 \cdot 4H_2O$ from an unknown Chinese source and when it ran out, we used $Sc(NO_3)_3 \cdot 6H_2O$ (Energy Chemicals) and $Sc(NO_3)_3 \cdot H_2O$ (Macklin) and although the masses were adjusted accordingly, the desired compounds could not be isolated.

- The novel $\{[(Sc(H_2O)_4)_4(H_2W_{12}O_{42})]^{4-}\}_\infty$ (**15**) could be synthesized and isolated in extremely low yield and the crystals only form after several months.

- Over the course of this work, one puzzling issue was the inability to synthesize/reproduce the trilacunary POM precursor: $[B\text{-}\alpha\text{-}BiW_9O_{33}]^{9-}$ following a well-known published procedure. It is known that both the trilacunary precursor and paratungstate-B are formed at the same pH window making it hard to isolate the desired compound without the other. In one experiment, three different polyanions could be isolated with $[H_2W_{12}O_{42}]^{10-}$ formed first followed by $[Bi_2(H_2O)_6W_2O_4(B\text{-}\beta\text{-}BiW_9O_{33})_2]$ (**17**) and lastly $[Bi_2(W_3O_{10})(B\text{-}\alpha\text{-}BiW_9O_{33})_3]^{23-}$ (**16**).

- When scandium nitrate, sodium tungstate, and germanium dioxide were mixed together in a stoichiometric ratio of 2:16:1 (Ge:W:Sc) two sandwich-type complexes; $[Sc_2Na_2(H_2O)_2(B\text{-}\alpha\text{-}GeW_9O_{34})_2]^{12-}$(**18**) and $[Sc_2(B\text{-}\beta\text{-}GeW_8O_{31})_2]^{14-}$ (**19**) were formed. Two types of needles **Na-18** (thick needles) and **Na-19** (thinner needles) formed

simultaneously, and we have not been able to find a way to preferentially isolate one product over the other.

Below are detailed descriptions of the inconclusive outcomes of this work.

8.1 Synthesis of Tetra-Scandium-Containing Heteropolytungstates
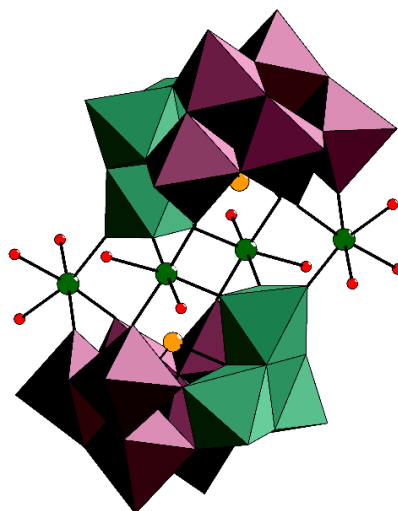
Figure 8.1. Combined polyhedral/ball-and-stick representation of $[Sc_4(H_2O)_{10}(B\text{-}\beta\text{-}XW_9O_{33})_2]^{n-}$. Colour code: WO_6, dark-pink; heteroatom ($X = As^{III}, Te^{IV}$), orange; O, red.

8.1.1   Synthesis Procedures

$Na_4[Sc_4(H_2O)_{10}(B\text{-}\beta\text{-}Te^{IV}W_9O_{33})_2]\cdot xH_2O$ (Na-13)

$Na_8[TeW_9O_{33}]\cdot 19.5H_2O$ **(Na-TeW9) (**0.285 g, 0.100 mmol) and $Sc(NO_3)_3\cdot 4H_2O$ (0.061 g, 0.200 mmol) were dissolved in 10 ml of water. The resulting pH of the solution was 3.7. The reaction mixture was vigorously stirred and heated at 75 ºC for 40 minutes. After cooling to room temperature, the solution was centrifuged and filtered. The final pH was 3.7. After the addition of 2 drops of 1M NaCl, the solution was left to evaporate slowly and colourless crystals formed within 1-2 weeks.

$Na_6[Sc_4(H_2O)_{10}(B\text{-}\beta\text{-}As^{III}W_9O_{33})_2]\cdot xH_2O$ (Na-14)

$Na_9[B\text{-}\alpha\text{-}As^{III}W_9O_{33}]\cdot 16H_2O$ **(Na-AsW9) (**0.300 g, 0.100 mmol) and $Sc(NO_3)_3\cdot 4H_2O$ (0.061 g, 0.200 mmol) were dissolved in 10 ml of water. The pH of the solution was adjusted from 6.1 to

5.0 using 4M HCl. The reaction mixture was vigorously stirred and heated at 75 ºC for 40 minutes. After cooling to room temperature, the solution was filtered. The final pH was 3.9. After the addition of 5 drops of 1M NaCl, the solution was left to evaporate slowly and colourless crystals formed within 2 weeks.

For both **Na-13** and **Na-14**, we were able to easily reproduce these compounds until we ran out of $Sc(NO_3)_3 \cdot 4H_2O$.

8.1.2   Single-Crystal X-Ray Diffraction

Table 8.1. Crystal data and structure refinement for **Na-13**.

Compound	**Na-13**
Formula Weight (g/mol)	Unknown
Crystal System	Triclinic
Space Group	P-1
a (Å)	12.8413(17)
b (Å)	12.8538(17)
c (Å)	16.180(2)
α (º)	91.586(6)
ß (º)	105.555(6)
γ (º)	101.691(5)
Volume (Å^3)	2509.9(60)
Z	2
$D_{calc.}$ (g/cm^3)	2.888
Absorption Coefficient (mm^{-1})	20.596
F(000)	1860
θ range for data collection	1.311 to 27.649
Completeness to θ$_{max}$	99.9%
Index Ranges	-16<=h<=16, -16<=k<=16, -20<=l<=20
Reflections Collected	96832
Unique Reflections	11561
R$_{int}$	0.0892
Absorption Correction	Semi-empirical from equivalents
Data/Restraints/Parameters	11561 / 0 / 357
Goodness of Fit on F^2	1.120
R$_1$[a] (I>2σ(I))	0.1079
wR$_2$[b] (all data)	0.2698

[a] $R_1 = \Sigma \|F_0|-|F_c\|/\Sigma|F_0|$, [b] $wR_2 = [\Sigma w(F_0^2 - F_c^2)^2 / \Sigma w(F_0^2)^2]^{1/2}$

Table 8.2. Comparison of unit cell parameters of **Na-13 and Na-14**.

Compound	**Na-13**	**Na-14**
Crystal System	Triclinic	Triclinic
Space Group	P-1	P-1(2)
a (Å)	12.8413(17)	12.8499(21)
b (Å)	12.8538(17)	12.8531(20)
c (Å)	16.180(2)	16.1103(27)
α (°)	91.586(6)	91.48(1)°
ß (°)	105.555(6)	105.39(1)°
γ (°)	101.691(5)	102.18(1)°
Volume (Å^3)	2509.9(60)	2498.18(59)
D$_{calc.}$ (g/cm^3)	2.888	3.319

8.1.3   Results and Discussion

8.1.3.1 Infrared (IR) spectroscopy

Fourier transform infrared (IR) spectra was recorded for **Na-13** and **Na-14.** The bending and asymmetric vibrations of crystallized water molecules are shown by a broad signal at around 3400 cm^{-1} and a narrow signal at around 1630 cm^{-1}. The vibration band at around 670 cm^{-1} and 900 cm^{-1} correspond to Te-O and As-O stretching modes from the TeO$_3$ and AsO$_3$ heterogroups, respectively. The W-O$_t$ and W-O$_b$-W stretching frequencies appear in the 932 - 880 cm^{-1} region of the spectra and the vibration frequency of the Sc-O bonds in the 777-795 cm^{-1} region. Finally, the W-O$_b$-W bending frequencies occur below 500 cm^{-1}.
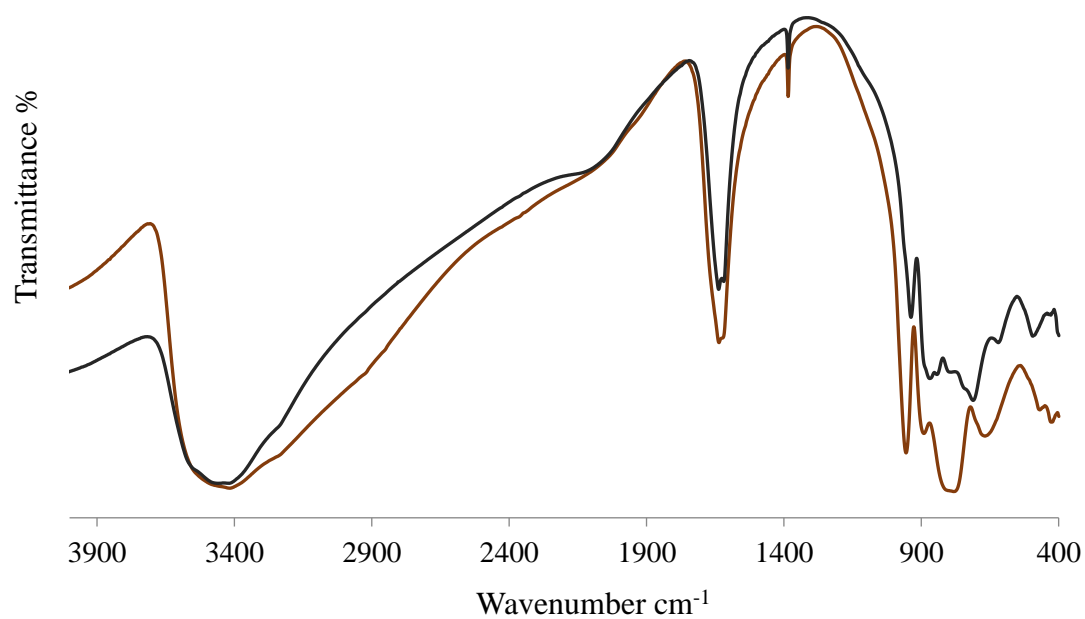
Figure 8.2. IR spectra of **Na-13** (dark orange) and **Na-TeW₉** (black).
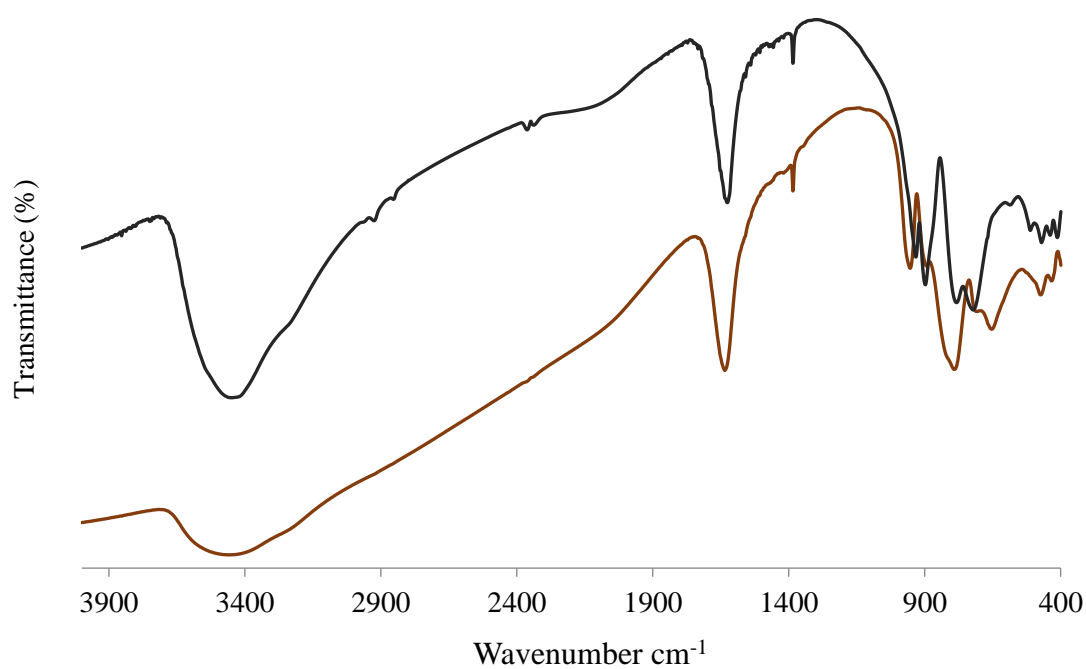
Figure 8.3. IR spectra of **Na-14** (dark orange) and the precursor **Na-AsW₉** (black).

8.1.3.2 Thermogravimetric analysis

Na-13 shows a rapid weight loss step in the range of 19-110°C. This corresponds to the loss of loosely and strongly bound crystal water molecules. The slow weight loss from 110 to 400 °C is likely due to the loss of coordinated water (i.e., the three aqua ligands of the outer Sc^{3+} ion and two from the inner Sc^{3+} ions. Above 400 °C, **Na-13** starts to decompose. It is at this point that other residual molecules such as some bridging oxygens of the polyanion start to get lost.
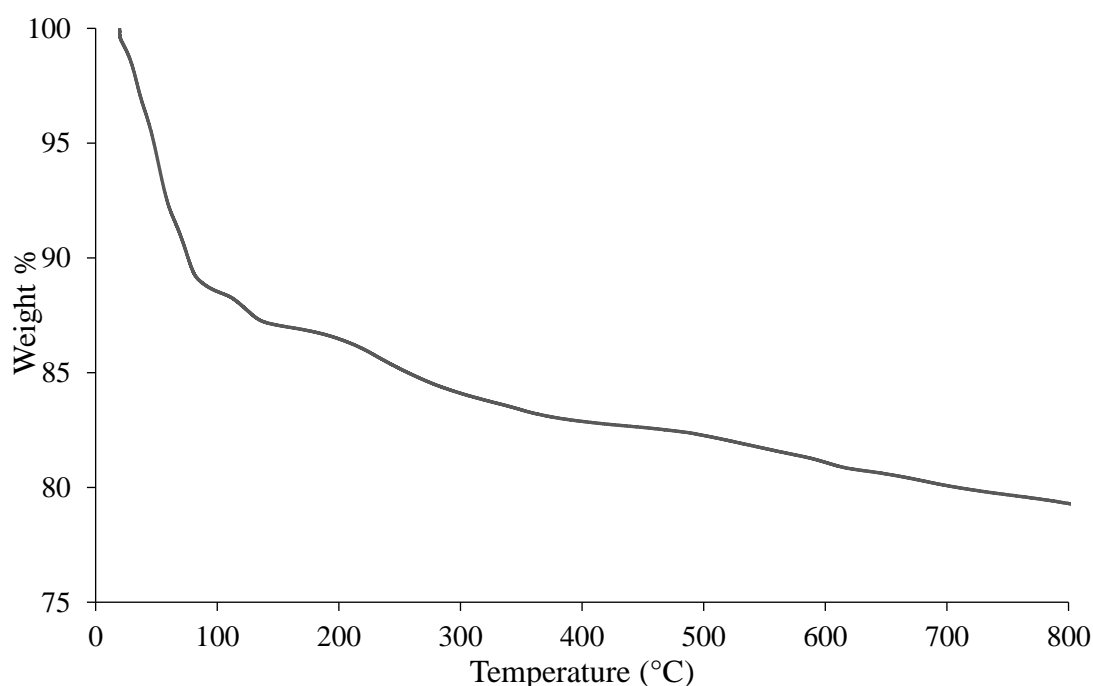
Figure 8.4. Thermogram of **Na-13**.

8.1.3.3 Structural description

The isostructural Krebs-type polyanions **13** and **14** are composed of two equivalent trilacunary $[\beta\text{-}XW_9O_{33}]^{n-}$ moieties linked to each other by four octahedrally coordinated Sc^{3+} ions to form a Krebs type polyanion with C_{2h} symmetry. The Sc^{3+} ions are arranged in pairs at two distinct positions: the outer position Sc^{3+} ions have three terminal aqua ligands while the inner two Sc^{3+} ions have only two terminal aqua ligands.

The Sc-O bond lengths of the inner Sc^{3+} ions range from 2.040(1) – 2.150(1) Å and those of the outer Sc^{3+} ion, 2.044(1) -2.145(1) Å. The longest bonds belong to the Sc-OH_2 bonds. Krebs and co-workers first reported this class of polyanions and their pioneering work has resulted in a large family of *3d-* transition-metal-disubstituted $[\{M(H_2O)_3\}_2(WO_2)_2(XW_9O_{33})_2]^{n-}$ species where M = Mn^{2+}, Fe^{3+}, Co^{2+}, Ni^{2+}, or Zn^{2+} and X = Sb^{3+}, Bi^{3+}). [1-3] Our research group synthesized $[Fe_4(H_2O)_{10}(\beta\text{-}Te^{IV}W_9O_{33})_2]^{4-}$ in 2002.[4] However the first scandium-containing Krebs-type polyanion; $[Sc_4(H_2O)_{10}(B\text{-}\beta\text{-}SbW_9O_{33})_2]^{6-}$ was reported in 2017 by the Zheng group. [5]

8.2 Synthesis of a three-dimensional framework, $\{(Sc(H_2O)_4)_4(H_2W_{12}O_{42})\}_{\infty}^{4-}$

Paratungstate-B $[H_2W_{12}O_{40}]^{10-}$ or $[W_{12}O_{40}(OH)_2]^{10-}$ is one of the most common isopolytungstates, which is stable in aqueous acidic solution. [6-7] $[H_2W_{12}O_{40}]^{10-}$ has been known to act a multidentate ligand which coordinates with alkaline metals, transition, post transition and lanthanide (rare earth) metals due to its high negative charges and active oxygen-rich surface [8-16] The result can be high-dimensional structures.

8.2.1   Synthesis

$Na_4[(Sc(H_2O)_4)_4(H_2W_{12}O_{42})]\cdot xH_2O$ (Na-15)

$Sc(NO_3)_3\cdot 4H_2O$ (0.0265 g, 0.35mmol) was dissolved in 10 ml of NaOAc buffer (pH 4.86, 0.5 M). $Na_{10}[H_2W_{12}O_{42}]\cdot 20H_2O$ (0.250 g, 0.072 mmol) was added to this solution and stirred until complete dissolution of the precursor (a milky white solution is observed which clears after 5 minutes). 0.2 ml of 1M NaOH was added dropwise and the pH was 4.9. The reaction solution was stirred for 30 minutes at room temperature and filtered. The filtrate was kept in a 25 ml beaker and it could evaporate slowly. Rod shaped crystals formed after several months.

8.2.2   Single-Crystal X-Ray Diffraction

Table 8.3. Crystal data and structure refinement for **Na-15**.

Compound	**Na-15**
Formula weight without water, g/mol	3572.08
Crystal system	*Monoclinic*
Space group	$P2_1/n$
a (Å)	15.3586(14)
B (Å)	11.7296(10)
C (Å)	18.1384(15)
α (°)	90
β (°)	109
γ (°)	90
Volume (Å^3); Z	3081.6(5)
Density (Mgm^{-3})	3.850
Abs. coef. (mm^{-1})	22.663
$F(000)$	3132
θ range (°)	2.301 to 27.571
Limiting indices	$-19 \leq h \leq 19$, $-14 \leq k \leq 15$, $-23 \leq l \leq 23$
Reflections collected	46353
Unique reflections [R_{int}]	7098 [0.2194]
Completeness to θ	99.6 (27.571)
Data / restraints /parameters	7098/0/230
GOOF on F^2	1.022
Final Rindices [I>2σ(I)][a]	$R_1 = 0.0550$, $wR_2 = 0.1538$
R indices (all data)[b]	$R_1 = 0.0625$, $wR_2 = 0.1573$

[a] $R_1 = \Sigma\|F_0\|-\|F_c\|/\Sigma\|F_0\|$, [b] $wR_2 = [\Sigma w(F_0^2 - F_c^2)^2/\Sigma w(F_0^2)^2]^{1/2}$

8.2.3   Results and Discussion

8.2.3.1 Structural description

$[(Sc(H_2O)_4)_4(H_2W_{12}O_{42})]^{4-}$ (**15**) consists of a paratungstate-B ion; $[H_2W_{12}O_{42}]^{10-}$ which acts as a hexadentate ligand and coordinates with six Sc^{3+} cations. The resulting structure is a three-dimensional network where $[H_2W_{12}O_{42}]^{10-}$ ions are connected to each other via $Sc(H_2O)_4^{3+}$ units. Two neighbouring $[H_2W_{12}O_{42}]^{10-}$ ions are connected to each other via two different types of connections. The first connection involves two $Sc(H_2O)_4^{3+}$ units linked to the paratungstate

ion via four terminal oxygen atoms. Each $Sc(H_2O)_4^{3+}$ unit connects to two WO_6 octahedra of each $[H_2W_{12}O_{42}]^{10-}$ ion. The second connection involves two $Sc(H_2O)_4^{3+}$ cations connecting to two neighbouring $[H_2W_{12}O_{42}]^{10-}$ polyanions via two terminal oxygen atoms of WO_6 octahedron from an edge shared triad. In other words, each Sc^{3+}, acts as a linking cation, joining three $[H_2W_{12}O_{42}]^{10-}$ ions via the terminal oxygen atoms of edge-shared and corner-shared WO_6 octahedra.

There are two types of Sc-O bonds with the first one resulting from the coordination of 4 aqua ligands (Sc-O$_{water}$ length of 2.386(11) - 2.416(75) Å. The remaining Sc-O bonds contain three terminal oxygen atoms of the tungsten atoms in three different $[H_2W_{12}O_{42}]^{10-}$ polyanions with a Sc−O$_{terminal}$ length of 2.363(87)-2.428(67) Å.
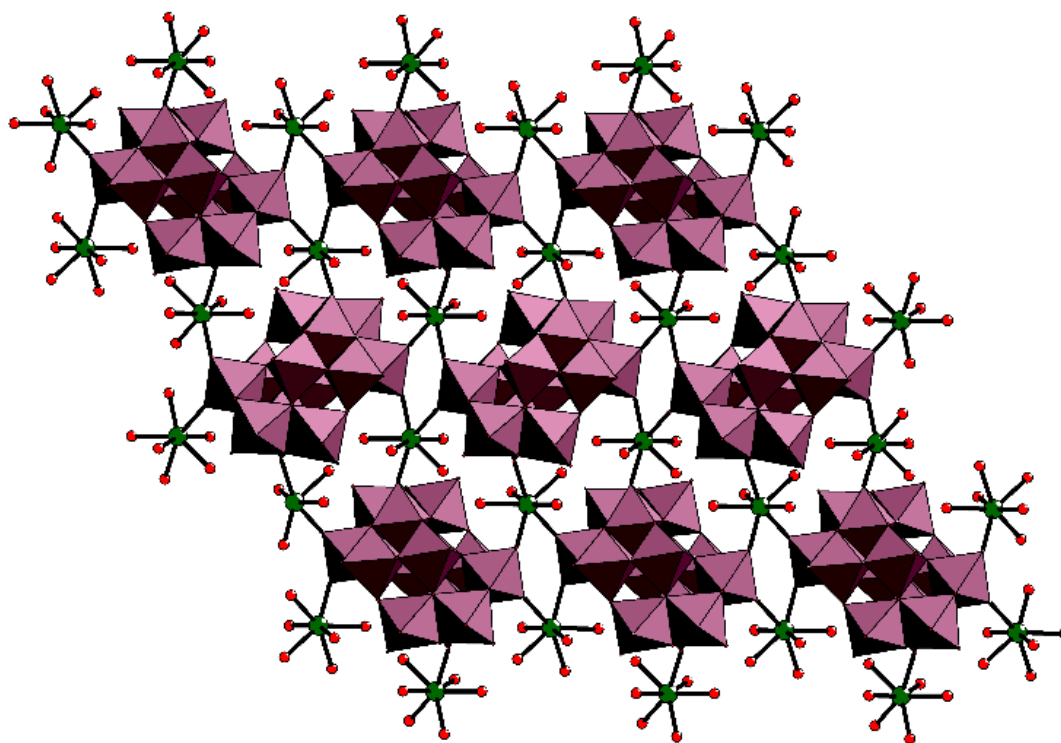
Figure 8.5. Combined polyhedral/ball-and-stick representation of $\{[(Sc(H_2O)_4)_2(H_2W_{12}O_{42})]^{4-}\}_\infty$ (**15**). Colour code: WO_6, dark-pink octahedra; Sc, green; O, red.

$\{[(Sc(H_2O)_4)_2(H_2W_{12}O_{42})]^{4-}\}_\infty$ (**15**) was originally synthesized by accident during attempts to prepare scandium-containing tungstobismuthates. A polyanion we once isolated but have problems reproducing is $[(Sc_2OH(H_2O)_4)_2(Sc(H_2O))_6Sc(H_2O)_2(W_3O_{12})_2(B\text{-}\beta\text{-}Bi^{III}W_9O_{33})_6]^{37-}$ had been made as follows:

 0.0265 g (0.35mmol) $Sc(NO_3)_3 \cdot 4H_2O$ (salt from an unknown academic source from China) was dissolved in 10 ml of NaOAc buffer (pH 5, 0.5 M). To this solution 0.250 g (0.35 mmol) of $Na_9[B\text{-}\alpha\text{-}BiW_9O_{33}] \cdot 16H_2O$ (**Na-BiW₉**) was added. The solution was stirred until complete dissolution of the precursor (a milky white solution is observed which clears after 5 minutes). 0.2 ml of 1M NaOH was added dropwise and the pH was 4.9. The reaction solution was stirred for 30 minutes at room temperature and filtered. The filtrate was kept in a 25 ml beaker and it could evaporate slowly. Rod shaped crystals formed after two weeks. However, on this occasion, rhombic shaped crystals formed after a week and it turns out that $[H_2W_{12}O_{42}]^{10-}$ had been made instead of the intended POM precursor $[B\text{-}\alpha\text{-}BiW_9O_{33}]^{9-}$.

8.3 The $Na_9[BiW_9O_{33}] \cdot 16H_2O$ Problem

According to the published procedure, by Yamase and co-workers, when an acidic solution of $Bi(NO_3)_3 \cdot 5H_2O$ is added to a hot solution (80°C) of $Na_2WO_4 \cdot 2H_2O$ and heated for 1 h, colourless crystals of $Na_9[BiW_9O_{33}] \cdot 16H_2O$ are expected to form upon cooling to room temperature. The final pH of the reaction should be 7.5.[17]

During our experiments, we continually had to adjust the pH to 7.5 using 1M NaOH (our pH was around 7.1). The resulting rhombic crystals were paratungstate-B which easily forms at pH 7.5-8.0.[18] These results suggest that bismuth nitrate acts as a structure directing agent for the formation of $[H_2W_{12}O_{42}]^{10-}$. This is not the first time that such an observation has been made. In 1975, Evans and Rollins isolated $Na_{10}[H_2W_{12}O_{42}] \cdot 20H_2O$ in an attempt to prepare a

heteropoly-tungstoaluminate complex. They dissolved sodium tungstate and aluminium nitrate in water and adjusted the pH to 7 using nitric acid. After boiling the solution for 10-15 minutes they obtained crystals of the sodium salt of paratungstate-B.[6] Based on this information, the authors concluded that $[H_2W_{12}O_{42}]^{10-}$ formation is highly favoured at around pH 7. With this acquired information, it was only befitting to perform the reaction by Evans and Rollins replacing Al^{3+} with Bi^{3+} and the results were quite interesting. (section **8.3.1**)

8.3.1   Synthesis of Na$_{23}$[Bi$_2$(W$_3$O$_{10}$)(*B-α*-BiW$_9$O$_{33}$)$_3$]·xH$_2$O (Na-16)

Na$_2$WO$_4$·2H$_2$O (5.00g, 15.2 mmol) and Bi(NO$_3$)$_3$·5H$_2$O (0.688g, 1.38 mmol) were dissolved in 10 ml of water. The pH of the solution was adjusted to 7 (from pH 9) using 6M HNO$_3$. The turbid solution was boiled for 15 minutes until it was clear. After cooling to room temperature, the final pH of the solution was 7.2. It was then left at room temperature and after a day, large rhombic crystals formed which were characterized by infrared (IR) spectroscopy and single crystal XRD as the sodium salt of paratungstate-B $[H_2W_{12}O_{42}]^{10-}$. After a week, a lot of larger cubic crystals of $[H_2W_{12}O_{42}]^{10-}$ and smaller ones of the sodium salt of $[Bi_2(W_3O_{10})(B\text{-}\alpha\text{-}BiW_9O_{33})_3]^{23-}$ (**16**) were formed. We repeated this reaction several times and each time $[H_2W_{12}O_{42}]^{10-}$ was formed first followed by **Na-16.**

$[H_2W_{12}O_{42}]^{10-}$ $[Bi_2(W_3O_{10})(B\text{-}\alpha\text{-}BiW_9O_{33})_3]^{23-}$ (**16**)
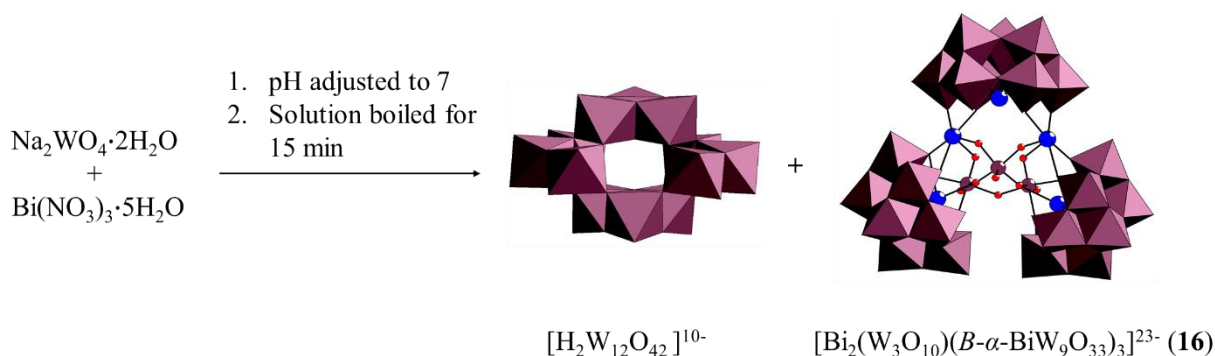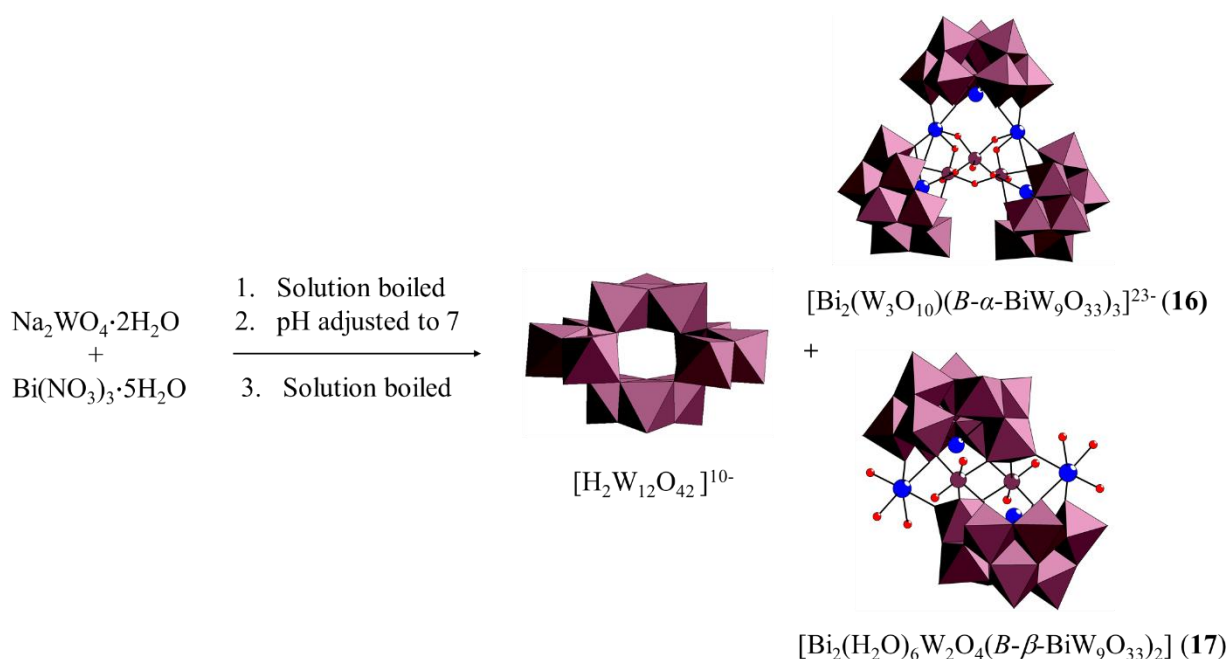
Scheme 1. Illustration of the original Evans and Rollins reaction (Al^{3+} replaced with Bi^{3+}).

We slightly adjusted the afore mentioned reaction, and the results were surprising.

8.3.2   Synthesis of Na$_8$[Bi$_2$(H$_2$O)$_6$W$_2$O$_4$(*B*-β-BiW$_9$O$_{33}$)$_2$]·xH$_2$O (Na-17)

After mixing of sodium tungstate and bismuth nitrate, the solution was boiled for 15 minutes before the pH of the solution was adjusted to 7. The resulting solution was boiled for a further 15 minutes after which was cooled and the pH was 6.6. After one day, large rhombic crystals of the sodium salt of [H$_2$W$_{12}$O$_{42}$]$^{10-}$ formed followed by a few rod-shaped crystals of Na$_8$[Bi$_2$(H$_2$O)$_6$W$_2$O$_4$(*B*-β-BiW$_9$O$_{33}$)$_2$]·xH$_2$O (**Na-17**) and some cubic crystals of **Na-16**.

$$Na_2WO_4 \cdot 2H_2O + Bi(NO_3)_3 \cdot 5H_2O \xrightarrow{\begin{array}{l}1.\ \text{Solution boiled}\\2.\ \text{pH adjusted to 7}\\3.\ \text{Solution boiled}\end{array}} [H_2W_{12}O_{42}]^{10-}$$

[Bi$_2$(W$_3$O$_{10}$)(*B*-α-BiW$_9$O$_{33}$)$_3$]$^{23-}$ (**16**)

+

[Bi$_2$(H$_2$O)$_6$W$_2$O$_4$(*B*-β-BiW$_9$O$_{33}$)$_2$] (**17**)

Scheme 2. Illustration of modified Evans and Rollins reaction (Al^{3+} replaced with Bi^{3+}).

8.3.3   Discussion

From our experimental observations, it is clear that in addition to the 7.5-8 pH domain, paratungstate-B readily forms around pH 6.6-7.2. This poses a great challenge when it comes to the isolation of pure polyoxometalates and in our case, this is the isolation of Na$_9$[BiW$_9$O$_{33}$]·16H$_2$O. Although we were able to isolate pure crystals of paratungstate after one day, we were unable to collect crystals of the three species separately as they grow simultaneously. As a result, it was impossible to obtain IR spectra of the pure compounds.
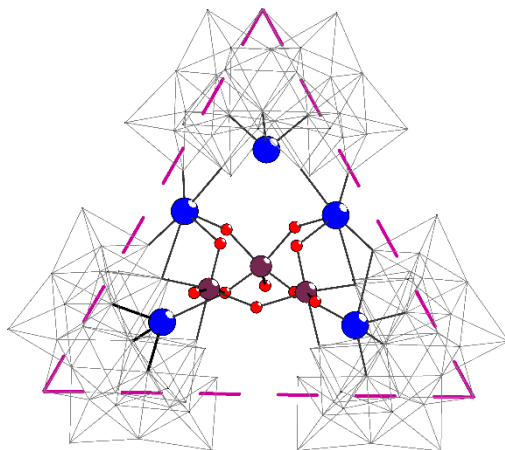
Figure 8.6. Combined polyhedral/ball-and-stick representation of $[Bi_2(W_3O_{10})(B\text{-}\alpha\text{-}BiW_9O_{33})_3]^{23-}$ (**16**). Colour code: WO_6, transparent octahedra; W, dark-pink; Bi, blue; O, red.

A closer look at $[Bi_2(W_3O_{10})(B\text{-}\alpha\text{-}BiW_9O_{33})_3]^{23-}$ (**16**) reveals that this polyanion consists of three $[B\text{-}\alpha\text{-}BiW_9O_{33}]^{9-}$ units which are connected to each other via a $\{Bi_2(W_3O_{10})\}$ core resulting in a triangular shaped structure. In this structure there are two types of Bi atoms: the tripodal (primary) Bi^{3+} of the BiO_3 unit and the hexacoordinated (secondary) connecting cation. The Bi-O distances in the BiO_3 unit are in the range of 2.115(27) - 2.180(26) Å and they vary a lot for the connecting bismuth atoms (2.105(28) - 2.867(27) Å). From this we could prove that the trilacunary precursor $[B\text{-}\alpha\text{-}BiW_9O_{33}]^{9-}$ can still be made but with obvious difficulties.

The other species that formed in the modified reaction was $[Bi_2(H_2O)_6W_2O_4(B\text{-}\beta\text{-}BiW_9O_{33})_2]^{8-}$ (**17**) which is a Krebs-type polyanion exhibiting two $[\beta\text{-}BiW_9O_{33}]^{9-}$ units that sandwich two Bi^{3+} ion and two W^{6+} ions.
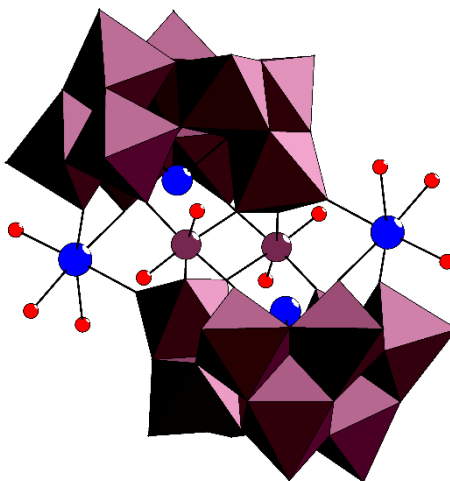
Figure 8.7. Combined polyhedral/ball-and-stick representation of $[Bi_2(H_2O)_6W_2O_4(B\text{-}\beta\text{-}BiW_9O_{33})_2]^{8-}$ (**17**). Colour code: WO_6, transparent octahedra; W, dark-pink; Bi, blue; O, red.

$[Bi_2(H_2O)_6W_2O_4(B\text{-}\beta\text{-}BiW_9O_{33})_2]^{8-}$ (**17**) could also be made using the following procedure: H_2WO_4 (1.85 g, 7,42 mmol) was dissolved in 10ml H_2O and the resulting pH of 3.0 adjusted to 7.3 using 8ml 2M NaOH. The reaction solution was heated at 45 °C for 5 minutes and solid $BiCl_3 \cdot H_2O$ added. The pH of 4.3 was increased to 6.7 and the solution stirred at 80°C for 24 hours. After cooling to room temperature, the pH was 6.6. A few rod-shaped crystals of $[Bi_2(H_2O)_6W_2O_4(B\text{-}\beta\text{-}BiW_9O_{33})_2]^{8-}$ (**17**) formed when the solution was stored at 4 °C. Simultaneously, crystals of paratungstate-B formed readily. We tried to vary the reaction time, temperature as well as varying the pH (ranging from 4-11) but we were not able to obtain favourable results.

8.4 Synthesis of Di-Scandium-Containing Tungstogermanates

Na$_{12}$[Sc$_2$Na$_2$(H$_2$O)$_2$(*B-α*-GeW$_9$O$_{34}$)$_2$]·xH$_2$O (Na-18) and Na$_{14}$[Sc$_2$(*B-β*-GeW$_8$O$_{31}$)$_2$]·xH$_2$O (Na-19)

Solid GeO$_2$ (0.05g, 0.5 mmol) and Na$_2$WO$_4$·2H$_2$O (1.32g, 4.0 mmol) were added to a solution

of Sc(NO$_3$)·H$_2$O (0.063g, 0.25 mmol) in 20 ml IM NaOAc (pH 5.90). The resulting reaction

mixture was stirred for an hour at 60°C. After cooling to room temperature, the pH was 8.91

and thick needle-shaped crystals of Na$_{12}$[Sc$_2$Na$_2$(H$_2$O)$_2$(*B-α*-GeW$_9$O$_{34}$)$_2$]·xH$_2$O (**Na-18**) and

thin long needles of Na$_{14}$[Sc$_2$(*B-β*-GeW$_8$O$_{31}$)$_2$]·xH$_2$O **(Na-19)** formed after the solution was left

for slow evaporation at 4°C.

8.4.1   Discussion

The reaction of scandium nitrate, sodium tungstate, and germanium dioxide at stoichiometric

ratio of 2:16:1 (Ge:W:Sc) in a sodium acetate solution (pH 5.9) at a high temperature resulted

in two sandwich-type complexes; [Sc$_2$Na$_2$(H$_2$O)$_2$(*B-α*-GeW$_9$O$_{34}$)$_2$]$^{12-}$(**18**) and [Sc$_2$(*B-β*-

GeW$_8$O$_{31}$)$_2$]$^{14-}$ **(19).** This reaction yielded thick needles of **Na-18** first followed by thinner

needles of **Na-19**. A rational procedure for the formation of **Na-18** would require a molar ratio

of Ge:W:Sc of 1:9:1 but we were able to synthesize it with a little less W. This could explain

why we obtained minute amounts of the compound. Thinner needles of **Na-19** formed almost

simultaneously. This compound is the most rational product of the two because of the molar

ratio of 1:8:1 (Ge: W: Sc). Although we could isolate the different types of crystals for single

crystal XRD, we were unable to collect them separately for further analysis. Over time we also

noticed the formation of a precipitate which further made it harder to isolate the two compounds

separately.

Table 8.4. Comparison of unit cell praramaters of **Na-18** and **Na-19**.

Compound	**Na-18**	**Na-19**
Crystal System	Triclinic	Triclinic
Space Group	P-1(2)	P-1(2)
a (Å)	11.3612(13	11.6982(9) Å
b (Å)	12.5598(14)	13.4512(11
c (Å)	18.535(2)	18.8303(15)
α (°)	101.17	102.28
ß (°)	94.28	103.22
γ (°)	107.22	108.96
Volume (Å^3)	2453.65(384)	2592.16(365)
D$_{calc.}$ (g/cm^3)	3.85217	3.13658
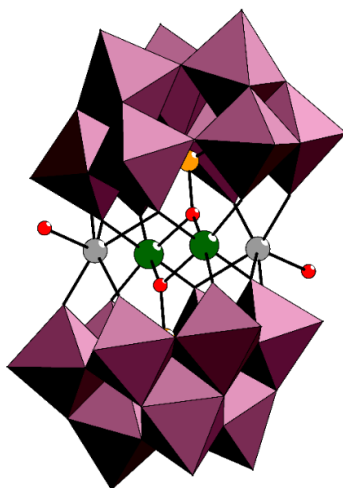
Figure 8.8. Combined polyhedral/ball-and-stick representation of $[(Na(H_2O))_2Sc_2(B\text{-}\alpha\text{-}GeW_9O_{34})_2]^{12-}$ (**18**). Colour code: WO_6, dark-pink octahedra; Sc, green; P, orange; Na, grey; O, red.

The structure of the polyanion **18** is based on Weakley-type sandwich complexes first reported in 1973.[19] It is formed by the fusion of two trilacunary $[\alpha\text{-}GeW_9O_{24}]^{10-}$ {GeW$_9$} via a tetranuclear central core in a centrosymmetric arrangement with an idealized C_{2h} symmetry. The tetranuclear central core of the polyanion **18**, is composed of two internal ScO$_6$ and two external NaO$_5$(H$_2$O) octahedra.
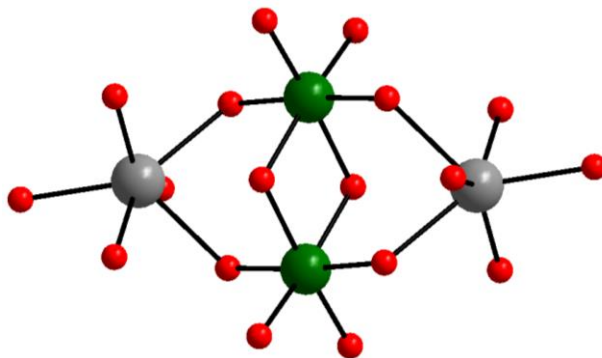
Figure 8.9. Ball-and-stick representation of the central tetranuclear $Na_2(OH_2)_2Sc_2O_{14}$ unit of $[(Na(H_2O))_2Sc_2(B\text{-}\alpha\text{-}GeW_9O_{34})_2]^{14-}$ (**18**). Colour code: Sc, green; Na, grey; O, red.

Each Sc^{3+} centre is adopts an octahedral geometry formed by one μ_2-O from a WO_6 octahedron, one μ_3-O from another WO_6 octahedron and one μ_3-O from the central GeO_4 tetrahedron on each GeW_9 unit. In other words, each scandium ion is linked to the two GeW_9 sub-units *via* four Sc-O-(W) bonds and two Sc-O-(Ge) bonds.
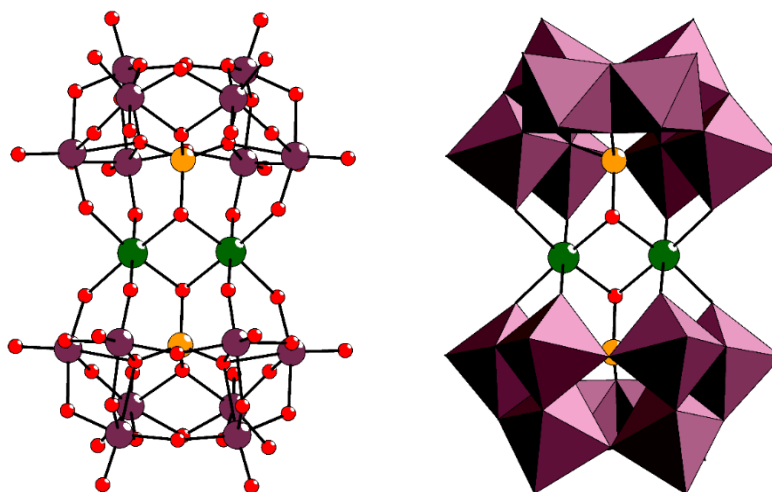
Figure 8.10. Ball-and-stick (left) and combined polyhedral/ball-and-stick (right) representations of $[Sc_2(B\text{-}\beta\text{-}GeW_8O_{31})_2]^{14-}$(**19**). Colour code: WO_6, dark-pink octahedra; W, dark-pink; Sc, green; Ge, orange; O, red.

Polyanion **19** consists of two equivalent octatungstogermanate $[B\text{-}\beta\text{-}GeW_8O_{31}]^{10-}$ {GeW_8} units connected by two Sc^{3+} centres, leading to a sandwich-type structure with C_{2h} symmetry. Each GeW_8 consists of two W_3O_{13} triads connected to a two edge-shared WO_6 octahedra, which are

stabilized by GeO_4 in the centre. The $[B\text{-}\beta\text{-}GeW_8O_{31}]^{10-}$ polyanion is not a very common lacunary polyoxotungstate which however can be imagined as being derived from a saturated β-Keggin isomer; $[SiW_{12}O_{40}]^{3-}$ where one W_3O_{13} triad and a WO_6 octahedron of the rotated triad have been lost. The $\{GeW_8\}$ unit was first reported in 2007 in $[Cu_5(2,2'\text{-}$ bpy)$_6(H_2O)][GeW_8O_{31}]$ and to date it has been reported in very few publications. [20-23]

The two equivalent Sc^{3+} ions have an octahedral coordination environment formed by four μ_2-O atoms; Sc-O distances of 2.20(1)-2.23(1) Å (terminal oxo ligands from two edge-shared octahedra in each GeW_8 unit) and two μ_3-O atoms, each from the terminal oxo ligand of GeO_4; Sc - O distances of 2.134(1) and 2.152(1) Å.

The occurrence of both $\{GeW_8\}$ and $\{GeW_9\}$ has been observed in several structures and as such a mixture of both polyanions **18** and **19** can be expected.[21-22] Since polyanion **19** is known for $\{GeW_8\}$, we believe that the Si- analogue could be obtained and this work is currently underway.

8.5 References

[1]   M. Piepenbrink, E. M. Limanski, B. Krebs, *Z. Anorg. Allg. Chem.* **2002**, *628*, 1187–
        1191.

[2]   M. Bösing, I. Loose, H. Pohlmann, B. Krebs, *Chem. Eur. J.* **1997**, *3*, 1232–1237.

[3]   I. Loose, E. Droste, M. Bösing, H. Pohlmann, M. H. Dickman, C. Rosu, M. T. Pope, B.
        Krebs, *Inorg. Chem.* **1999**, *38*, 2688–2694.

[4]   U. Kortz, M. G. Savelieff, B. S. Bassil, B. Keita, L. Nadjo, *Inorg. Chem.* **2002**, *41*,
        783–789.

[5]   Z. W. Cai, B. X. Liu, T. Yang, X. X. Li, S. T. Zheng, *Inorg. Chem. Commun.* **2017**, *80*,
        1–5.

[6]   H. T. Evans, O. W. Rollins, *Acta Crystallogr. Sect. B.* **1976**, *32*, 1565–1567.

[7]   M. T. Pope, *Heteropoly and Isopoly Oxometalates*, Springer-Verlag, 1983.

[8]   E. V. Peresypkina, A. V. Virovets, S. A. Adonin, P. A. Abramov, A. V. Rogachev, P.
        L. Sinkevich, V. S. Korenev, M. N. Sokolov, *J. Struct. Chem.* **2014**, *55*, 295–298.

[9]   S. V. Radio, G. M. Rozantsev, V. N. Baumer, O. V. Shishkin, *J. Struct. Chem.* **2011**,
        52, 111–117.

[10]   Z. H. Xu, X. L. Wang, Y. G. Li, E. B. Wang, C. Qin, Y. L. Si, *Inorg. Chem. Commun.*
        2007, *10*, 276–278.

[11]   C. Giménez-Saiz, J. R. Galán-Mascaròs, S. Triki, E. Coronado, L. Ouahab, *Inorg.
        Chem.* **1995**, *34*, 524–526.

[12]   C. Y. Sun, S. X. Liu, L. H. Xie, C. L. Wang, B. Gao, C. D. Zhang, Z. M. Su, *J. Solid
        State Chem.* **2006**, *179*, 2093–2100.

[13]   B. Yan, N. K. Goh, L. S. Chia, *Inorg. Chim. Acta.* **2004**, *357*, 490–494.

[14]   I. Loose, M. Bösing, R. Klein, B. Krebs, R. P. Schulz, B. Scharbert, *Inorg. Chim. Acta.*

1997, *263*, 99–108.

[15]   X. Zhang, J. Dou, D. Wang, Y. Zhang, Y. Zhou, R. Li, S. Yan, Z. Ni, J. Jiang, *Cryst. Growth Des.* **2007**, 1699–1705.

[16]   X. Zhang, D. Wang, J. Dou, S. Yan, X. Yao, J. Jiang, *Inorg. Chem.* **2006**, *45*, 10629–10635.

[17]   B. Botar, T. Yamase, E. Ishikawa, *Inorg. Chem. Commun.* **2000**, *3*, 579–584.

[18]   H. Von D'Amour, R. Allmann, *Zeits. Kristallogr. NCS.* **1972**, *136*, 23–47.

[19]   T. J. R. Weakley, H. T. Evans, J. S. Showell, G. F. Tourné, C. M. Tourné, *J. Chem. Soc. Chem. Commun.* **1973**, 139–140.

[20]   C. M. Wang, S. T. Zheng, G. Y. Yang, *Inorg. Chem.* **2007**, *46*, 616–618.

[21]   Z. Zhang, Y. Qi, C. Qin, Y. Li, E. Wang, X. Wang, Z. Su, L. Xu, *Inorg. Chem.* **2007**, *46*, 8162–8169.

[22]   N. H. Nsouli, A. H. Ismail, I. S. Helgadottir, M. H. Diekman, J. M. Clemente-Juan, U. Kortz, *Inorg. Chem.* **2009**, *48*, 5884–5890.

[23]   W. Liu, R. Al-Oweini, K. Meadows, B. S. Bassil, Z. Lin, J. H. Christian, N. S. Dalal, A. M. Bossoh, M. Mbomekallé,Mbomekallé, P. De Oliveira, J. Iqbal, U.Kortz, *Inorg. Chem.* **2016**, *55*, 10936−10946.